Variations in Size and Optical Properties of Dissolved Organic Matter During Mixing at Large River Confluences: Implications for Source Discrimination in the Boreal Zone

by

Jinping Xue

A thesis submitted in partial fulfillment of the requirements for the degree of

Master of Science

in

Soil Science

Department of Renewable Resources
University of Alberta

ABSTRACT

The functionality of dissolved organic matter (DOM) in natural waters depends on its size and composition. Identifying the sources and associated properties of DOM is vital to understand its effects on downstream ecosystems. River mixing has great potential to alter DOM quality, but its role in large boreal river confluences remains largely unknown, which limits our ability to realize the exact magnitude and composition of DOM exported to the ocean.

Using asymmetrical flow field-flow fractionation (AF4) with offline excitation emission matrices (EEMs) measurements and parallel factor (PARAFAC) analysis, we found that inputs of DOM from the major tributaries shifted DOM quality in a typical large boreal river, namely, the lower Athabasca River (LAR). Flowing downstream, DOM tended to be higher in concentrations of dissolved organic carbon (DOC) and degrees of humification and aromaticity. Seasonal variations of DOM as a result of spring freshet were observed, during which times DOM tended to be higher in molecular mass (e.g., size) and richer in protein-like (i.e., tryptophan-like) relative to humic-like components. Source discrimination of DOM was more apparent under base flow conditions compared with the snowmelt period.

In addition, conservative mixing behaviors of DOM at river confluences were observed. Contrasting mixing patterns among mixing zones suggest that both hydrological conditions and river geomorphology affect mixing patterns of DOM between the LAR and its tributaries. Our results demonstrate that DOM could be used as a *quasi*-conservative tracer during mixing at large river confluences. Findings from this study will enhance our ability to determine sources of DOM and to distinguish trends of mixing between the mainstem and the tributaries for DOM-associated trace elements in the boreal zone.

PREFACE

This research was supported by the Natural Sciences and Engineering Research Council of Canada, Alberta Innovates, and the Canadian Oil Sands Innovation Alliance. We are also grateful to the Canadian Foundation for Innovation, the Government of Alberta, and the University of Alberta Faculty of Agriculture, Life and Environmental Sciences for funding the SWAMP laboratory facility.

Chapter 2 was written as a manuscript to be submitted for publication. I was responsible for the sample collection in the spring of 2019. I also performed the sample & data analyses and wrote the manuscript. William Shotyk and Chad W. Cuss were supervisory authors and co-authors on the manuscript, and were involved in concept formation, manuscript composition, and editing.

A version of Chapter 2 will be submitted as Jin-Ping Xue, Chad W. Cuss, Tommy Noernberg, Muhammad B. Javed, Na Chen, Rick Pelletier, Yu Wang, William Shotyk. (2020) "Variations in Size and Optical Properties of Dissolved Organic Matter During Mixing at Large River Confluences: Implications for Source Discrimination in the Boreal Zone" to a peer-reviewed journal. Chad W. Cuss, Jin-Ping Xue, and Muhammad B. Javed contributed to the data collection. Na Chen and Yu Wang provided valuable suggestions for the initial preparation of the manuscript. Tommy Noernberg provided technical assistance during two sampling campaigns. Rick Pelletier made the map of the Athabasca River watershed with the data I provided.

To my family

"I am writing a longer letter than usual because there is not enough time to write a short one"

Blaise Pascal, *Lettres Provinciales* (ca. 1657)

ACKNOWLEDGMENTS

It is with my sincere gratitude that I thank my supervisor Dr. William Shotyk for his boundless support along the two-year journey in Canada. Thank you for giving me the opportunity to explore such a fantastic area of research. You have broadened my scientific horizon and taught me how to treat scientific work. Your wisdom and kindness guided me to be a better man. A special thank you to Dr. Chad Cuss who got me involved in the world of DOM and AF4, and taught me practical skills for lab instruments and data analyses with great patience and understanding, which served as a solid basis for the completion of the thesis. My sincere thanks to Dr. William Shotyk, Dr. Scott Chang, and Dr. David Olefeldt for serving as examiners; also a special thank you to Dr. Scott Chang for chairing the exam.

I sincerely acknowledge support from members of the SWAMP laboratory. Thanks to Iain Grant-Weaver and Dr. Muhammad (Babar) Javed for scientific discussions/training and lab/field support. Thanks to Tommy Noernberg for leading our Athabasca field trips, as well as Tracy Gartner for administrative support. Thanks to Na Chen and Yu Wang for their comments and suggestions along the way. Thanks to Carla Germani, Marjan Ghotbizadeh, Andrii Oleksandrenko, Ron Goyhman, Dulani Kandage, and Dr. Fiorella Barraza Castelo for your kindness and generosity. Thanks to Dr. Lina Du and Dr. Yifeng Zhang, I will keep our memories in mind all the time.

Last but certainly not least, I would like to thank my family and friends who were so supportive throughout my oversea journey. A special thanks to my grandma, who was always by my side and I wish you well. A big thank you to my previous supervisors Dr. Dingyong Wang and Dr. Yongmin Wang, who have always encouraged me to pursue my scientific aspirations. Thank you to Dr. Scott Chang for your valuable help for my MSc application. Thank you to Dr. Tariq Siddique for your great support, your teaching style impressed me. A special thank you to my friend Jinghe Jiang, you taught me a lot about life. I am also very grateful to have met so many wonderful people in Edmonton, you will be greatly missed.

No one truly leaves! My sincerest thanks to one and all!

Jinping Xue

TABLE OF CONTENTS

LIST OF FIGURES

LIST OF TABLES

1.0 INTRODUCTION

1.1 DISSOLVED ORGANIC MATTER IN FRESHWATERS

Dissolved organic matter (DOM) is a complex molecular mixture that is generally defined as that fraction which passes through a 0.45 μm filter (range used 0.2–1.22 μm). A key component in the global carbon cycle (Perdue and Ritchie, 2014), it is supplied to surface waters from both external (allochthonous, e.g., terrestrial ecosystem) and internal (autochthonous, e.g., algae and macrophytes) sources. As such, DOM is heterogeneous in its chemical composition, which largely impacts its reactivity and ecological role in surface waters (Fellman, Hood and Spencer, 2010; Stubbins et al., 2014).

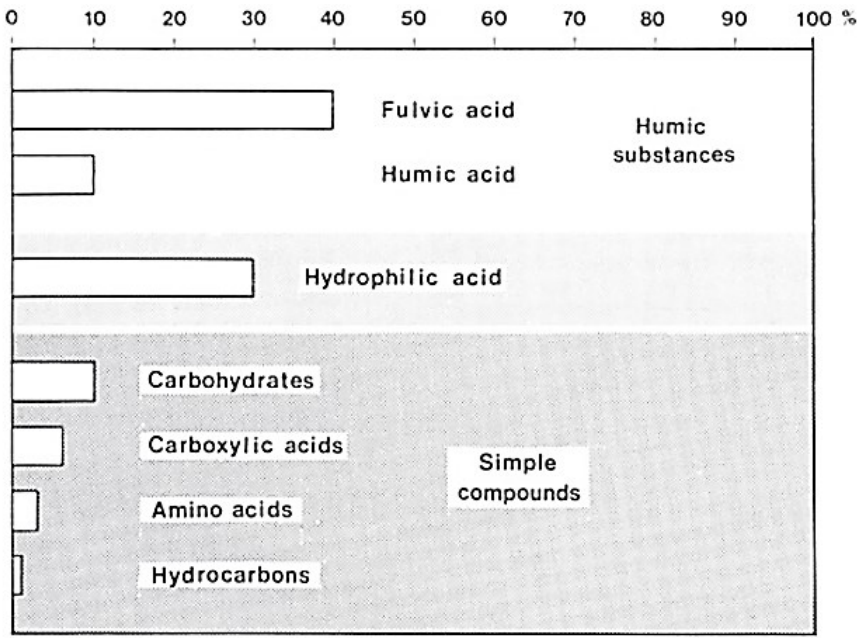

Figure 1-1 The abundance of organic compounds of dissolved organic carbon (DOC) for average river water with a DOC of 5 mg/l, adapted from *Figure 4.1* in Thurman (1985).

Given that DOM is difficult to quantify as a result of its structural complexity, measurements of dissolved organic carbon (DOC), which accounts for ~50% of DOM (Moody and Worrall, 2017),

are preferred for describing natural water samples. The abundance of major compounds constituting DOC for average river water with a DOC of 5 mg/l is shown in Figure 1-1 (Thurman, 1985). Aquatic fulvic and humic acids make up a large proportion of DOC (Figure 1-1), thus serving as the dominant group of natural organic compounds in water. This thesis focuses on DOM in freshwaters, while comprehensive reviews on other aquatic ecosystems, such as estuarine waters (Bauer and Bianchi, 2011) and seawater (Dittmar and Stubbins, 2014), are also available.

1.1.1 Sources and Properties of Dissolved Organic Matter to Surface Waters

Autochthonous and allochthonous DOM sources in natural waters are summarized in Figure 1-2 (Thurman, 1985).

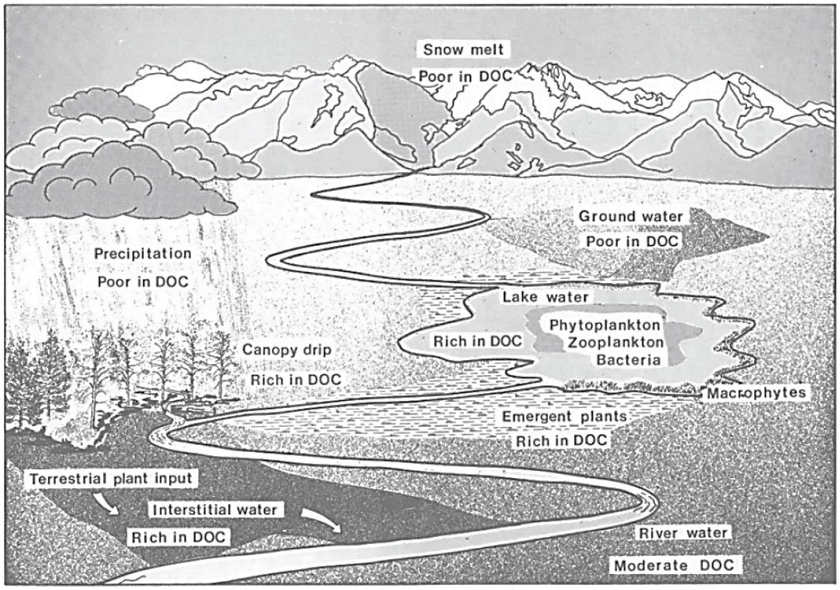

Figure 1-2 Allochthonous and autochthonous dissolved organic matter sources in natural waters, adapted from *Figure 2.1* in Thurman (1985).

In general, the majority of autochthonous DOM in freshwaters is derived from algae,

including phytoplankton and periphyton in lentic and lotic ecosystems, respectively, and macrophytes (e.g., liverworts) (Bertilsson and Jones, 2003). The organic compounds derived from phytoplankton can be released upon cell death or from actively growing cells. Such internally produced constituents are either available for microorganisms or can be transformed via a variety of pathways (e.g., photodegradation) (Figure 1-3). Similar mechanisms are also found for the extracellular release of DOM from macrophytes. Notably, the organic material released during active growth mainly comprises of biologically labile compounds with low molecular weight. Altogether, autochthonous DOM serves as a major nutrient source for aquatic microorganisms and hence regulates the structure and function of microbial communities (Thurman, 1985).

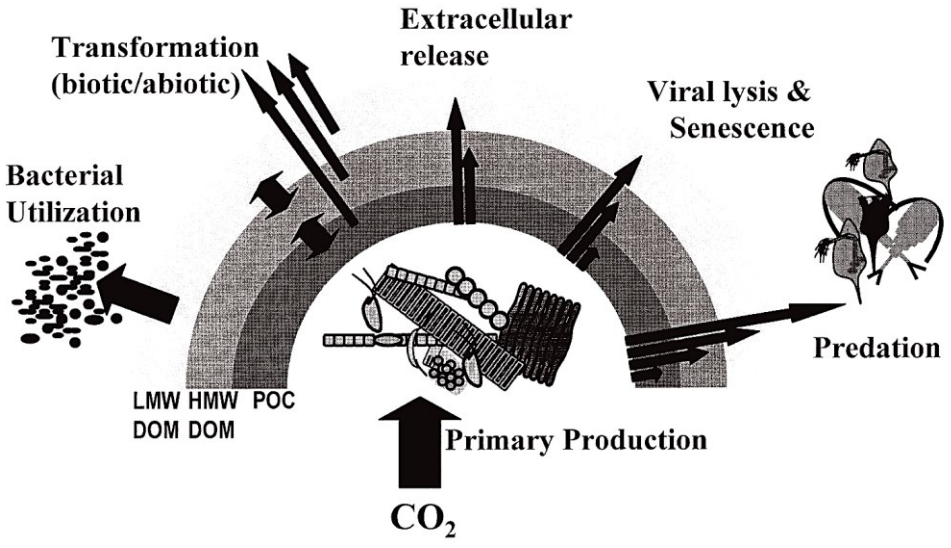

Figure 1-3 Production and transformation of dissolved organic matter (DOM) from aquatic phytoplankton and macrophytes. Arrows denote fluxes; POC indicates particulate organic matter; LMW and HMW DOM are low molecular weight and high molecular weight DOM, respectively, from *Figure 1* of Bertilsson and Jones (2003).

Allochthonous DOM in freshwaters mainly comes from soil and terrestrial plants, especially

in small to moderate-sized rivers. It is widely accepted that DOM from soil is much more decomposed compared with that from vascular plants (Thurman, 1985). Inputs of allochthonous DOM into freshwaters are largely associated with surface runoff and result from the balance between production and loss from the soil solution and the hydrological conditions (Aitkenhead-Peterson, McDowell and Neff, 2003).

1.1.2 Chemical and Biological Interactions of Dissolved Organic Matter

Dissolved organic matter plays a significant role in affecting aquatic chemistry and biology. For instance, DOM can influence acid-base balance as well as the fate, transport, and bioavailability of trace metals through complexation (Oliver, Thurman and Malcolm, 1983; Worms et al., 2019). It serves as the major source for potentially toxic by-products during water disinfection (Perdue and Ritchie, 2014). Meanwhile, it can attenuate ultraviolet-B (UV-B) radiation and thus protect aquatic biota from harmful UV exposure (Stubbins et al., 2014). Lastly, it fuels microbial food webs (Thurman, 1985).

1.1.2.1 Dissolved Organic Matter and The Acid-Base Chemistry of Freshwaters

The large-scale research effort for studying the acid-base properties of DOM was initiated in the 1980s, in order to reveal the influence of acidic precipitation on aquatic environments (Oliver, Thurman and Malcolm, 1983). Various studies have examined that long-term (i.e., natural) decreases in pH and alkalinity in rivers were largely related to elevated inputs of natural organic acids and could be estimated via empirical models of the acid-base chemistry of DOM (Perdue and Ritchie, 2014).

1.1.2.2 The Interaction Between Dissolved Organic Matter and Trace Metals

In natural waters, a metal-organic complex is formed when a metal ion (electron acceptor) associates with a ligand (electron donor), which is a charged or uncharged molecular species (Nieboer and Richardson, 1980). Various organic functional groups acting as ligands are involved into metal-OM interactions in natural systems (Nieboer and Richardson, 1980). The speciation of a metal can be defined as the distribution of a specific species of the metal among its various chemical forms which together make up the total concentration of that element in a water sample (Florence, Batley and Benes, 1980). For a metal-organic complex, the stability relies on thermodynamic data (e.g., stability constant), and its magnitude is highly related to environmental parameters (e.g., pH), and the properties of the organic ligand(s), and the metal (Florence, Batley and Benes, 1980; Nieboer and Richardson, 1980). It is widely accepted that metal-organic complexes can exert strong influences on metal speciation, thus regulating their potential availability or toxicity to aquatic biota (Yamashita and Jaffé, 2008).

Pioneering works on classification of either metal ions or ligands or both proposed three distinct categories, namely, "hard", "soft", and borderline (e.g., the scheme of Pearson's Hard and Soft Acids and Bases, HSAB) (Ahrland, Chatt and Davies, 1958; Pearson, 1968a; Pearson, 1968b; Nieboer and Richardson, 1980). A hard Lewis acid usually is a charged ion that is small in size and is low in polarizability (e.g., K^+, Na^+, Mg^{2+}, Ca^{2+}), while a soft Lewis acid refers to the ion of low oxidation states and high polarizability (e.g., Cu^{2+}, Au^+, Hg^{2+}, Cd^{2+}) (Pearson, 1968a). Also, hard Lewis bases include H_2O, O^{2-}, OH^-, F^-, Cl^-, NO_3^-, etc. and examples of soft bases are I^-, CN^-, and R^-, S^{2-}, CO. Complete lists of Lewis acids and bases can be found elsewhere (Pearson, 1968a). The key point of the HSAB theory is that, under comparable conditions of acid-base strength, hard Lewis acids tend to bind with hard Lewis bases and soft Lewis acids prefer soft bases. The HSAB thus has great implications on most of the inorganic coordination chemistry.

It should be noted that the Irving-Williams series (e.g., Mn < Fe < Co < Ni < Cu) regarding the order of stability of some organic complexes of divalent cations can be applied without considering the nature of ligands (Irving and Williams, 1948). Such an observation also serves as a key basis for studying metal-organic complexation in nature. Generally, DOM in natural waters has more abundant O-containing functional groups than N-containing and S-containing groups. However, complexation between soft or borderline Lewis acid ions (e.g., Ni^{2+}, Cu^{2+}, and Hg^{2+}) and N- and S-containing groups has been found to be more stable than those of O-containing groups, which are usually bound with hard Lewis acid ions (e.g., $A1^{3+}$, Mn^{2+}) (Nieboer and Richardson, 1980).

A vast array of analytical approaches is available to determine the chemical speciation of trace metals in natural waters (Florence, Batley and Benes, 1980). Those techniques can be basically divided into two categories, namely, calculation (e.g., chemical speciation models) and experimental methods. The development of chemical speciation models largely relies on knowledge of metal binding by DOM from both field and laboratory studies (Perdue and Ritchie, 2014). Large efforts have been made to incorporate competitive effects of H^+, other metal ions, and ligands into speciation models, which in turn enhanced their predictive capabilities of metal-DOM interactions. Some relatively early models are briefly reviewed by Perdue and Ritchie (2014). Those models consist of the competitive Gaussian distribution model, models V and VI, and the family of nonideal competitive adsorption models, while all of which are largely dwarfed by their oversimplication on DOM binding sites. As such, the first priority for those modelling studies will be to resolve the relative concentrations and strengths of these binding sites (Perdue and Ritchie, 2014). Additionally, earlier modelling studies have also been evaluated by Florence, Batley and Benes (1980), who indicated the importance of the measurement of the equilibrium constants for chemical speciation calculations. It should be noted that the biotic ligand model is now widely accepted to model metal speciation related to toxicity (Figure 1-4) (Paquin et al., 2002).

Experimental methods place the different metal species into experimentally defined categories according to their behavior during chemical analysis (Florence, Batley and Benes, 1980). Briefly, ion selective electrode (ISE) is a species-specific technique and responds to only to the activity of the free metal ion (Florence, Batley and Benes, 1980). It can be used to differentiate a free metal cation from its complexed forms (Perdue and Ritchie, 2014). Unfortunately, concentrations of trace metals (e.g., Cu, Pb, Cd, and Zn) are usually too low in natural waters for determination by ISE (Florence, Batley and Benes, 1980; Perdue and Ritchie, 2014). Anodic stripping voltammetry (ASV) is widely used to distinguish labile (e.g., free metal ion plus metal complexes) and nonlabile forms of a metal cation (Perdue and Ritchie, 2014). This method is considered to be more sensitive than the ISE technique. For ASV-labile measurements, preliminary separations and blanks can be avoided, and the risk for contamination is minimal (Florence, Morrison and Stauber, 1992). Cathodic stripping voltammetry with excellent sensitivity can also be used to distinguish between labile and nonlabile forms of a metal (Florence, 1986). Furthermore, similar information can be derived from cation exchange, which is applicable to metal cations that cannot be oxidized or reduced in aqueous solution (Backes and Tipping, 1987; Florence, Morrison and Stauber, 1992).

Chelation-solvent extraction methods have been used to determine organically complexed metal in natural waters (Florence, Batley and Benes, 1980), although it suffers from underestimation on the percentage of metal-organic forms. Dialysis, electrophoresis, ultrafiltration, and centrifugation are all capable of differentiating metals associated with colloidal particles from their ionic species (Florence, Batley and Benes, 1980). Available analytical methods such as X-ray absorption spectroscopy and spectrophotometric techniques (e.g., UV–Visible absorbance and fluorescence) are also widely used to characterize DOM and its binding with metals in aquatic environments (Karlsson and Persson, 2010; Kikuchi et al., 2017). Altogether, a series of metals (e.g., Al, Fe, Cu, Hg, Pb, and Ag) are demonstrated to form strong complexes with DOM in many freshwaters (Warren and Haack,

2001; Perdue and Ritchie, 2014). Reviews on analytical methods that are capable of distinguishing chemical forms of trace metals in early studies are referred to Florence, Batley and Benes (1980), Florence (1986), and Florence, Morrison and Stauber (1992).

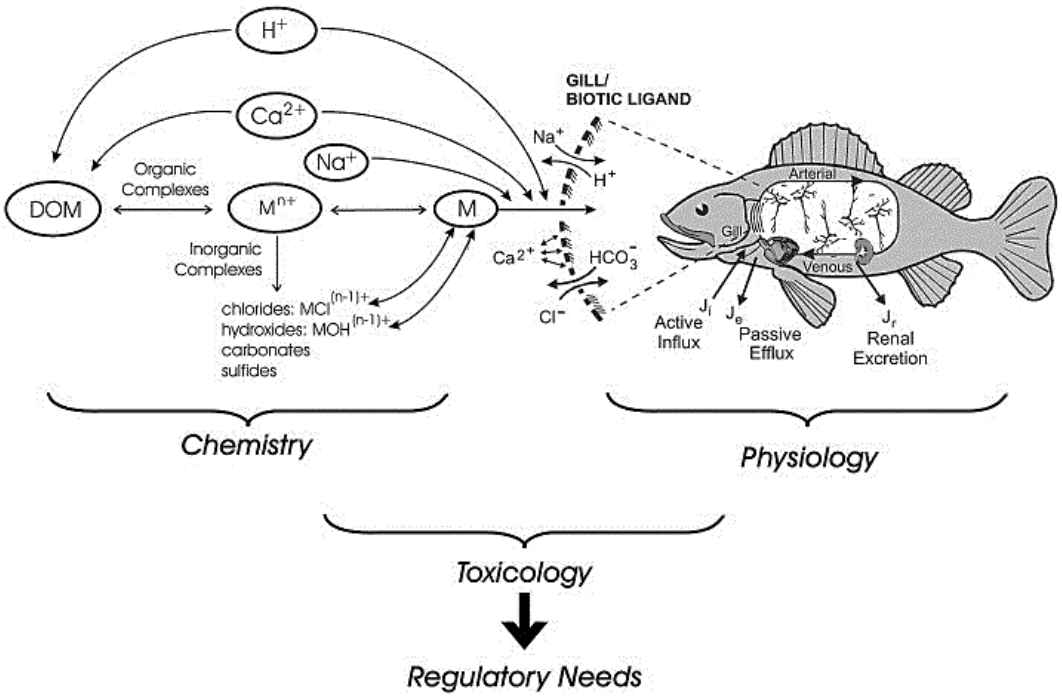

Figure 1-4 The biotic ligand model from *Figure 1* of Paquin et al. (2002).

1.1.2.3 Dissolved Organic Matter and Disinfection By-Products

Starting from the 1970s, the generation of chloroform and other halogenated organics as disinfection by-products in treated drinking water has been identified and a large body of studies has been conducted on this topic (Perdue and Ritchie, 2014). To date, various by-products have been identified and the corresponding concentrations and adverse effects on health have been widely evaluated (Perdue and Ritchie, 2014). It is well recognized that DOM serves as the basis of such by-products (e.g., trihalomethane) in disinfected water. Meanwhile, the measurement of trihalomethane formation potential (THMEP) has been integrated as a routine component for water treatment

processes. Efforts on the removal of DOM before chlorination also led to advances in isolation techniques of DOM from water (e.g., ultrafiltration) (Perdue and Ritchie, 2014). Reviews related to the effects of DOM on the formation of disinfection by-products can be found elsewhere (Nikolaou and Lekkas, 2001; Urbansky and Magnuson, 2002).

1.1.2.4 Dissolved Organic Matter and UV-Visible Radiation

Dissolved organic matter comprises a continuum of organic molecules, part of which contain chromophores and fluorophores and can interact with UV and visible radiation. In this process, electrons in molecules containing chromophores or fluorophores are excited to higher electronic energy states. Photochemical reactions of DOM can thus be facilitated by the absorbed energy (Miller, 1998). Dissolved organic matter may experience direct photodegradation, during which its electronically excited components undergo specific chemical reaction(s). Additionally, it may serve as a photosensitizing agent and transfer energy to other constituents of natural waters (Perdue and Ritchie, 2014). Photobleaching, the process during which the color of DOM fades when exposing to solar radiation, can also facilitate the formation of inorganic carbon (e.g., HCO_3^-, CO_2 and CO) (Gao and Zepp, 1998).

1.1.2.5 Dissolved Organic Matter and Its Ecosystem Services

The flow of matter and energy through different trophic levels are essential to the function of an ecosystem (Foreman and Covert, 2003). Dissolved organic matter is widely known as a key component of aquatic food webs by supplying nutrients and energy to microorganisms (Fellman et al., 2009). The availability of labile DOM thus has significant effects on stream ecology (Fischer et al., 2002; Foreman and Covert, 2003), although other factors such as physical (e.g., salinity, pH, oxygen concentrations, and pressure) and biotic (e.g., competition and predation) forces are also

responsible for structuring microbial communities (Foreman and Covert, 2003).

1.2 DISSOLVED ORGANIC MATTER IN BOREAL RIVERS

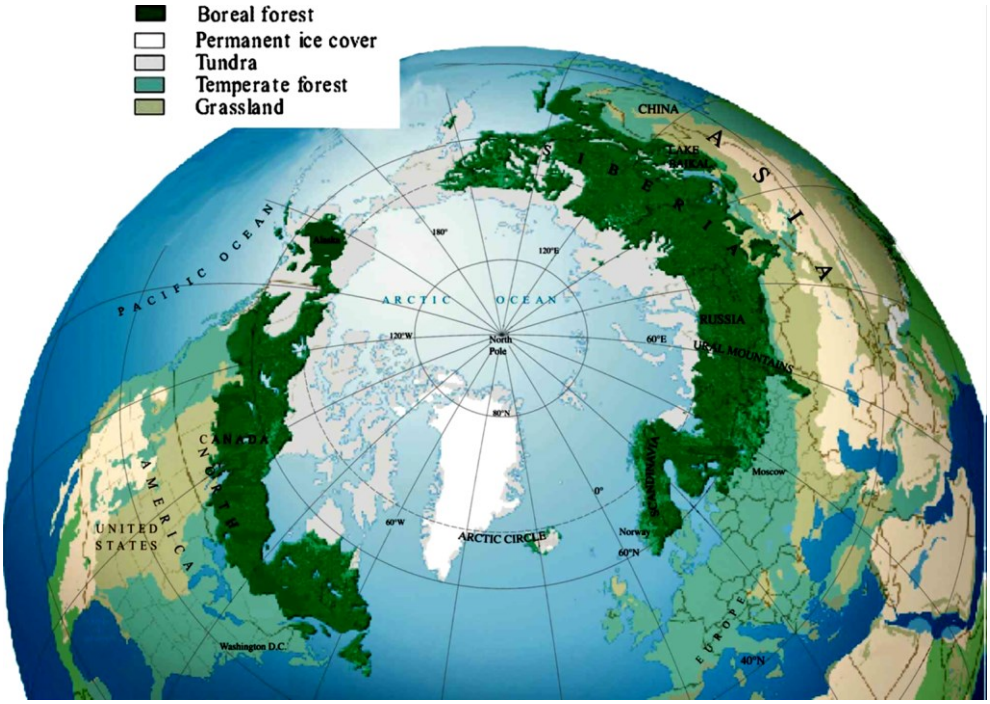

Figure 1-5 Boreal forests (in green) distributed in North America and Eurasia from *Figure 1* of Yoon and Chen (2006).

The boreal forest, also known as the taiga, is the largest terrestrial biome, covering ~11% of the Earth's land surface (Bonan and Shugart, 1989). Geographically, it is located between latitudes 45° and 70° N (DeAngelis, 2019), and the majority is distributed in North America and Eurasia (Figure 1-5). The part in North America stretches from northern Alaska (US) to Newfoundland & Labrador (Canada), between the treeless tundra to the north and the mixed forest of the south. The boreal forest

largely consists of trees that are young relative to those in temperate zones. Furthermore, it is regularly influenced by forest fires, insects, and other natural disturbances (DeAngelis, 2019).

Fluvial networks in the boreal biome are extremely dense and complex and are closely coupled to land (Hutchins, Prairie and del Giorgio, 2019). Given the prevalence of terrestrial organic-rich systems (e.g., peatlands) in the boreal zone (Shotyk, 1988; Gorham, 1991), boreal rivers receive great attention as large amounts of terrestrial DOM are released into adjacent freshwaters, potentially rendering boreal rivers significant in the regional and global carbon budgets (Lapierre et al., 2013; Hutchins, Prairie and del Giorgio, 2019). Therefore, examining the key drivers responsible for the spatial variability of DOM in boreal rivers will be helpful to predict the direction and magnitude of its riverine fluxes and its potential influences on downstream ecosystems.

To date, a large amount of work has been done on DOM in the boreal zone (Dillon and Molot, 1997; Ågren et al., 2008; Spencer et al., 2009; Wilson and Xenopoulos, 2009; Franke, Hamilton and Ziegler, 2012; Kothawala et al., 2015). A series of factors have thus been reported to influence fluvial DOM quality, such as climatic factors and the proportion of wetlands and agricultural lands (Andersson and Nyberg, 2008; Wilson and Xenopoulos, 2009; Laudon et al., 2012). Seasonal variations of DOM quality were also well studied in the boreal biome, and the shift of DOM quality between snowmelt and base flow has been widely documented (Moore, 2003; Finlay et al., 2006; Ågren et al., 2008).

1.3 MIXING OF DISSOLVED ORGANIC MATTER AT LARGE RIVER CONFLUENCES

River channel confluences serve as a key component of fluvial systems. Junction scours are often prevalent at river confluences, and fluid acceleration and helical secondary flow cells are important

parts of junction-flow dynamics (Parsons et al., 2008). Turbulence generated by the shear-layer may exert a significant influence on confluence scour and mixing rates (Parsons et al., 2008). The complete mixing of two large rivers may require a long distance (e.g., ~400 km) (Parsons et al., 2008). Three-dimensional flow structures and channel scale flow circulation are identified respectively, for slower and rapid mixing cases. These variables control mixing, which will be fast or slow depending on the structure and amount of circulation (Parsons et al., 2008).

Mixing phenomena occur in a variety of aquatic environments, such as the river confluences or the estuaries connecting the riverine and marine systems (Simon et al., 2019). Both spatial and temporal aspects of DOM are combined in a unique way during flow mixing, exerting great influence on carbon pools in natural waters (Simon et al., 2019). To date, a large body of studies has been conducted on mixing in estuaries (Zhou et al., 2016). Nonetheless, little information is available regarding the physical mixing of riverine waters (Simon et al., 2019).

Previous studies have examined the non-conservative behavior of DOM during flow mixing at river confluences (Moreira-Turcq et al., 2003; Lambert et al., 2016), implying changes of DOM quality (Aucour et al., 2003; Simon et al., 2019). A detailed summary is available regarding geochemical processes and corresponding explanations for the non-conservative behavior of DOM during flow mixing at river confluences (Simon et al., 2019). Those processes consist of sorption, release, flocculation/coagulation, and fractionation (McKnight et al., 1992; Aucour et al., 2003; Simon et al., 2019). Given the non-conservative behavior of DOM, the relationship between sources and the quality of DOM may not exist (McKnight et al., 1992). Altogether, the research gap on riverine mixing largely limits the discrimination of sources of DOM and ultimately our understanding of the evolution of DOM along the river continuum to the ocean, at the regional and global scales.

Figure 1-6 The mixing zone between the Horse River ("black waters") and the LAR upstream of Fort McMurray (Credit: William Shotyk and Jinping Xue).

The development of the bituminous sands in northern Alberta has received much attention due to the potential release of organic and inorganic contaminants into the lower Athabasca River (LAR) (Zhang et al., 2016; Shotyk et al., 2017; Sun et al., 2017). The delayed mixing in the LAR is obvious and visible as some of its tributaries contain abundant DOM as a result of their drainage basins being rich in peatlands (Figure 1-6), where the DOM pool is largely dominated by inputs of plant-derived polysaccharides such as cellulose and phenolic compounds from lignin (Gorham, 1991; D'Andrilli et al., 2010). In peatlands, DOM experiences significant transformations as a result of processes such as humification (Chanton et al., 2008). Decomposition of OM in peat is thought to be limited due largely to low activity of the enzyme phenol oxidase led by the absence of oxygen, thus resulting in high levels of high molecular weight (HMW) DOM in shallow layers of *Sphagnum*-dominated peatlands (Chanton et al., 2008; D'Andrilli et al., 2010; Ward and Cory, 2015). Furthermore, production and decomposition of peat largely occur in porewaters (D'Andrilli et al., 2010). Unsaturated/aromatic compounds are found to be reactive compounds in the peat profile, dominating the DOM pool in surface porewater (D'Andrilli et al., 2010; Ward and Cory, 2015).

Changes of DOM quality with depth are usually not so significant, and refractory, less aromatic DOM tends to accumulate along the vertical gradient due to anoxic conditions, slow hydrologic transport, and possibly microbial activity (Chanton et al., 1995; D'Andrilli et al., 2010; Tfaily et al., 2018).

Mixing phenomena also need to be considered for water quality monitoring in rivers potentially influenced by industry, especially when the mixing zone coincides with the area of potential contamination (Cuss et al., 2020). Therefore, the study of flow mixing in the LAR will be of great significance for the regional source discrimination of DOM. Moreover, given the prevalence of flow mixing in large boreal rivers, the study on the mixing behavior of DOM in the LAR is also of broader significance, lending support for the understanding of the geochemical behavior of DOM in other large boreal rivers.

1.4 CHARACTERIZATION OF DISSOLVED ORGANIC MATTER

Knowledge of DOM structural chemistry is necessary for a better understanding of its geochemical behavior in natural waters. Subtle changes in DOM composition can alter its biological and chemical properties, which, in turn, affect the potential reactivity toward a diverse suite of aquatic organisms.

1.4.1 Optical Characterization

Advances in spectroscopic techniques (e.g., absorbance and fluorescence) offer reliable information about composition of DOM in aquatic ecosystems in a rapid, precise, and inexpensive manner (Fellman, Hood and Spencer, 2010). Given that both measurements require absorption of UV-visible light by DOM moieties, these techniques thus only provide information on the chromophoric components of DOM (CDOM) instead of the total DOM pool. To date, a variety of optical

approaches ranging from simple indicators and excitation emission matrices-parallel factor analysis (EEM-PARAFAC) can be used to interpret optical data of DOM (Figure 1-7), allowing for qualitative and quantitative characterization of DOM (Fellman, Hood and Spencer, 2010; Stubbins et al., 2014).

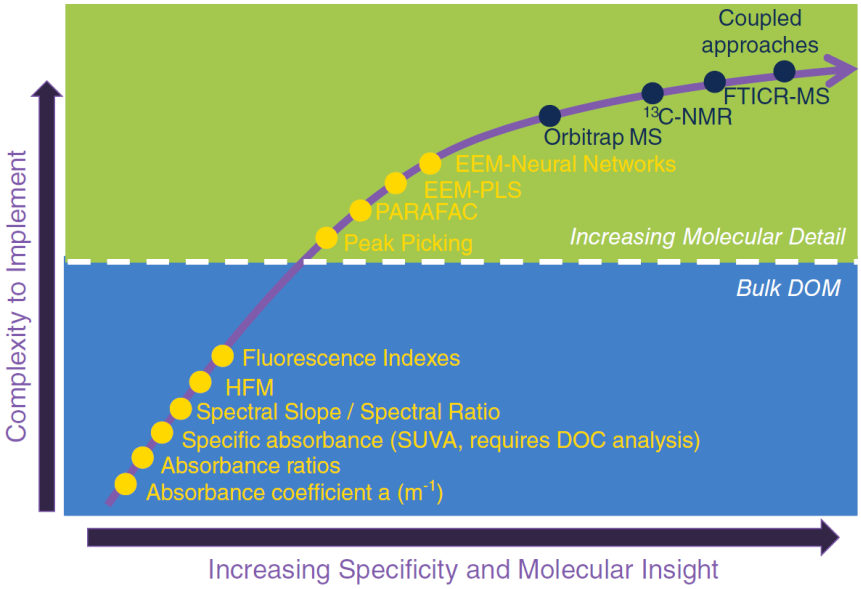

Figure 1-7 Conceptual diagram of the relevance of molecular insight and the level of analytical complexity, from *Figure 1* of McCallister, Ishikawa and Kothawala (2018). Names of analytical techniques for DOM characterization are differentiated into optical (yellow) and molecular (deep blue). All techniques below the dashed line evaluate bulk DOM, while those above the line can be used to get detailed molecular insight of DOM.

The absorption spectrum for CDOM exhibits an exponential increase in absorption following the decrease in wavelength from the visible into the UV range. A detailed summary of absorbance indicators is reported elsewhere (Minor et al., 2014; Hansen et al., 2016). A sub-fraction of DOM fluoresces under ultraviolet light. This property is used to characterize changes in DOM composition in aquatic ecosystems. To date, molecular fluorescence spectroscopy has been considered to be a promising tool for characterizing the chemical composition of DOM (Fellman, Hood and Spencer,

2010). The application of molecular fluorescence spectroscopy depends on the type of data collected (e.g., EEMs) and the corresponding data analysis performed (Fellman, Hood and Spencer, 2010; Stubbins et al., 2014). Distinct peak types are defined mainly based on excitation and emission maxima, with their sources and composition well documented (Fellman, Hood and Spencer, 2010).

Various fluorescence indicators have been developed to quantify differences in fluorescence properties of DOM as reviewed elsewhere (Fellman, Hood and Spencer, 2010). More detailed insights into the biogeochemical processing of DOM can be obtained by using multivariate approaches (e.g., PARAFAC), through which underlying signals (i.e., components) with chemical significance can be identified (Stedmon and Bro, 2008; Murphy et al., 2013).

Currently, standardized data treatment and interpretation techniques (e.g., DOMFluor and drEEM) for EEMs data have made the analysis of fluorescence powerful, potentially allowing for a large-scale inter-laboratory comparison of DOM quality from various natural water samples (Stedmon and Bro, 2008; Murphy et al., 2013). In addition, the online library of PARAFAC components (OpenFluor) also allows for statistical comparisons with any newly generated components (Murphy et al., 2014).

Attempts have been conducted to link results from EEMs analyses to chemical functional group information revealed by nuclear magnetic resonance (NMR). Distributions of elemental formulae can also be examined from the Fourier transform ion cyclotron resonance mass spectrometer (FT-ICR-MS). Nevertheless, such studies are currently limited to a fraction of the DOM pool, as these tools usually require an isolation and concentration step prior to use. The options for isolation and concentration of DOM samples were recently reviewed with great detail (Minor et al., 2014).

1.4.2 Mass Spectrometry

Applications of mass spectrometry (MS) to DOM have been conducted for several decades (Manskaya and Drozdova, 1968; Schnitzer and Khan, 1978). In order to improve the resolution and selectivity, separation techniques were largely coupled to MS (e.g., Liquid chromatography (LC)-MS, Gas chromatography (GC)-MS, pyrolysis-GC-MS, and direct temperature (DT)-resolved MS) (Mopper et al., 2007). In general, only specific DOM fractions or components can be identified and quantified using MS, instead of the structure and composition of bulk DOM in natural systems (Manskaya and Drozdova, 1968; Mopper et al., 2007). Also, various ionization techniques (e.g., atmospheric pressure electrospray ionization, atmospheric pressure chemical ionization, matrix-assisted laser desorption/ionization) were combined with different mass analyzers (e.g., quadrupole ion trap and quadrupole time of flight). In light of the further combination with several extraction and pre-separation techniques (e.g., solid-phase extraction (SPE), ultrafiltration (UF), high-performance liquid chromatography (HPLC), and GC), the MS ionization techniques significantly improved selectivity and spectral interpretation. Such technical advances, in turn, greatly facilitated characterization of key components within previously unknown fraction of DOM (Mopper et al., 2007).

Although novel insights regarding specific DOM components have been gained following application of aforementioned MS techniques, characterization of DOM in highly complex systems was limited due to poor MS resolution (i.e., the ability of a mass spectrometer to distinguish between ions of two distinct mass-to-charge ratios) (Mopper et al., 2007). The introduction of the FT-ICR-MS in recent years has received much attention for the analysis of DOM. Generally, FT-ICR-MS is one of the techniques that can observe a vast array of individual DOM components (Minor et al., 2014). In most cases, DOM needs to be firstly isolated from the water samples (Minor et al., 2014). The significantly-high resolving power of FT-ICR-MS allows for the differentiation of masses of

several thousands of DOM compounds with small errors. For instance, errors in mass-to-charge ratio (m/z) for individual DOM components can reach < 0.5 ppm for components of ~400 Da (Minor et al., 2014). Meanwhile, it could assign empirical formulae including key heteroatoms of DOM such as N, S, and P, besides C, H, and O (McCallister, Ishikawa and Kothawala, 2018). Such information can be used for the categorization of DOM components. Sample preparation, peak assignment, and data interpretation are reviewed extensively by Mopper et al. (2007). In comparison to the Orbitrap MS, FT-ICR-MS generally provides much higher mass resolution. Differences between Orbitrap and FT-ICR-MS instruments also include the field applied (e.g., electrostatic field for Orbitraps and superconducting magnets for FT-ICR-MS).

1.4.3 Nuclear Magnetic Resonance

The presence of surrounding functional groups can influence the resonance frequency of atomic nuclei (commonly ^{1}H, ^{13}C, ^{15}N, or ^{31}P), inducing the shift in resonance frequency of a particular atom (McCallister, Ishikawa and Kothawala, 2018). Such mechanisms constitute the principle of NMR. More detailed reviews of NMR methodology and its applications to DOM characterization are elsewhere (Mopper et al., 2007; Hertkorn et al., 2013).

This technique is usually combined with FT-ICR-MS to provide a large picture of DOM composition, allowing an opportunity to reveal various molecular structures comprising DOM and their chemical reactivity (Hertkorn et al., 2013). Currently, there is also elevated interest in detailed molecular analysis of DOM after chromatographic separation, for instance, through HPLC-NMR (Simpson et al., 2004). It should also be mentioned that DOM needs to be isolated from samples and concentrated before NMR analysis, and inorganic ions must be removed (Minor et al., 2014).

1.4.4 Other Methods

Other methods for the structural characterization of DOM such as Fourier-transform infrared spectroscopy (FTIR) (Minor et al., 2014), natural abundance isotopic approaches (McCallister, Ishikawa and Kothawala, 2018), thermal analysis techniques (e.g., differential thermal analysis) (Plante, Fernández and Leifeld, 2009), and electron spin resonance spectroscopy (Paul et al., 2006) were also reported elsewhere.

1.5 FLOW-FIELD FLOW FRACTIONATION AND SIZE SEPARATION OF DISSOLVED ORGANIC MATTER

1.5.1 Introduction, Theory and Basic Principles

Field-flow fractionation (FFF) is a versatile separation technique. Its history can be traced back to the work of J. Calvin Giddings in the 1960s (Giddings, 1966). Following that, he and his colleges at the University of Utah integrated the principle and theory of FFF and developed a variety of FFF techniques (flow FFF, sedimentation FFF, thermal FFF, electrical FFF, and gravitational FFF). The basic theory of flow FFF was proposed in the 1970s (Giddings, Yang and Myers, 1976a; Giddings, Yang and Myers, 1976b; Wahlund et al., 1986), and the initial concept of AF4 (i.e., asymmetric channel) occurred in 1987 (Wahlund and Giddings, 1987).

To date, the instrumentation of flow-field flow fractionation (FlFFF) has matured (Podzimek, 2011), allowing a series of applications such as the separation of natural colloidal particles (Kammer, Baborowski and Friese, 2005; Baalousha et al., 2006; Cuss, Grant-Weaver and Shotyk, 2017), engineered nanoparticles (Mitrano et al., 2012; Montaño et al., 2019), proteins (Kim and Moon, 2009), and polymers (Wittgren et al., 1998; Ehrhart, Mingotaud and Violleau, 2011).

Theoretically, asymmetrical flow field-flow fractionation (AF4) is a chromatography-like

technique but without a stationary phase (Podzimek, 2011). The separation of particles in AF4 taking place in a thin empty channel is by channel flow (i.e., for migration of sample components) where a perpendicular cross-flow is applied to retard sample migration, and particles are separated following their hydrodynamic properties (Giddings, 1993). Also, AF4 takes great advantage of the diffusion features of particles. Small particles (smaller Stokes' diameter) are moved away from the accumulation wall with higher diffusion coefficients than that of large particles toward the channel center where the axial flow is faster. As such, small particles will be eluted earlier than large particles in a flowing stream characterized by parabolic flow profiles in the normal mode (i.e., Brownian separation) (Podzimek, 2011).

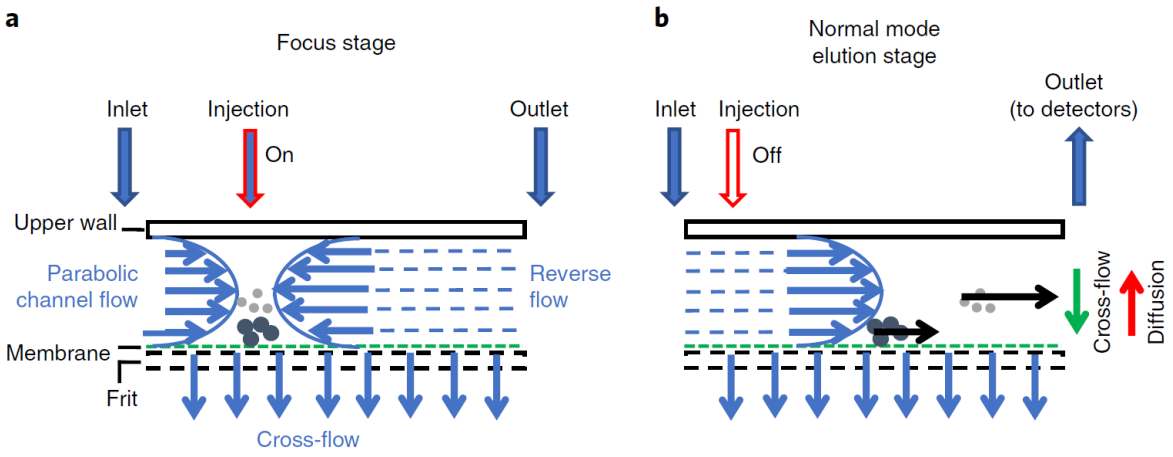

Figure 1-8 Schematic view of the AF4 separation principle adapted from *Figure 1* of Zhang and Lyden (2019). In detail, a and b denote side views of the AF4 channel with a height of several hundreds of micrometers (not to scale). The directions of all the arrowheads are the same as the flow direction. For cross-flow induced particle movement, the direction is represented by the fine green arrows; while the direction of particle movement due to their diffusion is indicated by the fine red arrows.

Generally, there are three steps in the AF4 analysis for size-based separation of particles, namely, injection, focusing, and elution (Podzimek, 2011). As shown in Figure 1-8 adapted from Zhang and Lyden (2019), in the focus stage (Figure 1-8a), inlet and outlet flows with opposing directions (fine blue arrows) are balanced to meet near the injection port. Meanwhile, the eluent (*carrier* in some literature) moves exclusively in cross direction, passes the permeable membrane, and exits from the channel. The injected samples will move along a thin band focused by the two opposing flows, prior to the elution mode (Figure 1-8b).

In the elution stage, a single direction of laminar flow from the inlet to the outlet can be produced, and particles with a smaller hydrodynamic size and higher diffusion coefficients will be eluted much earlier, while larger particles will be eluted later. For fundamental descriptions related to the theory and principles, instrumentation, and data processing, see Wahlund and Giddings (1987), Podzimek (2011), and the FFF handbook (Schimpf, Caldwell and Giddings, 2000).

1.5.2 Applications of Flow-Field Flow Fractionation to Dissolved Organic Matter

To date, a large body of literature has used FIFFF to characterize DOM quality from different perspectives, including the molar mass distribution (Hassellöv, 2005; Cuss and Guéguen, 2012; Zhou et al., 2016), the relationship between size and optical properties (Guéguen and Cuss, 2011; Cuss and Guéguen, 2015), variations of DOM composition as a function of size (Stolpe et al., 2010; Lin and Guo, 2020), etc. Such applications are of great significance for understanding the geochemical behavior of DOM in the environment.

For instance, Zhou et al. (2016) showed evidence of contrasting estuarine mixing of different size fractions of DOM by identifying its optical properties and size distribution using FIFFF coupled to optical detectors. The advance in DOM size characterization also allows the determination of the

distribution of trace elements as a function of size (Cuss, Grant-Weaver and Shotyk, 2017; Cuss et al., 2018; Worms et al., 2019).

Although optical detectors (absorbance and fluorescence) are usually coupled with FIFFF for providing optical composition of colloidal DOM, other instruments such as inductively coupled plasma mass spectrometry (ICP-MS) and high-resolution mass spectrometers can also be connected to provide elemental and isotopic analysis related to DOM properties (Stubbins et al., 2014; Cuss, Grant-Weaver and Shotyk, 2017).

1.6 OBJECTIVES

The objectives of the study were: 1) to determine the major sources of DOM from tributaries to a large boreal river, namely, the lower Athabasca River through size and optical properties in two different seasons (i.e., fall and spring); 2) to test if DOM properties can be used as *quasi*-conservative tracers of mixing processes in the river at/near confluences between tributaries and the main stem of the LAR.

1.7 REFERENCES

Ågren A., Buffam I., Berggren M., Bishop K., Jansson M. and Laudon H. (2008) Dissolved organic carbon characteristics in boreal streams in a forest-wetland gradient during the transition between winter and summer. *J. Geophys. Res.* **113**, G03031.

Ahrland S., Chatt J. and Davies N. R. (1958) The relative affinities of ligand atoms for acceptor molecules and ions. *Q. Rev. Chem. Soc.* **12**, 265.

Aitkenhead-Peterson J. A., McDowell W. H. and Neff J. C. (2003) 2 - Sources, Production, and Regulation of Allochthonous Dissolved Organic Matter Inputs to Surface Waters. In *Aquatic ecosystems* (eds. S. Findlay and R. L. Sinsabaugh). Academic Press. Amsterdam, London, pp. 25–70.

Andersson J.-O. and Nyberg L. (2008) Spatial variation of wetlands and flux of dissolved organic carbon in boreal headwater streams. *Hydrol. Process.* **22**, 1965–1975.

Aucour A.-M., Tao F.-X., Moreira-Turcq P., Seyler P., Sheppard S. and Benedetti M.F. (2003) The Amazon River: behaviour of metals (Fe, Al, Mn) and dissolved organic matter in the initial mixing at the Rio Negro/Solimões confluence. *Chem. Geol.* **197**, 271–285.

Baalousha M., Kammer F. V. D., Motelica-Heino M., Hilal H. S. and Le Coustumer P. (2006) Size fractionation and characterization of natural colloids by flow-field flow fractionation coupled to multi-angle laser light scattering. *J. Chromatogr. A* **1104**, 272–281.

Backes C. A. and Tipping E. (1987) An Evaluation of the Use of Cation-Exchange Resin for the Determination of Organically-Complexed Al in Natural Acid Waters. *Int. J. Environ. Anal. Chem.* **30**, 135–143.

Bauer J. E. and Bianchi T. S. (2011) 5.02 - Dissolved organic carbon cycling and transformation. In *Treatise on estuarine and coastal science* (eds. E. Wolanski and D. S. McLusky). Academic Press. London, Waltham, MA, pp. 7–67.

Bertilsson S. and Jones J. B. (2003) 1 - Supply of dissolved organic matter to aquatic ecosystems: autochthonous sources. In *Aquatic ecosystems* (eds. S. Findlay and R. L. Sinsabaugh). Academic Press. Amsterdam, London, pp. 3–24.

Bonan G. B. and Shugart H. H. (1989) Environmental factors and ecological processes in boreal forests. *Annu. Rev. Ecol. Syst.* **20**, 1–28.

Chanton J. P., Bauer J. E., Glaser P. A., Siegel D. I., Kelley C. A., Tyler S. C., Romanowicz E. H. and Lazrus A. (1995) Radiocarbon evidence for the substrates supporting methane formation within northern Minnesota peatlands. *Geochim. Cosmochim. Acta* **59**, 3663–3668.

Chanton J. P., Glaser P. H., Chasar L. S., Burdige D. J., Hines M. E., Siegel D. I., Tremblay L. B. and Cooper W. T. (2008) Radiocarbon evidence for the importance of surface vegetation on fermentation and methanogenesis in contrasting types of boreal peatlands. *Glob. Biogeochem. Cycle* **22**, GB4022.

Cuss C. W., Donner M. W., Grant-Weaver I., Noernberg T., Pelletier R., Sinnatamby R. N. and Shotyk W. (2018) Measuring the distribution of trace elements amongst dissolved colloidal species as a fingerprint for the contribution of tributaries to large boreal rivers. *Sci. Total Environ.* **642**, 1242–1251.

Cuss C. W., Ghotbizadeh M., Grant-Weaver I., Javed M. B., Noernberg T. and Shotyk W. (2020) Delayed mixing of iron-laden tributaries in large boreal rivers: implications for iron transport, water quality and monitoring. *J. Hydrol.*, 125747.

Cuss C. W., Grant-Weaver I. and Shotyk W. (2017) AF4-ICPMS with the 300 Da membrane to resolve metal-bearing “colloids” < 1 kDa: optimization, fractogram deconvolution, and advanced quality control. *Anal. Chem.* **89**, 8027–8035.

Cuss C. W. and Guéguen C. (2012) Determination of relative molecular weights of fluorescent components in dissolved organic matter using asymmetrical flow field-flow fractionation and parallel factor analysis. *Anal. Chim. Acta* **733**, 98–102.

Cuss C. W. and Guéguen C. (2015) Relationships between molecular weight and fluorescence properties for size-fractionated dissolved organic matter from fresh and aged sources. *Water Res.* **68**, 487–497.

D'Andrilli J., Chanton J. P., Glaser P. H. and Cooper W. T. (2010) Characterization of dissolved organic matter in northern peatland soil porewaters by ultra high resolution mass spectrometry. *Org. Geochem.* **41**, 791–799.

DeAngelis D. L. (2019) The boreal forest ecosystem. In *Encyclopedia of ecology* (eds. B. D. Fath and S. E. Jørgensen). Elsevier. Amsterdam, pp. 479–483.

Dillon P. J. and Molot L. A. (1997) Effect of landscape form on export of dissolved organic carbon, iron, and phosphorus from forested stream catchments. *Water Resour. Res.* **33**, 2591–2600.

Dittmar T. and Stubbins A. (2014) 12.6 - Dissolved organic matter in aquatic systems. In *Treatise on geochemistry* (eds. H. D. Holland and K. K. Turekian). Elsevier Ltd. Amsterdam, Netherlands, Oxford, England, Waltham, Massachusetts, pp. 125–156.

Ehrhart J., Mingotaud A.-F. and Violleau F. (2011) Asymmetrical flow field-flow fractionation with multi-angle light scattering and quasi elastic light scattering for characterization of poly(ethyleneglycol-b-ε-caprolactone) block copolymer self-assemblies used as drug carriers for photodynamic therapy. *J. Chromatogr. A* **1218**, 4249–4256.

Fellman J. B., Hood E., Edwards R. T. and Jones J. B. (2009) Uptake of allochthonous dissolved organic matter from soil and salmon in coastal temperate rainforest streams. *Ecosystems* **12**, 747–759.

Fellman J. B., Hood E. and Spencer R. G. M. (2010) Fluorescence spectroscopy opens new windows into dissolved organic matter dynamics in freshwater ecosystems: A review. *Limnol. Oceanogr.* **55**, 2452–2462.

Finlay J., Neff J., Zimov S., Davydova A. and Davydov S. (2006) Snowmelt dominance of dissolved organic carbon in high-latitude watersheds: Implications for characterization and flux of river DOC. *Geophys. Res. Lett.* **33**, L10401.

Fischer H., Sachse A., Steinberg C. E. W. and Pusch M. (2002) Differential retention and utilization of dissolved organic carbon by bacteria in river sediments. *Limnol. Oceanogr.* **47**, 1702–1711.

Florence T. M. (1986) Electrochemical approaches to trace element speciation in waters. A review. *Analyst* **111**, 489–505.

Florence T. M., Batley G. E. and Benes P. (1980) Chemical speciation in natural waters. *Crit. Rev. Anal. Chem.* **9**, 219–296.

Florence T. M., Morrison G. M. and Stauber J. L. (1992) Determination of trace element speciation and the role of speciation in aquatic toxicity. *Science of The Total Environment* **125**, 1–13.

Foreman C. M. and Covert J. S. (2003) 14 - Linkages between Dissolved Organic Matter Composition and Bacterial Community Structure. In *Aquatic ecosystems* (eds. S. Findlay and R. L. Sinsabaugh). Academic Press. Amsterdam, London, pp. 343–362.

Franke D., Hamilton M. W. and Ziegler S. E. (2012) Variation in the photochemical lability of dissolved organic matter in a large boreal watershed. *Aquat. Sci.* **74**, 751–768.

Gao H. and Zepp R. G. (1998) Factors Influencing Photoreactions of Dissolved Organic Matter in a Coastal River of the Southeastern United States. *Environ. Sci. Technol.* **32**, 2940–2946.

Giddings J. C. (1966) A new separation concept based on a coupling of concentration and flow nonuniformities. *Sep. Sci.* **1**, 123–125.

Giddings J. C. (1993) Field-flow fractionation: analysis of macromolecular, colloidal, and particulate materials. *Science* **260**, 1456–1465.

Giddings J. C., Yang F. J. and Myers M. N. (1976a) Flow-field-flow fractionation: a versatile new separation method. *Science* **193**, 1244–1245.

Giddings J. C., Yang F. J. and Myers M. N. (1976b) Theoretical and experimental characterization of flow field-flow fractionation. *Anal. Chem.* **48**, 1126–1132.

Gorham E. (1991) Northern Peatlands: Role in the Carbon Cycle and Probable Responses to Climatic Warming. *Ecol. Appl.* **1**, 182–195.

Guéguen C. and Cuss C. W. (2011) Characterization of aquatic dissolved organic matter by asymmetrical flow field-flow fractionation coupled to UV-Visible diode array and excitation emission matrix fluorescence. *J. Chromatogr. A* **1218**, 4188–4198.

Hansen A. M., Kraus T. E. C., Pellerin B. A., Fleck J. A., Downing B. D. and Bergamaschi B. A. (2016) Optical properties of dissolved organic matter (DOM): Effects of biological and photolytic degradation. *Limnol. Oceanogr.* **61**, 1015–1032.

Hassellöv M. (2005) Relative molar mass distributions of chromophoric colloidal organic matter in coastal seawater determined by Flow Field-Flow Fractionation with UV absorbance and fluorescence detection. *Mar. Chem.* **94**, 111–123.

Hertkorn N., Harir M., Koch B. P., Michalke B. and Schmitt-Kopplin P. (2013) High-field NMR spectroscopy and FTICR mass spectrometry: powerful discovery tools for the molecular level characterization of marine dissolved organic matter. *Biogeosciences* **10**, 1583–1624.

Hutchins R. H. S., Prairie Y. T. and del Giorgio P. A. (2019) Large-scale landscape drivers of CO_2, CH_4 , DOC, and DIC in boreal river networks. *Global Biogeochem. Cycles* **33**, 125–142.

Irving H. and Williams R. J. P. (1948) Order of Stability of Metal Complexes. *Nature* **162**, 746–747.

Kammer F. V. D., Baborowski M. and Friese K. (2005) Field-flow fractionation coupled to multi-

angle laser light scattering detectors: Applicability and analytical benefits for the analysis of environmental colloids. *Anal. Chim. Acta* **552**, 166–174.

Karlsson T. and Persson P. (2010) Coordination chemistry and hydrolysis of Fe(III) in a peat humic acid studied by X-ray absorption spectroscopy. *Geochim. Cosmochim. Acta* **74**, 30–40.

Kikuchi T., Fujii M., Terao K., Jiwei R., Lee Y. P. and Yoshimura C. (2017) Correlations between aromaticity of dissolved organic matter and trace metal concentrations in natural and effluent waters: A case study in the Sagami River Basin, Japan. *Sci. Total Environ.* **576**, 36–45.

Kim K. H. and Moon M. H. (2009) Development of a multilane channel system for nongel-based two-dimensional protein separations using isoelectric focusing and asymmetrical flow field-flow fractionation. *Anal. Chem.* **81**, 1715–1721.

Kothawala D. N., Ji X., Laudon H., Ågren A. M., Futter M. N., Köhler S. J. and Tranvik L. J. (2015) The relative influence of land cover, hydrology, and in‐stream processing on the composition of dissolved organic matter in boreal streams. *J. Geophys. Res.-Biogeosci.* **120**, 1491–1505.

Lambert T., Bouillon S., Darchambeau F., Massicotte P. and Borges A. V. (2016) Shift in the chemical composition of dissolved organic matter in the Congo River network. *Biogeosciences* **13**, 5405–5420.

Lapierre J.-F., Guillemette F., Berggren M. and del Giorgio P. A. (2013) Increases in terrestrially derived carbon stimulate organic carbon processing and CO_2 emissions in boreal aquatic ecosystems. *Nat. Commun.* **4**, 2972.

Laudon H., Buttle J., Carey S. K., McDonnell J., McGuire K., Seibert J., Shanley J., Soulsby C. and Tetzlaff D. (2012) Cross-regional prediction of long-term trajectory of stream water DOC response to climate change. *Geophys. Res. Lett.* **39**, L18404.

Lin H. and Guo L. (2020) Variations in colloidal DOM composition with molecular weight within individual water samples as characterized by flow field-flow fractionation and EEM-PARAFAC analysis. *Environ. Sci. Technol.* **54**, 1657–1667.

Manskaya S. M. and Drozdova T. V. (1968) *Geochemistry of Organic Substances.* Elsevier Science, Burlington.

McCallister S. L., Ishikawa N. F. and Kothawala D. N. (2018) Biogeochemical tools for characterizing organic carbon in inland aquatic ecosystems. *Limnol. Oceanogr. Lett.* **3**, 444–457.

McKnight D. M., Bencala K. E., Zellweger G. W., Aiken G. R., Feder G. L. and Thorn K. A. (1992) Sorption of dissolved organic carbon by hydrous aluminum and iron oxides occurring at the confluence of Deer Creek with the Snake River, Summit County, Colorado. *Environ. Sci. Technol.* **26**, 1388–1396.

Miller W. L. (1998) Effects of UV Radiation on Aquatic Humus: Photochemical Principles and Experimental Considerations. In *Aquatic Humic Substances* (eds. D. O. Hessen and L. J.

Tranvik). Springer Berlin Heidelberg. Berlin, Heidelberg, pp. 125–143.

Minor E. C., Swenson M. M., Mattson B. M. and Oyler A. R. (2014) Structural characterization of dissolved organic matter: a review of current techniques for isolation and analysis. *Environ. Sci.-Process Impacts* **16**, 2064–2079.

Mitrano D. M., Barber A., Bednar A., Westerhoff P., Higgins C. P. and Ranville J. F. (2012) Silver nanoparticle characterization using single particle ICP-MS (SP-ICP-MS) and asymmetrical flow field flow fractionation ICP-MS (AF4-ICP-MS). *J. Anal. At. Spectrom.* **27**, 1131.

Montaño M. D., Kammer F. von der, Cuss C. W. and Ranville J. F. (2019) Opportunities for examining the natural nanogeochemical environment using recent advances in nanoparticle analysis. *J. Anal. At. Spectrom.* **34**, 1768–1772.

Moody C. S. and Worrall F. (2017) Modeling rates of DOC degradation using DOM composition and hydroclimatic variables. *J. Geophys. Res.-Biogeosci.* **122**, 1175–1191.

Moore T. R. (2003) Dissolved organic carbon in a northern boreal landscape. *Global Biogeochem. Cycles* **17**, 1109.

Mopper K., Stubbins A., Ritchie J. D., Bialk H. M. and Hatcher P. G. (2007) Advanced instrumental approaches for characterization of marine dissolved organic matter: extraction techniques, mass spectrometry, and nuclear magnetic resonance spectroscopy. *Chem. Rev.* **107**, 419–442.

Moreira-Turcq P. F., Seyler P., Guyot J. L. and Etcheber H. (2003) Characteristics of organic matter in the mixing zone of the Rio Negro and Rio Solimões of the Amazon River. *Hydrol. Process.* **17**, 1393–1404.

Murphy K. R., Stedmon C. A., Graeber D. and Bro R. (2013) Fluorescence spectroscopy and multi-way techniques. PARAFAC. *Anal. Methods* **5**, 6557.

Murphy K. R., Stedmon C. A., Wenig P. and Bro R. (2014) OpenFluor– an online spectral library of auto-fluorescence by organic compounds in the environment. *Anal. Methods* **6**, 658–661.

Nieboer E. and Richardson D. H.S. (1980) The replacement of the nondescript term ‘heavy metals’ by a biologically and chemically significant classification of metal ions. *Environ. Pollut. Series B, Chemical and Physical* **1**, 3–26.

Nikolaou A. D. and Lekkas T. D. (2001) The role of natural organic matter during formation of chlorination by-products: a review. *Acta Hydrochim. Hydrobiol.* **29**, 63–77.

Oliver B. G., Thurman E. M. and Malcolm R. L. (1983) The contribution of humic substances to the acidity of colored natural waters. *Geochim. Cosmochim. Acta* **47**, 2031–2035.

Paquin P. R., Gorsuch J. W., Apte S., Batley G. E., Bowles K. C., Campbell P. G.C., Delos C. G., Di Toro D. M., Dwyer R. L., Galvez F., Gensemer R. W., Goss G. G., Hogstrand C., Janssen C. R., McGeer J. C., Naddy R. B., Playle R. C., Santore R. C., Schneider U., Stubblefield W. A.,

Wood C. M. and Wu K. B. (2002) The biotic ligand model: a historical overview. *Comp. Biochem. Physiol. C-Pharmacol. Toxicol. Endocrinol.* **133**, 3–35.

Parsons D. R., Best J. L., Lane S. N., Kostaschuk R. A., Hardy R. J., Orfeo O., Amsler M. L. and Szupiany R. N. (2008) Large River Channel Confluences. In *River confluences, tributaries, and the fluvial network* (eds. S. P. Rice, A. G. Roy and B. L. Rhoads). John Wiley & Sons, Ltd. Hoboken, N.J., pp. 73–91.

Paul A., Stösser R., Zehl A., Zwirnmann E., Vogt R. D. and Steinberg C. E. W. (2006) Nature and abundance of organic radicals in natural organic matter: effect of pH and irradiation. *Environ. Sci. Technol.* **40**, 5897–5903.

Pearson R. G. (1968a) Hard and soft acids and bases, HSAB, part 1: Fundamental principles. *J. Chem. Educ.* **45**, 581–587.

Pearson R. G. (1968b) Hard and soft acids and bases, HSAB, part II: Underlying theories. *J. Chem. Educ.* **45**, 643–648.

Perdue E. M. and Ritchie J. D. (2014) 7.8 - Dissolved organic matter in freshwaters. In *Treatise on geochemistry* (eds. H. D. Holland and K. K. Turekian). Elsevier Ltd. Amsterdam, Netherlands, Oxford, England, Waltham, Massachusetts, pp. 237–272.

Plante A. F., Fernández J. M. and Leifeld J. (2009) Application of thermal analysis techniques in soil science. *Geoderma* **153**, 1–10.

Podzimek S. (2011) Asymmetric flow field flow fractionation. In *Light scattering, size exclusion chromatography and asymmetric flow field flow fractionation* (ed. S. Podzimek). John Wiley & Sons, Ltd. Hoboken, New Jersey, pp. 259–305.

Schimpf M. E., Caldwell K. and Giddings J. C. (2000) *Field-flow fractionation handbook.* Wiley-Interscience, New York, Chichester.

Schnitzer M. and Khan S. U. (1978) *Soil Organic Matter.* Elsevier Science, Amsterdam.

Shotyk W. (1988) Review of the inorganic geochemistry of peats and peatland waters. *Earth-Sci. Rev.* **25**, 95–176.

Shotyk W., Bicalho B., Cuss C. W., Donner M. W., Grant-Weaver I., Haas-Neill S., Javed M. B., Krachler M., Noernberg T., Pelletier R. and Zaccone C. (2017) Trace metals in the dissolved fraction (<0.45μm) of the lower Athabasca River: Analytical challenges and environmental implications. *Sci. Total Environ.* **580**, 660–669.

Simon C., Osterholz H., Koschinsky A. and Dittmar T. (2019) Riverine mixing at the molecular scale – An ultrahigh-resolution mass spectrometry study on dissolved organic matter and selected metals in the Amazon confluence zone (Manaus, Brazil). *Org. Geochem.* **129**, 45–62.

Simpson A. J., Tseng L.-H., Simpson M. J., Spraul M., Braumann U., Kingery W. L., Kelleher B. P. and Hayes M. H. B. (2004) The application of LC-NMR and LC-SPE-NMR to compositional

studies of natural organic matter. *Analyst* **129**, 1216–1222.

Spencer R. G. M., Aiken G. R., Butler K. D., Dornblaser M. M., Striegl R. G. and Hernes P. J. (2009) Utilizing chromophoric dissolved organic matter measurements to derive export and reactivity of dissolved organic carbon exported to the Arctic Ocean: A case study of the Yukon River, Alaska. *Geophys. Res. Lett.* **36**, L06401.

Stedmon C. A. and Bro R. (2008) Characterizing dissolved organic matter fluorescence with parallel factor analysis: a tutorial. *Limnol. Oceanogr. Methods* **6**, 572–579.

Stolpe B., Guo L., Shiller A. M. and Hassellöv M. (2010) Size and composition of colloidal organic matter and trace elements in the Mississippi River, Pearl River and the northern Gulf of Mexico, as characterized by flow field-flow fractionation. *Mar. Chem.* **118**, 119–128.

Stubbins A., Lapierre J.-F., Berggren M., Prairie Y. T., Dittmar T. and del Giorgio P. A. (2014) What's in an EEM? Molecular signatures associated with dissolved organic fluorescence in boreal Canada. *Environ. Sci. Technol.* **48**, 10598–10606.

Sun C., Shotyk W., Cuss C. W., Donner M. W., Fennell J., Javed M., Noernberg T., Poesch M., Pelletier R., Sinnatamby N., Siddique T. and Martin J. W. (2017) Characterization of Naphthenic Acids and Other Dissolved Organics in Natural Water from the Athabasca Oil Sands Region, Canada. *Environ. Sci. Technol.* **51**, 9524–9532.

Tfaily M. M., Wilson R. M., Cooper W. T., Kostka J. E., Hanson P. and Chanton J. P. (2018) Vertical Stratification of Peat Pore Water Dissolved Organic Matter Composition in a Peat Bog in Northern Minnesota. *J. Geophys. Res. Biogeosci.* **123**, 479–494.

Thurman E. M. (1985) *Organic geochemistry of natural waters.* Springer Netherlands, Dordrecht.

Urbansky E. T. and Magnuson M. L. (2002) Analyzing drinking water for disinfection byproducts. *Anal. Chem.* **74**, 260A-267A.

Wahlund K. G. and Giddings J. C. (1987) Properties of an asymmetrical flow field-flow fractionation channel having one permeable wall. *Anal. Chem.* **59**, 1332–1339.

Wahlund K. G., Winegarner H. S., Caldwell K. D. and Giddings J. C. (1986) Improved flow field-flow fractionation system applied to water-soluble polymers: programming, outlet stream splitting, and flow optimization. *Anal. Chem.* **58**, 573–578.

Ward C. P. and Cory R. M. (2015) Chemical composition of dissolved organic matter draining permafrost soils. *Geochim. Cosmochim. Acta* **167**, 63–79.

Warren L. A. and Haack E. A. (2001) Biogeochemical controls on metal behaviour in freshwater environments. *Earth-Sci. Rev.* **54**, 261–320.

Wilson H. F. and Xenopoulos M. A. (2009) Effects of agricultural land use on the composition of fluvial dissolved organic matter. *Nat. Geosci.* **2**, 37–41.

Wittgren B., Borgström J., Piculell L. and Wahlund K.-G. (1998) Conformational change and aggregation of κ-carrageenan studied by flow field-flow fractionation and multiangle light scattering. *Biopolymers* **45**, 85–96.

Worms I. A. M., Chmiel H. E., Traber J., Tofield-Pasche N. and Slaveykova V. I. (2019) Dissolved organic matter and associated trace metal dynamics from river to lake, under ice-covered and ice-free conditions. *Environ. Sci. Technol.* **53**, 14134–14143.

Yamashita Y. and Jaffé R. (2008) Characterizing the interactions between trace metals and dissolved organic matter using excitation-emission matrix and parallel factor analysis. *Environ. Sci. Technol.* **42**, 7374–7379.

Yoon J.-H. and Chen T.-C. (2006) Maintenance of the boreal forest rainbelts during northern summer. *J. Climate* **19**, 1437–1449.

Zhang H. and Lyden D. (2019) Asymmetric-flow field-flow fractionation technology for exomere and small extracellular vesicle separation and characterization. *Nat. Protoc.* **14**, 1027–1053.

Zhang Y., Shotyk W., Zaccone C., Noernberg T., Pelletier R., Bicalho B., Froese D. G., Davies L. and Martin J. W. (2016) Airborne petcoke dust is a major source of polycyclic aromatic hydrocarbons in the Athabasca oil sands region. *Environ. Sci. Technol.* **50**, 1711–1720.

Zhou Z., Stolpe B., Guo L. and Shiller A. M. (2016) Colloidal size spectra, composition and estuarine mixing behavior of DOM in river and estuarine waters of the northern Gulf of Mexico. *Geochim. Cosmochim. Acta* **181**, 1–17.

2.0 VARIATIONS IN SIZE AND OPTICAL PROPERTIES OF DISSOLVED ORGANIC MATTER DURING MIXING AT LARGE RIVER CONFLUENCES: IMPLICATIONS FOR SOURCE DISCRIMINATION IN THE BOREAL ZONE

2.1 ABSTRACT

The functionality of dissolved organic matter (DOM) in natural waters depends on its size and composition. Identifying the sources and associated properties of DOM is vital to understand its effects on downstream ecosystems. River mixing has great potential to alter DOM quality, but its role in large boreal river confluences remains largely unknown, which limits our ability to realize the exact magnitude and composition of DOM eventually exported to the ocean.

Using asymmetrical flow field-flow fractionation (AF4) with offline excitation emission matrices (EEMs) measurements and parallel factor (PARAFAC) analysis, we found that inputs of DOM from the major tributaries shifted DOM quality in a typical large boreal river, namely, the lower Athabasca River (LAR). Flowing downstream, DOM tended to be higher in concentrations of dissolved organic carbon (DOC) and degrees of humification and aromaticity. Seasonal variations of DOM as a result of spring freshet were observed, during which times DOM tended to be higher in molecular mass (e.g., size) and richer in protein-like (i.e., tryptophan-like) relative to humic-like components. Source discrimination of DOM was more apparent under base flow conditions compared with the snowmelt period.

In addition, conservative mixing behaviors of DOM at river confluences were observed. Contrasting mixing patterns among mixing zones suggest that both hydrological conditions and river geomorphology affect mixing patterns of DOM between the LAR and its tributaries. Our results demonstrate that DOM could be used as a *quasi*-conservative tracer during mixing at large river confluences. Findings from this study will enhance our ability to determine sources of DOM and to distinguish trends of mixing between the mainstem and the tributaries for DOM-associated trace elements in the boreal zone.

2.2 INTRODUCTION

Rivers serve as the major routes by which water and nutrients reach the oceans (Battin et al., 2008; Allen and Pavelsky, 2018). Boreal river networks are closely coupled to organic-rich terrestrial systems (e.g., peatlands) (Shotyk, 1988; Yu et al., 2011), thus constituting a key component responsible for global carbon flows in the terrestrial-aquatic continuum (Hutchins, Prairie and del Giorgio, 2019; Gómez-Gener et al., 2020). Dissolved organic matter (DOM), a complex molecular mixture of degradation products and products of microbial synthesis (Kellerman et al., 2015; Zark and Dittmar, 2018), represents a major part of the carbon flow in fluvial systems. It plays significant roles in fueling aquatic food webs (Keil and Kirchman, 1991; Wetzel, 1992) and in regulating the acid-base balance (Oliver, Thurman and Malcolm, 1983), as well as fate, transport, and bioavailability of trace metals and organic pollutants (Hassett, 2006; Latch and McNeill, 2006; Aiken, Hsu-Kim and Ryan, 2011; Oleinikova et al., 2017; Worms et al., 2019). Metabolism of DOM in rivers also plays a large role in controlling the magnitude of carbon dioxide degassing to the atmosphere (Battin et al., 2008; Allen and Pavelsky, 2018). As such, unraveling sources and associated properties of DOM is of vital importance to better understand its effect on downstream ecosystems (Wilson and Xenopoulos, 2009; Spencer et al., 2014; Hemingway et al., 2019), with implications for the geochemical behavior of trace elements (TEs) in the boreal zone.

The functionality of DOM depends on its chemical reactivity, which is largely associated with its size and composition (Amon and Benner, 1996; Fellman, Hood and Spencer, 2010; Guéguen et al., 2012; Cuss and Guéguen, 2015; Kellerman et al., 2015; Zhou et al., 2016; Lin and Guo, 2020). The bulk DOM contains components with various sizes, among which colloidal organic matter constitutes a major part in freshwaters (Guéguen and Cuss, 2011; Zhou et al., 2016; Broder, Knorr and Biester, 2017). Given the colloidal nature of riverine DOM (e.g., small size and large specific

surface area), a vast array of functional groups of this active substance are potentially available to interact with TEs, regulating their fate, transport, and bioaccessibility in freshwaters (Roditi, Fisher and Sañudo-Wilhelmy, 2000; Cuss et al., 2018; Worms et al., 2019; Wang, Cuss and Shotyk, 2020). The size feature of colloidal DOM has also been linked to its source and composition (Cuss and Guéguen, 2015). For instance, aromatic structures and higher molecular weight dominate the chromophoric fraction of the DOM pool (CDOM) of terrestrial origin (e.g., lignin) in natural systems, while lower molecular weight compounds (e.g., carbohydrates and amino acids) constitute the majority of autochthonous DOM of algal and macrophyte origin (Fellman, Hood and Spencer, 2010; Guéguen and Cuss, 2011; Lee et al., 2018). Moreover, the utilization efficiency of DOM by microbes has been evaluated based on size properties (Amon and Benner, 1996). Altogether, it is apparent that the size properties of colloidal DOM should be well considered in order to provide key insights into the biogeochemical cycling of DOM in freshwaters.

Mixing phenomena occur in a variety of aquatic environments, such as river confluences or the estuaries connecting freshwater and marine systems (Parsons et al., 2008; Simon et al., 2019). To date, a large body of studies has been conducted on mixing in estuaries (Stedmon and Markager, 2003; Abdulla, Minor and Hatcher, 2010; Zhou et al., 2016), relative to fluvial systems (Lambert et al., 2016; Simon et al., 2019). At river confluences, the non-conservative behavior of DOM during flow mixing has been examined (Moreira-Turcq et al., 2003; Lambert et al., 2016), implying changes of DOM quality (Aucour et al., 2003; Simon et al., 2019). Geochemical processes responsible for such changes consist of sorption, release, flocculation/coagulation, and fractionation (McKnight et al., 1992; Aucour et al., 2003; Simon et al., 2019). Although studies on DOM during riverine mixing have been increasing (Simon et al., 2019), information on spatial and temporal variations in DOM quality at large river confluences (channels >100 m wide) remains scarce (Parsons et al., 2008; Simon et al., 2019). This lack of knowledge, to a great extent, limits the discrimination of sources of DOM

at regional and global scales. For instance, the quality of DOM sources may not persist downstream as a result of non-conservative mixing behavior at large river confluences (McKnight et al., 1992), which ultimately narrows our understanding of the evolution of DOM along the river continuum to the ocean.

Asymmetrical flow field-flow fractionation (AF4) is a versatile separation technique (Wahlund and Giddings, 1987). To date, the instrumentation of AF4 has matured (Podzimek, 2011), allowing a series of applications such as the separation of natural colloidal particles (Cuss, Grant-Weaver and Shotyk, 2017; Wang, Cuss and Shotyk, 2020), engineered nanoparticles (Mitrano et al., 2012; Wang, Cuss and Shotyk, 2020), proteins (Kim and Moon, 2009), and polymers (Ehrhart, Mingotaud and Violleau, 2011). When coupled to ultraviolet-visible (UV-Vis) absorbance and fluorescence spectroscopy, the continuous size spectra of DOM can be examined (Guéguen and Cuss, 2011; Zhou et al., 2016; Cuss and Guéguen, 2012a). Also, detailed mapping of the fluorescence properties produces excitation emission matrices (EEM), which can be connected to the size-fractionated fluorescent organic matter, providing in-depth information about its source, chemical reactivity, and diagenetic state (Guéguen and Cuss, 2011; Stubbins et al., 2014; Lin and Guo, 2020). Especially when the overlapping peaks in EEMs are decomposed into their underlying chemical components by a multi-way data analysis approach (parallel factor analysis, PARAFAC) (Stedmon and Bro, 2008; Cuss and Guéguen, 2012a; Murphy et al., 2013; Stubbins et al., 2014), a direct comparison can be made with those components commonly found in aquatic ecosystems worldwide (Murphy et al., 2014; Parr et al., 2014). Although the application of AF4 coupled with optical detectors for characterizing DOM properties in freshwaters has also been increasing (Cuss and Guéguen, 2015; Zhou et al., 2016; Lin and Guo, 2020), studies on variations of DOM during river mixing at large confluences are very scarce.

The objectives of the study were: 1) to determine the major sources of DOM from tributaries

to a large boreal river, namely, the lower Athabasca River (LAR) through size and optical properties in two different seasons (i.e., fall and spring); 2) to test if DOM properties can be used to as *quasi*-conservative tracers of mixing processes in the river at/near confluences between tributaries and the main stem of the LAR.

2.3 MATERIALS AND METHODS

2.3.1 Study Area

The Athabasca River originates from the glaciers of the Columbia Icefields in Jasper National Park and extends over 1,200 km before emptying into Lake Athabasca. From here, waters flow to the Mackenzie River and eventually reach the Arctic ocean. The LAR (i.e., lower Athabasca River), defined as the reach starting downstream of Fort McMurray flowing toward the mouth of the Athabasca River (Figure 2-1a), has received the lion's share of attention as a result of its complex hydrological and geochemical settings and concerns of potential contamination by metals and organic pollutants from the oil sands industry (Shotyk et al., 2017; Sun et al., 2017; Lima and Wrona, 2019). Tributaries of the LAR are characterized by elevated DOM largely due to their drainage basins (e.g., peatlands) (Guéguen et al., 2012; Cuss et al., 2018; Cuss et al., 2019). Delayed mixing between tributaries and the LAR has been observed, and the mixing zones coincide with the oil sands industry, potentially rendering source discrimination of DOM difficult (Cuss et al., 2020a). Spring freshet between April and June significantly contributes to the seasonal variability of the concentration of DOM, flow rate, and turbidity both in the LAR and its tributaries (Yi et al., 2015; Cuss et al., 2020b). Thus, the LAR serves as an ideal setting for tracking the sources and evolution of DOM from terrestrial landscapes to the receiving freshwater ecosystems under different hydrological regimes in the boreal zone.

2.3.2 Sample Collection

Given the annual hydrological cycle in the LAR (Figure S2-1), major inputs of DOM to the river are expected to be different between fall and spring. For instance, DOM inputs in fall are dominated by tributaries and groundwaters. In contrast, spring freshet exerts more influence in late May carrying a unique DOM fingerprint. Representative field campaigns occurred in the fall of 2018 (Sept. 25–Oct. 03) and spring of 2019 (May 14–18 and May 25–27) with 95 and 108 water samples taken at 49 and 52 sites, respectively. Sampling sites were designated along the LAR at five mainstem transects (e.g., T1–T5) each including samples from west, middle, and east (Figure 2-1a). Samples at each location were also collected at different water depths. Furthermore, sampling was conducted at the outlet of eight tributaries (e.g., Little Fishery R., LFR; McLean Creek, MLC; Beaver R., BR; Muskeg R., MUR; Mackay R., MKR; Ells R., ER; Tar R., TAR; and Pierre R., PR) (Figure 2-1a). Lastly, samples were obtained in three major mixing zones between the LAR and three other tributaries (i.e., Horse R., HR; Clearwater R., CL; and Steepbank R., SB) (see Figures 2-1b–f).

Exceptional quality control measures were taken for equipment cleaning and preparation, sample collection and analysis following Spencer and Coble (2014). Samples were collected via a peristaltic pump coupled with acid cleaned tubing, bottles, and syringes. Adequate purging was guaranteed to stabilize water quality measurements, and parameters were determined through a field multiparameter meter (YSI Pro Plus, Yellow Springs, OH, USA). The pH and electrical conductivity were determined at all sampling sites. Syringe filters (0.22 μm PTFE) and glass vials were rinsed using river water at each site prior to sample collection. Samples were immediately stored in dark and cool conditions with ice packs after collection and during transport until returning to the lab where they were kept refrigerated at 4 °C prior to analysis. Detailed information about general equipment preparation and water sample collection procedures can be found elsewhere (Cuss et al., 2019).

2.3.3 Analytical Methods

In this study, dissolved organic carbon (DOC) was quantified as the CO_2 produced during combustion following acid sparging (Shimadzu TOC-5000A, Kyoto, Japan). Major anions (Cl^- and SO_4^{2-}) and cations (Na^+, K^+, Mg^{2+}, Ca^{2+}) were determined by ion chromatography (Dionex ICS 2500, Sunnyvale, California, USA) and inductively coupled argon plasma optical emission spectrometer (Thermo Fisher Scientific iCAP 6300, Waltham, Massachusetts, USA), respectively. Fluorescence EEM spectra were measured in ratio (S/R) mode using an Agilent G1321B fluorescence detector (Agilent Technologies, Santa Clara, USA) (Cuss and Guéguen, 2015). Excitation-emission wavelength ranges were set as 220–450 nm and 280–550 nm with 1 nm and 5 nm intervals, respectively, and wavelengths were also calibrated following routine procedures (Cuss et al., 2019). The EEM of Milli-Q water was measured and subtracted on a daily basis to eliminate background noise and reduce scatter. Absorbance spectra were measured over a wavelength range of 200–640 nm using a diode array detector (Agilent G4212B, Agilent Technologies, Santa Clara, USA), and part of the spectra (220–550 nm) were used to correct for the inner-filtering effect (Kothawala et al., 2013).

2.3.4 Optical Indicators

A total of 203 filtered samples were analyzed for absorbance and fluorescence of DOM. Three distinct subsamples of each sample were injected and measured to minimize the noise-to-signal ratio for a robust PARAFAC model, and to improve the accuracy of measurement for fluorescence intensities (Cuss et al., 2019).

Fluorescence indices of the relative extent of humification (HIX) and autotrophic productivity (BIX) were calculated following Zsolnay et al. (1999) and Huguet et al. (2009). Elevated HIX values are related to high fluorescence emission at longer wavelengths, suggesting

greater contributions from complex molecules (Zsolnay et al., 1999). For BIX, recently produced DOM of autochthonous origin is characterized by values larger than 1. The fluorescence index (FIX) was determined to identify the relative contribution of terrestrial and microbial sources to the bulk DOM pool (McKnight et al., 2001).

The Napierian absorption coefficient at 254 nm (A_{254}) was selected to quantify the CDOM content (Ågren et al., 2008). Specific UV adsorption at 254 nm ($SUVA_{254}$), an indicator of DOM aromaticity, was calculated through normalizing A_{254} by DOC concentration (Weishaar et al., 2003). We also calculated the E2/E3 ratio (E2:E3) as the absorbance at 254 nm divided by that at 365 nm. Notably, E2:E3 ratios can not only serve as molecular weight proxies (Peuravuori and Pihlaja, 1997; Ågren et al., 2008), but also show correlations with the quantum yields of singlet oxygen ($^1O_2$) and hydrogen peroxide (H_2O_2) (Dalrymple, Carfagno and Sharpless, 2010), being a potentially valuable index to reflect the photo-degradability and photo-reactivity of DOC (Chow et al., 2013).

2.3.5 EEM-PARAFAC

The PARAFAC analysis was performed on Matlab R2017b (MathWorks) using a total of 664 EEMs (including 55 size-fractionated EEMs) after spectra correction with a combination of DOMFluor and drEEM toolboxes developed by Stedmon and Bro (2008) and Murphy et al. (2013), respectively. Before processing EEMs, Milli-Q water blanks were subtracted on a daily basis. Fluorescence intensities were also normalized to Raman units (r.u.) (Lawaetz and Stedmon, 2009). Excitation wavelengths <240 nm were removed due to a low noise-to-signal ratio. First and second Raman and Rayleigh scatter peaks were recognized and eliminated. Blank subtraction, Raman normalization, and scatter removal were performed via an elaborated EEM-Cut algorithm (Cuss and Guéguen, 2012b).

The PARAFAC model was constrained to non-negative values, and an eight-component

model was successfully derived (Figure 2-2 and Figure S2-2) and validated using split-half analysis (Figures S2-3 and S2-4) (Murphy et al., 2013). Random initialization was conducted to guarantee that the solution was not a local minimum (Stedmon and Bro, 2008). The fluorescence of each Ex/Em pair in EEMs was normalized to the corresponding DOC concentration of the sample, in favor of the subsequent principal component analysis (PCA) analysis to ascertain the actual trends of fluorescence variability (Korak et al., 2014; Burns et al., 2016). We also compared PARAFAC components via comPARAFAC (Parr et al., 2014), through which quantitative comparisons were conducted across up to 38 additional PARAFAC models using a modified Tucker's Congruence Coefficient (mTCC) (Table S2-1). Moreover, spectra of components were uploaded into the online spectral database (OpenFluor, https://openfluor.lablicate.com/) for quantitative matches with any set of published spectra in the database (Figure S2-5) (Murphy et al., 2014).

It is well-known that certain parameters like pH, ionic strength, and iron concentration could affect DOM fluorescence (Poulin, Ryan and Aiken, 2014; Zhang and He, 2015). Here we reasoned that these parameters would exert little influence on fluorescence measured in the study. First, the pH of samples from the LAR was similar (ranging from 8.0 to 8.7) and are unlikely to account for alteration of DOM quality (Guéguen et al., 2012). Besides, the ionic strengths of samples were not markedly different. Given the similar Fe:DOM ratio in the LAR and insensitivity of EEMs for PARAFAC modeling (Poulin, Ryan and Aiken, 2014), it was also considered that the alteration of DOM quality by Fe concentration would not be significant (Guéguen et al., 2012; Cuss et al., 2019).

2.3.6 Size Separation

Size-based separation of DOM was performed via a Postnova AF2000 Multiflow FFF fractionation system with a 300-Da (Dalton = atomic mass unit) polyethersulfone membrane (Postnova Analytics, Salt Lake City, Utah, USA), coupled to on-line diode array and fluorescence detectors (Agilent

Technologies G4212 DAD and G1321B FLD, Santa Clara, California, USA). This specific application of AF4 was originally developed by Guéguen and Cuss (2011), and was optimized and successfully applied elsewhere (Cuss and Guéguen, 2015; Cuss, Grant-Weaver and Shotyk, 2017; Cuss et al., 2018).

Briefly, the ionic strength and pH of the carrier fluid were adjusted to values similar to the physicochemical condition of the LAR (300 μS cm^{-1} and 8) using a buffer made from ultrapure $(NH_4)_2CO_3$ (Sigma-Aldrich, St. Louis, Missouri, USA) (Cuss et al., 2018), to provide an analysis of DOM quality based on *in situ* conditions (Montaño et al., 2019). A blank (e.g., eluent) was analyzed before each sample to minimize memory effects. In practice, the accumulation of DOM on/in membranes may change the accuracy of size measurements of DOM by AF4 (Cuss, Grant-Weaver and Shotyk, 2017), such that the relationship between retention time and the molecular mass at peak maximum of DOM for each fractogram (M_p) needs to be calibrated on a daily basis. A mixture of bromophenol blue (Sigma-Aldrich, St. Louis, Missouri, USA) and polystyrene-sulfonate Na salt standards (PSS-Polymer Standards Service-USA, Inc., Amherst, Massachusetts) was used to calibrate the channel over a range of 0.69–20.7 kDa (Cuss et al., 2018). The slope and intercept of the size calibration curve varied over the time course of measurement, with average values of (± 1 SD; standard deviation):

$$\log(t_R - t_0) = [0.574 \pm 0.019] \cdot \log(M) - [1.479 \pm 0.064], \quad R^2 = 0.998 \pm 0.002 \qquad (1),$$

for $n = 24$ calibrations, void time t_0, retention time t_R, and molecular mass M. Also, M_p was calculated using the average slope and intercept of the two calibration curves that bracketed every alternating series of ten samples and blanks. Some DOM moieties may not absorb light, so that A_{254} serves only as a proxy for DOM, suitable for estimating its size properties (Wang, Cuss and Shotyk, 2020). Detailed information for AF4 instrumentation (e.g., flow program), analytical conditions, quality control, and optimization steps can be found elsewhere (Cuss, Grant-Weaver and Shotyk, 2017).

2.3.7 Data Analysis

Spearman's rank order correlation was applied to DOM quality measurements (DOC concentration, M_p, BIX, HIX, FIX, A_{254}, E2:E3, $SUVA_{254}$, and PARAFAC components C1–C8) separately for samples from mainstem and tributaries, and mixing zones, in OriginPro 2020b (OriginLab Corporation, Northampton, Massachusetts, USA). Data transformations were used to ensure that the distribution of each variable was normally distributed, including the log transformation for DOC, A_{254}, C1, C2, C5 and C7 and cubic root transformation for C8. Outliers and normality tests were performed using Grubb's test and the Kolmogorov–Smirnov test at significance levels of 0.05 and 0.001, respectively. Principal component analysis was applied to each data subset in OriginPro 2020b. Three and 2 outliers were detected for the mainstem and tributaries, and mixing zone data sets, respectively; however, these values reflected correct measurements and natural levels of variation in the system. Further testing also revealed that these values exerted little influence on both the variation explained by, and the loadings of most principal components (PCs). Hence, these values were included in the Spearman's correlation and PCA analyses.

2.4 RESULTS

2.4.1 Concentration, Size and Optical Properties of DOM

Tables 2-1 and 2-2 provide statistical data about DOM quality indicators in mainstem transects (T1–T5) and key tributaries of the LAR, respectively. The spectra of 8 PARAFAC-derived fluorescent components were characterized as six humic-like (C1–C6) and two protein-like (C7, C8) (see Figure 2-2 and Figure S2-2), with their potential sources, molecular association, and reactivity summarized in Table 2-3. Quantitative comparisons of components via comPARAFAC revealed that, except for C8, the rest exactly matched (i.e., mTCC > 0.95) those from previous studies (Table S2-1). In

addition, results from OpenFluor showed that C6 did not match any of the published models in the online database (Figure S2-5).

2.4.2 DOM in the LAR and Its Tributaries

The first three PCs were selected for PCA analysis based on the scree plot (Figure S2-6a), accounting for 86.8% of the total variance (Figure 2-3). The first PC (PC1) is largely driven by the majority of variables (e.g., C1–C6, A_{254}, DOC, $SUVA_{254}$, and E2:E3) (Figures 2-3c–d). Along PC1, scores of mainstem samples from fall and spring were differentiated (Figures 2-3a–b), and scores of tributaries were separated from those of mainstem samples in the fall (Figures 2-3e–f). Taken together, PC1 was largely representative for both seasonal and source-based variations in DOM quality. The second PC (PC2) was mainly controlled by BIX, C7, C8 and HIX (Figure 2-3c). Spatial variations (e.g., T1–T5) in DOM quality in the LAR in both seasons were, to a large extent, indicated on the 2D space of PC1 and PC2 (Figures 2-3e–g).

Given the geographical setting of major tributaries (e.g., HR and CL) located downstream of T1 and eastside of the LAR (Figure 2-1a), it was supposed that at least DOM in T1 and the west of T2 would be distinct from the others. Such a pattern was especially obvious in the fall where scores of samples from T1 and west of T2 were well separated from those of the rest (Figure 2-3e). Indeed, there was a clear gradient of scores at T2 running from the east side close to CL, through the middle, over to the west side in the fall, clustered with T1 (Figure 2-3e, from the lower right-hand side to the upper left-hand side). The scores of samples collected from the west side of T3 were also clustered nearer to these other samples compared to the east side and middle, where scores of samples plotted largely close to those of the east side of T2. For downstream sites T4 and T5, scores of samples were largely grouped together halfway between those of CL and T1 (Figure 2-3e). In addition, scores of

tributaries (ER, MUR, CL, TAR, and PR) plotted close to those of the mainstem, and specifically the score of CL was close to those of T2 (east) and T3 (east and middle).

In the spring, scores of samples from T1 were still largely clustered (on PC1 and PC2), and scores for samples from the west of T2 were also well separated from those of the middle and east on PC2 (Figure 2-3g). Notably, the score cluster of samples from the west side of T2 largely deviated from those of T1 in spring in contrast to the fall. Scores for samples from T3, T4, and T5 were more spread out on PC1 and PC2, without any apparent organization from east to west or upstream to downstream. Scores of most tributary samples were separated from those of the mainstem, with three exceptions: ER, MUR, and CL (Figure 2-3g). Also, the score of CL was much closer to those of the east and middle sides of T2 relative to the west.

The third PC (PC3) was strongly controlled by FIX, M_p and $SUVA_{254}$ (Figure 2-3d), where scores of mainstem samples in the fall and spring were largely clustered and scores of tributary samples in different seasons were largely differentiated, with the exception of CL which was clustered with the mainstem samples (Figures 2-3b, 2-3f, 2-3h). Figure 2-4 shows correlations between the concentration of DOC, and the size and optical properties of DOM.

2.4.3 DOM in Mixing Zones

The first two PCs were selected for PCA analysis based on the scree plot (Figure S2-6b), accounting for 79.5% of the total variance (Figure 2-5). Scores on PC1 largely distinguished samples from different mixing transects in both the fall and the spring (Figures 2-5c–d). An exception was that scores from samples collected along AR-HR in the spring were largely separated on PC2 (Figure 2-5d). Spatial variations in DOM quality in mixing zones (i.e., PC1) were strongly controlled by C1–C6, DOC, A_{254}, $SUVA_{254}$, BIX, E2:E3, and FIX (Figure 2-5b). The variability in scores of DOM quality in the fall and spring were largely separated on PC2 relative to PC1 (Figure 2-5a). Seasonal

variability (i.e., PC2) was driven to a great extent by C7–C8, M_p, BIX, and HIX (Figure 2-5b), which were higher in the spring compared to the fall. Figure 2-6 shows correlations between DOC concentration, size, and optical indices for mixing zones.

In the fall, scores of samples from different sides of mixing transects were well differentiated (e.g., AR-CL and CL-CL, and AR-HR and HR-HR), except that the clusters of scores from AR-SB and SB-SB were partially overlapping (Figure 2-5c). At the mainstem side, scores of AR-CL samples were largely mixed with the score cluster of AR-HR. Also, scores of samples at the end of the CL mixing zone (e.g., AR-CL05) were mixed with AR-SB samples (e.g., AR-SB02). Scores of AR-SB samples were located close to scores of CL-CL samples. Notably, scores of AR-CL showed progressive changes during mixing (on PC1 and PC2, except for samples on AR-CL02). At the tributary side, the score clusters from CL-CL and the majority of SB-SB (except for the SB-SB01 sample) were grouped together on PC1. Also, scores of HR-HR were well separated from those of CL-CL and SB-SB and showed progressive changes during mixing, becoming more similar to the LAR side of the mixing transects.

In the spring, the differentiation of scores of samples at different sides of the mixing zone was not as clear as in fall (Figure 2-5d). Scores of samples from different sides of HR and SB mixing zones were differentiated to a large extent, respectively, while the clusters of scores from AR-CL and CL-CL were overlapping. At the mainstem side, scores of AR-HR partially mixed with those of AR-CL and AR-SB (Figure 2-5d). The distribution of scores of AR-HR was heterogeneous and no progressive pattern during mixing was observed. Scores of AR-CL were largely mixed with those of AR-SB and partially mixed with those of HR-HR and SB-SB. The majority of scores of AR-SB was located close to those of CL-CL and those scores were also partially mixed with those of HR-HR. At the tributary side, scores of HR-HR samples were mixed with those of SB-SB. Also, scores of both HR-HR and SB-SB were largely separated from those of CL-CL (Figure 2-5d). Notably, the scores

of HR-HR changed progressively during mixing (e.g., PC1), becoming more similar to the LAR side of the mixing transects. In contrast, the changing pattern of scores of SB-SB was not progressive during mixing relative to that of HR-HR.

2.5 DISCUSSION

2.5.1 DOM Sources During Base Flow

Our results reveal that DOM quality along the LAR shifted significantly during base flow and the snowmelt period (Figure 2-3). To examine probable DOM inputs (e.g., tributaries and groundwaters), we first studied variations in DOM quality in the fall, in the absence of the influence of snowmelt.

2.5.1.1 Upstream of Industry

At T1, DOM quality was largely uniform among different locations (west, middle, and east) (Figure 2-3e), suggesting that the river was well mixed at this transect. The exception to this trend occurred at the surface (i.e., 0.3/0.9 m) of the west side, which was characterized with lower DOC-normalized concentrations of C1–C8 and M_p (0.93 ± 0.009 kDa, 95% CI) and higher FIX (1.56) compared with other sites (M_p: 1.03 ± 0.0001 to 1.11 ± 0.01 kDa, 95% CI; FIX: 1.49 ± 0.02). Moving downstream to T2, the DOM on the west side shared similar size and optical properties to those of T1 (Figure 2-3e), highlighting the conservative behavior of DOM (i.e., a negligible chemical modification of DOM composition) during long-distance transport (e.g., ~20 km on the west side) (Stedmon and Markager, 2003; Holmes et al., 2008; Wickland et al., 2012). Besides, from the west to the east, the concentration of DOC, degree of humification, CDOM (A_{254}), DOC-normalized concentrations of C1–C6 (i.e., humic-like), and aromaticity increased (Figures 2-3c, 2-3e), but the proportion of fresh DOM (BIX) decreased. This trend points to inputs of allochthonous DOM from DOM-rich tributaries

(e.g., Horse R. and Clearwater R.) at the east side of the river (Figure 2-1a) (Yi et al., 2015; Cuss et al., 2018; Cuss et al., 2019). This is expected given that DOM in these tributaries is contributed from catchments that are dominated by wetlands where DOM experiences significant transformations as a result of processes such as humification (Chanton et al., 2008; Guéguen et al., 2012; Cuss et al., 2019). Based on other findings for wetlands, it is expected that this DOM is characterized by a high aromatic carbon pool dominated by inputs of plant-derived polysaccharides such as cellulose and phenolic compounds from lignin (Gorham, 1991; Battin, 1998; D'Andrilli et al., 2010). In addition, the score of the CL sample was more similar to those of the east side at T2 relative to that of the HR, which deviated most from the cluster (Figure 2-3e). Such a pattern indicates that DOM from the Horse R. had properties that were very distinct from transect T1 and the west side of transect T2. Interestingly, the DOM quality in the middle of T2 was different from both the west and east sides, possibly suggesting the evolution of DOM during the mixing of the tributaries and the mainstem (Cuss et al., 2020a).

2.5.1.2 Midstream

Flowing downstream to T3, similar to T2, scores from samples collected from the west side were well separated from those of the middle and east (Figure 2-3e). The quality of DOM on the west at T3 also exhibited great similarity to that of the middle of T2, but largely deviated from the west of T2. Such patterns suggest that dispersion of DOM from the middle of T2 partially masked the original DOM quality on the west within a short distance (e.g., ~17 km) (Figure 2-1a). In the meantime, the quality of DOM in the east and middle sides of T3 resembled that of the east of T2, indicating the negligible role of MLC (at the east side of the LAR between T2 and T3, see Figure 2-1a) in altering DOM quality, and the delayed mixing behavior of HR and CL along the river (Stedmon and Markager, 2003; Cuss et al., 2020a). One exception to the middle and east cluster occurred at

depth (i.e., 0.6/0.9 m) on the east, characterized by especially lower DOC-normalized concentrations of C1–C6 relative to others (Figure 2-3d), indicating the heterogeneity of DOM quality with depth at the east side.

2.5.1.3 Downstream of Industry

Moving downstream of industry, samples from T4 had similar DOM composition to those from T5, except one sample (i.e., 0.3/3.5 m) from the west, which was separated from the others (Figure 2-3e). This surface sample tended to have more terrestrial DOM fingerprints indicated by elevated HIX and lower BIX (Figure 2-3g), but was characterized by lower fluorescence intensities on C1–C8, suggesting a unique local DOM source with properties similar to CL, but having minimal influence on downstream DOM quality (e.g., T5) (Figure 2-3e). Altogether, DOM downstream (e.g., T4 and T5) was characterized by higher concentrations of DOC, greater DOC-normalized concentrations of C1–C6, and greater degrees of humification and aromaticity compared with that of upstream (e.g., T1) (Figure 2-3c). Taken together, these changes reflect the significant impact of terrestrial DOM inputs from wetlands by tributaries on DOM quality downstream (Yi et al., 2015; Cuss et al., 2019).

2.5.1.4 Natural vs. Industrial Inputs

The DOM quality along and across the river became increasingly similar to tributaries from upstream to downstream. Specifically, the Clearwater R. (flow rate: ~130 m^3 s^{-1}) contributed a unique DOM fingerprint to the LAR which ultimately changed the nature of DOM on the river compared to DOM pool (e.g., low aromaticity) from upstream (Figure 2-3e) (Guéguen et al., 2012). Also, the Ells, Pierre and Tar Rivers were much closer to those of T4 and T5, suggesting a probable DOM source downstream of industrial operations.

The scores from Beaver R. and McLean Creek, which flow through the operational areas for

the oil sands industry, were grouped together far away from those of the mainstem and the other tributaries (Figure 2-3e), indicating unique DOM quality. This conclusion is consistent with the findings of Sun et al. (2017), who claimed that the naphthenic acids in Beaver R. and McLean Creek had a relatively similar composition to oil sands process-affected water (OSPW) and other natural bitumen-impacted waters, distinguishing them from other tributaries. Given recent advances in disentangling organic fingerprints for natural bitumen impacted groundwater and OSPW (Ahad et al., 2020; Hewitt et al., 2020), additional study is needed for a clear understanding of dominant sources of DOM in Beaver R. and McLean Creek in order to assess the potential influence of the oil sands industry on the local water quality.

Cuss et al. (2019) found that both saline and non-saline groundwaters were marked by a high proportion of protein-like fluorescent components, likely coming from autochthonous DOM sources (e.g., algae and microorganisms) (Osburn et al., 2011; Coble et al., 2014). Although groundwater samples were not studied here, the trend of DOM towards a more humified composition from upstream to downstream suggests that groundwater inputs were not a major source of DOM in the LAR (Figure 2-3e).

2.5.2 Snowmelt and Its Effect on DOM Quality

2.5.2.1 Changes in DOM Quality from Fall to Spring

In addition to spatial variations in DOM quality observed under baseflow condition, a large difference in DOM quality between fall base flow conditions and the period following spring snowmelt was observed (Figure 2-3a). The spring freshet serves as a main hydrological regime in the annual water cycle of the LAR (Figure S2-1) (Woo and Thorne, 2003; Yi et al., 2015), and generally results in an annual flushing and carries a unique DOM fingerprint in boreal rivers (Ågren et al., 2008; Cao et al., 2016). The T1 site was valuable to compare changes in DOM quality in the

mainstem that were driven by snowmelt with those in fall, before the introduction of DOM from tributaries (e.g., LFR, HR, and CLR) and potential influences from industry downstream. Elevated concentrations of DOC were observed in the late part of the snowmelt period (Table 2-1), which was consistent to previous studies (Findlay and Sinsabaugh, 2003; Avagyan et al., 2016). Given that snow normally contains very low concentrations of DOC (Wallis, Hynes and Telang, 1981; Yi et al., 2015), the elevated levels of DOC could be responsible by erosion of organic materials (e.g., leaf leachates) in the upper shallow organic-rich surface layer of soils from wetlands and boreal forests upstream of the LAR during the late spring freshet (O'Donnell et al., 2010; Wickland et al., 2012; Cade-Menun et al., 2013; Yi et al., 2015; Cuss et al., 2019).

The molecular mass (i.e., size) of DOM and degree of aromaticity (e.g., $SUVA_{254}$) were higher in spring compared to the fall, suggesting that additional terrestrial DOM (i.e., high molecular weight aromatic carbon) was transported into the river during spring freshet (Miller and McKnight, 2010; Mann et al., 2012; Wickland et al., 2012; Walker, Amon and Stedmon, 2013; Burns et al., 2016). In addition, the lower BIX values in spring samples suggest decreased contribution from recently produced DOM of microbial origin (Parlanti et al., 2000; Wilson and Xenopoulos, 2009). It should be noted that in the peatlands, decomposition of OM is thought to be limited due largely to low activity of the enzyme phenol oxidase led by the absence of oxygen, thus resulting in high levels of high molecular weight (HMW) DOM in shallow layers of *Sphagnum*-dominated peatlands (Chanton et al., 2008; D'Andrilli et al., 2010; Ward and Cory, 2015). The DOC-normalized Fmax values of all PARAFAC components (C1–C8) were lower in the fall compared to the spring (Figure 2-3c), consistent with the findings of Walker, Amon and Stedmon (2013). It should be noted that the extent of the increase of C7 and C8 (e.g., ~2–5 times) between fall and spring was much higher than that of C1–C6 (e.g., ~1.5–2.5 times). It was supposed that the increase of C1–C6 indicates terrestrial DOM input as soils richer in humic-like components are flushed into rivers during spring freshet,

while that of protein-like components (C7 and C8) could be largely attributed to ice melt occurring upstream of the LAR, wherein DOM fluorescence is dominantly protein-like (Hood et al., 2009; Mann et al., 2012). The increase of C7 and C8 could also result from the long residence time and increased microbial processing of DOM during transport of snowmelt into the river (Striegl et al., 2005; Mann et al., 2012). It is unlikely that snow contributed such DOM fingerprints in the LAR as was reported by Yi et al. (2015), who showed distinct DOM composition between snow and surface waters in the Athabasca oil sands region using electrospray ionization Fourier transform ion cyclotron resonance mass spectrometry. Additionally, the absence of tyrosine-like fluorophores in this period could be explained by its rapid biogeochemical transformation or physical mixing with other OM pools within the stream channel which masks its spectral signature (Barker et al., 2013).

2.5.2.2. Spatial Variations in DOM Quality

During the late snowmelt period, variation of DOM quality along the river could also be tracked (e.g., T1–T2, see Figures 2-3e, 2-3f). Similar to the fall, DOM quality at the T1 site was largely uniform across the transect, and was also distinct from other mainstem sites (Figure 2-3e). From T1 to the east side and middle at T2, DOM quality changed significantly (Figure 2-3e), and was generally characterized by elevated DOC, CDOM content (i.e., A_{254}), C1–C4 and C6 intensities, but lower BIX and microbial humic-like C5 (Figure 2-3c). Similar to the fall, this pattern was reflective of the dominant role of tributary inputs in altering DOM quality. Besides, the HIX increased in the east and middle sides of T2, but decreased on the west. Thus, tributary inputs dominated changes of DOM quality largely on the east and middle sides at T2. Also, the PARAFAC-derived components (e.g., C7 and C8) increased significantly from T1 to T2 on the west side and showed a significantly negative correlation to HIX ($p < 0.001$, see Figure 2-4). Given that C8 was previously found in recycled water treatment plants (Figure S2-6) (Murphy et al., 2011), it was speculated that a unique

DOM source of microbial origin (e.g., Fort McMurray wastewater treatment plant) upstream from T2 on the west may have a local impact on DOM quality.

Molecular mass increased significantly on the middle and west sides (i.e., ~0.10 kDa) from T1 to T2 relative to that of the east (i.e., similar values) (Figure 2-3e). Moreover, A_{254} increased more (i.e., ~10 m^{-1}) on the middle and west sides, and less (~5 m^{-1}) at the east. The average molecular mass and A_{254} at T1 were 1.26 ± 0.03 kDa and 29.8 ± 0.3 m^{-1}, respectively, similar to those of the CL (e.g., 1.21 ± 0.05 kDa and 33.0 m^{-1}, respectively). However, molecular mass and A_{254} at the HR were 1.33 ± 0.05 kDa and 70.0 m^{-1}, respectively. As such, it seems that the HR plays a larger role in altering DOM quality on the middle and west sides of T2 in spring through riverine mixing processes relative to the CL, although the influence of the wastewater treatment plant could not be well resolved at this stage. It is unlikely that tributary upstream of T2 on the west side (e.g., LFR, see Figure 2-1) is responsible for such patterns due to its similar M_p (i.e., 1.23 ± 0.05 kDa) to that of the T1. Taken together, we reasoned that HR input probably dominated DOM quality at the middle and west sides of T2 in spring, while CL temporarily exerted more influence on the east side. Lastly, scores of the middle and west sides of T2 were mixed with those of T3–T5 where no apparent organization of DOM quality indicators from east to west or upstream to downstream was observed, likely due to the overwhelming effect of snowmelt in the LAR (Yi et al., 2015).

2.5.3. Behavior of DOM in Mixing Zones

In this study, the properties and behaviors of DOM in mixing zones at river confluences were investigated to provide novel insights for source discrimination of DOM. In the fall, our data clearly showed changing patterns of DOM along the LAR as a result of tributary inputs via mixing processes (Figure 2-5c). Generally, DOM at the AR-HR largely shared similar properties, reflective of conservative transport of DOM in the LAR. At the HR-HR side, progressive changes of DOM along

the river were examined. The samples of HR-HR were collected over a distance of < 5 km before merging with the CL outflow, which does not allow much time for degradation or adsorption processes (Moreira-Turcq et al., 2003; Mann et al., 2012; Walker, Amon and Stedmon, 2013). Therefore, we reason that DOM variations at the HR-HR side were largely a result of physical mixing processes along the shoreline (e.g., dilution) (Cuss et al., 2020a), thus highlighting that DOM can be used as a *quasi*-conservative tracer during mixing processes over short distances in the LAR (Jiang et al., 2017). Notably, contrasting mixing patterns of DOM were found between the CL and HR mixing transects. That is, changes of DOM quality were mainly found in the AR-CL side instead of the tributary side (e.g., CL-CL), roughly following the order of AR01-CL, AR03-CL, AR04-CL, AR02-CL, and AR05-CL as they moved downstream (Figure 2-5c).

Generally, the bed height discordance was greater at HR (i.e., the depth at inflow was shallower than the LAR at HR, but it was the same or deeper at the CL). Also, the volumetric flow at HR was lower, so that upwelling from the LAR underneath the HR inflow caused faster mixing at the shore compared to the CL (Rutherford, 1994; Gaudet and Roy, 1995; Parsons et al., 2008). Moreover, the CL likely had a primarily "vertical shear layer" because the influx from the CL and its associated depth were sufficient to penetrate far enough into the LAR. As such, the shear forces that are caused by friction with the banks of the river were dispersed at the shear layer between the LAR and the CL (Rutherford, 1994; Parsons et al., 2008). These underlying mechanisms that cause delayed mixing are responsible for the contrasting patterns of mixing zones between the CL and HR mixing transects (Cuss et al., 2020a). Along the mainstem side of AR-SB mixing zone, DOM quality was highly heterogeneous. However, at the SB-SB side, SB-SB01 was well separated from the others, suggesting a faster mixing rate between SB and the LAR relative to that of HR, which could be attributed to the high junction angle between the SB and the mainstem (Parsons et al., 2008).

During the period following snowmelt, mixing patterns differed from those in fall.

Specifically, no apparently progressive changes of DOM along the AR-CL or CL-CL mixing transects was observed possibly due to the occurrence of more turbulence in the spring compared with fall. Similar to the fall, DOM quality changed progressively at the HR-HR side with an order of HR01-HR, HR02-HR, HR04-HR, HR05-HR, and HR03-HR. The patterns of DOM at the AR-HR were heterogeneous. For the AR-SB mixing zone, DOM quality at the mainstem side was relatively uniform, but the SB-SB side was not. A general trend could be roughly derived as DOM quality changed towards that of the mainstem as sample at the end of the SB-SB side resembled that of the mainstem, suggesting the progressive dilution of SB by the LAR along the bank from upstream to downstream. Interestingly, given that SB is shallow and the flow is relatively low, similar mixing behavior as the HR is expected in the spring (Parsons et al., 2008). Taken together, we highlight that hydrological conditions (e.g., spring freshet) and river geomorphology collectively affect *quasi*-conservative mixing patterns of DOM between the LAR and its tributaries, thus exerting influences on downstream water quality (Parsons et al., 2008; Lynch et al., 2019).

2.5.4. Implications for Carbon-Cycle and Trace Element Geochemistry

Boreal systems play a key role in the global carbon cycle and are experiencing rapid changes as a result of climate change (e.g., rising temperatures). Examining key factors regulating the variability of DOM in this biome would thus strengthen our ability to predict the transformations and associated changes in roles of DOM in these complex fluvial networks (Hutchins, Prairie and del Giorgio, 2019; Gómez-Gener et al., 2020). There are several drivers affecting DOM in the LAR. Under base flow conditions, DOM quality shifts progressively toward that of major tributaries (e.g., CL) in the LAR. Given that watersheds draining these tributaries (e.g., CL) are dominated by wetlands (Cuss et al., 2018), such variations highlight the importance of wetlands in altering DOM at the regional scale. Our results are consistent with previous work, which demonstrates that terrestrially derived DOM

dominates boreal rivers relative to DOM from aquatic organisms (Schumacher et al., 2006; Wilson and Xenopoulos, 2009; Hutchins, Prairie and del Giorgio, 2019). Altogether, these reflect the collective influence of surrounding soils, wetlands, regional vegetation, and climate.

Tributaries in the LAR drain a large area of peatlands where large amounts of aromatic DOM can be leached (Khadka, Munir and Strack, 2016). Export of DOM largely depends on annual runoff, potentially making waterborne release pathways a key driver of downstream carbon pool and composition (Michaelson et al., 1998; Jager, Wilmking and Kukkonen, 2009; Walker, Amon and Stedmon, 2013; Broder, Knorr and Biester, 2017). Conservative mixing and transport are suggested by the concentration and DOM quality gradients in this study, potentially strengthening our ability to distinguish trends of mixing between the mainstem and the tributaries for DOM and trace elements. Also, in the LAR at least, most alterations are likely to occur after mixing and not during mixing, rendering the study of great significance at the regional scale.

Spring snowmelt serves as a major hydrological regime in the boreal zone and greatly affects DOC fluxes along the terrestrial-aquatic continuum (Avagyan et al., 2016). For instance, Finlay et al. (2006) estimated that a large proportion (e.g., ~55%) of Arctic river DOC flux happens during snowmelt. As such, considering seasonal variations in DOM quality in large boreal rivers (e.g., LAR) is of great significance for understanding the global carbon cycle. Our results showed that DOC concentration increased in the period immediately following snowmelt, and its composition shifted towards having more biologically labile components (e.g., protein-like), consistent with previous studies in cold regions (Michaelson et al., 1998; Hood, Williams and McKnight, 2005; Finlay et al., 2006; Ågren et al., 2008; Mann et al., 2012; Avagyan et al., 2016; Hemingway et al., 2019).

The development of the bituminous sands in northern Alberta has received much attention due to the potential release of trace elements into the LAR. Knowledge of trace element speciation in the LAR is thus of great significance to an understanding of aquatic toxicity and bioaccumulation

(Florence, Batley and Benes, 1980; Florence, Morrison and Stauber, 1992). The colloidal form of some metals may account for the majority of the traditionally defined dissolved fraction (<0.45 μm) in natural waters (Florence, Batley and Benes, 1980). In the case of DOM, much of it is in colloidal form with a varying origin and composition in natural waters (Florence, Batley and Benes, 1980). Among properties of colloidal DOM, the size is related to its utilization efficiency by microbes, and thus, has received great attention (Amon and Benner, 1996; Roditi, Fisher and Sañudo-Wilhelmy, 2000; Zhou et al., 2016). Given that DOM is a key carrier facilitating the transport of trace elements in boreal waters (Oleinikova et al., 2017), variations in the size and speciation of DOM-associated TEs would certainly affect their bioavailability for aquatic organisms. The changing nature of DOM in the LAR thus underscores the importance of separating and measuring the size-based distribution of trace elements amongst colloidal DOM using cutting-edge analytical instruments such as AF4 and AF4-ICPMS (Guéguen and Cuss, 2011; Cuss et al., 2018). Results from such studies would certainly improve the understanding of TE sources and forms, with implications for their bioaccessibility.

2.6 CONCLUSIONS

The integration of high-resolution sampling in the LAR allows us to resolve DOM sources and mixing processes in a large boreal river (e.g., the LAR) through size and optical properties. Results showed that DOM quality shifted progressively along the LAR due largely to inputs of terrestrial aromatic carbon through tributaries (e.g., Clearwater R.) from wetlands and their physical dispersion across the river. Flowing downstream, DOM tended to be higher in concentrations of DOC, and degrees of humification and aromaticity. Seasonal variations of DOM quality in the LAR as a result of spring freshet were observed, during which times DOM tended to be higher in molecular mass and richer in protein-like components (C7–C8) compared with humic-like components (C1–C6).

Source discrimination of DOM was thus more obvious at the base flow condition relative to the snowmelt period.

Conservative mixing patterns of DOM across all mixing zones were more apparent in the base flow condition compared to the period of spring freshet, due to the overwhelming effect of snowmelt which largely masked mixing patterns. We thus concluded that DOM can be used a *quasi*-conservative tracer during mixing at river confluences in the boreal zone. Contrasting mixing patterns in different mixing transects suggested that hydrological conditions (e.g., spring freshet) and river geomorphology collectively affect the mixing of DOM between the LAR and its tributaries. Such findings will enhance our ability to determine sources of DOM and to distinguish trends of mixing between the mainstem and the tributaries for DOM-associated trace elements. They will also provide new insights into the metal-binding properties of DOM exported from terrestrial ecosystems under different hydrological conditions.

2.7 ACKNOWLEDGMENTS

This work was supported by the Natural Sciences and Engineering Research Council of Canada, Alberta Innovates, and the Canadian Oil Sands Innovation Alliance. We are also grateful to the Canadian Foundation for Innovation, the Government of Alberta, and the University of Alberta Faculty of Agriculture, Life and Environmental Sciences for funding the SWAMP laboratory facility.

2.8 REFERENCES

Abdulla H. A. N., Minor E. C. and Hatcher P. G. (2010) Using two-dimensional correlations of ^{13}C NMR and FTIR to investigate changes in the chemical composition of dissolved organic matter along an estuarine transect. *Environ. Sci. Technol.* **44**, 8044–8049.

Ågren A., Buffam I., Berggren M., Bishop K., Jansson M. and Laudon H. (2008) Dissolved organic carbon characteristics in boreal streams in a forest-wetland gradient during the transition

between winter and summer. *J. Geophys. Res.* **113**, G03031.

Ahad J. M. E., Pakdel H., Gammon P. R., Mayer B., Savard M. M., Peru K. M. and Headley J. V. (2020) Distinguishing natural from anthropogenic sources of acid extractable organics in groundwater near oil sands tailings ponds. *Environ. Sci. Technol.* **54**, 2790–2799.

Aiken G. R., Hsu-Kim H. and Ryan J. N. (2011) Influence of dissolved organic matter on the environmental fate of metals, nanoparticles, and colloids. *Environ. Sci. Technol.* **45**, 3196–3201.

Allen G. H. and Pavelsky T. M. (2018) Global extent of rivers and streams. *Science* **361**, 585–588.

Amon R. M. W. and Benner R. (1996) Bacterial utilization of different size classes of dissolved organic matter. *Limnol. Oceanogr.* **41**, 41–51.

Aucour A.-M., Tao F.-X., Moreira-Turcq P., Seyler P., Sheppard S. and Benedetti M.F. (2003) The Amazon River: behaviour of metals (Fe, Al, Mn) and dissolved organic matter in the initial mixing at the Rio Negro/Solimões confluence. *Chem. Geol.* **197**, 271–285.

Avagyan A., Runkle B. R. K., Hennings N., Haupt H., Virtanen T. and Kutzbach L. (2016) Dissolved organic matter dynamics during the spring snowmelt at a boreal river valley mire complex in Northwest Russia. *Hydrol. Process.* **30**, 1727–1741.

Barker J. D., Dubnick A., Lyons W. B. and Chin Y.-P. (2013) Changes in dissolved organic matter (DOM) fluorescence in proglacial Antarctic streams. *Arct. Antarct. Alp. Res.* **45**, 305–317.

Battin T. J. (1998) Dissolved organic matter and its optical properties in a blackwater tributary of the upper Orinoco river, Venezuela. *Org. Geochem.* **28**, 561–569.

Battin T. J., Kaplan L. A., Findlay S., Hopkinson C. S., Marti E., Packman A. I., Newbold J. D. and Sabater F. (2008) Biophysical controls on organic carbon fluxes in fluvial networks. *Nat. Geosci.* **1**, 95–100.

Broder T., Knorr K.-H. and Biester H. (2017) Changes in dissolved organic matter quality in a peatland and forest headwater stream as a function of seasonality and hydrologic conditions. *Hydrol. Earth Syst. Sci.* **21**, 2035–2051.

Burns M. A., Barnard H. R., Gabor R. S., McKnight D. M. and Brooks P. D. (2016) Dissolved organic matter transport reflects hillslope to stream connectivity during snowmelt in a montane catchment. *Water Resour. Res.* **52**, 4905–4923.

Cade-Menun B. J., Bell G., Baker-Ismail S., Fouli Y., Hodder K., McMartin D. W., Perez-Valdivia C. and Wu K. (2013) Nutrient loss from Saskatchewan cropland and pasture in spring snowmelt runoff. *Can. J. Soil. Sci.* **93**, 445–458.

Cao X., Aiken G. R., Spencer R. G.M., Butler K., Mao J. and Schmidt-Rohr K. (2016) Novel insights from NMR spectroscopy into seasonal changes in the composition of dissolved organic matter exported to the Bering Sea by the Yukon River. *Geochim. Cosmochim. Acta* **181**, 72–88.

Chanton J. P., Glaser P. H., Chasar L. S., Burdige D. J., Hines M. E., Siegel D. I., Tremblay L. B. and Cooper W. T. (2008) Radiocarbon evidence for the importance of surface vegetation on fermentation and methanogenesis in contrasting types of boreal peatlands. *Glob. Biogeochem. Cycle* **22**, GB4022.

Chen M., Price R. M., Yamashita Y. and Jaffé R. (2010) Comparative study of dissolved organic matter from groundwater and surface water in the Florida coastal Everglades using multi-dimensional spectrofluorometry combined with multivariate statistics. *Appl. Geochem.* **25**, 872–880.

Chow A. T., Dai J., Conner W. H., Hitchcock D. R. and Wang J.-J. (2013) Dissolved organic matter and nutrient dynamics of a coastal freshwater forested wetland in Winyah Bay, South Carolina. *Biogeochemistry* **112**, 571–587.

Coble P., Spencer R. G. M., Andy Baker and Reynolds D. M. (2014) Aquatic Organic Matter Fluorescence. In *Aquatic organic matter fluorescence* (eds. Paula G. Coble, Jamie Lead, Andy Baker, Darren M. Reynolds and Robert G. M. Spencer). Cambridge University Press. New York, NY, USA, pp. 75–122.

Cuss C. W., Donner M. W., Grant-Weaver I., Noernberg T., Pelletier R., Sinnatamby R. N. and Shotyk W. (2018) Measuring the distribution of trace elements amongst dissolved colloidal species as a fingerprint for the contribution of tributaries to large boreal rivers. *Sci. Total Environ.* **642**, 1242–1251.

Cuss C. W., Donner M. W., Noernberg T., Pelletier R. and Shotyk W. (2019) EEM-PARAFAC-SOM for assessing variation in the quality of dissolved organic matter: simultaneous detection of differences by source and season. *Environ. Chem.* **16**, 360–374.

Cuss C. W., Ghotbizadeh M., Grant-Weaver I., Javed M. B., Noernberg T. and Shotyk W. (2020a) Delayed mixing of iron-laden tributaries in large boreal rivers: implications for iron transport, water quality and monitoring. *J. Hydrol.*, 125747.

Cuss C. W., Glover C. N., Javed M. B., Nagel A. and Shotyk W. (2020b) Geochemical and biological controls on the ecological relevance of total, dissolved, and colloidal forms of trace elements in large boreal rivers: review and case studies. *Environ. Rev.* **28**, 138–163.

Cuss C. W., Grant-Weaver I. and Shotyk W. (2017) AF4-ICPMS with the 300 Da membrane to resolve metal-bearing “colloids” < 1 kDa: optimization, fractogram deconvolution, and advanced quality control. *Anal. Chem.* **89**, 8027–8035.

Cuss C. W. and Guéguen C. (2012a) Determination of relative molecular weights of fluorescent components in dissolved organic matter using asymmetrical flow field-flow fractionation and parallel factor analysis. *Anal. Chim. Acta* **733**, 98–102.

Cuss C. W. and Guéguen C. (2012b) Impacts of microbial activity on the optical and copper-binding properties of leaf-litter leachate. *Front. Microbiol.* **3**, 166.

Cuss C. W. and Guéguen C. (2015) Relationships between molecular weight and fluorescence

properties for size-fractionated dissolved organic matter from fresh and aged sources. *Water Res.* **68**, 487–497.

D'Andrilli J., Chanton J. P., Glaser P. H. and Cooper W. T. (2010) Characterization of dissolved organic matter in northern peatland soil porewaters by ultra high resolution mass spectrometry. *Org. Geochem.* **41**, 791–799.

Dalrymple R. M., Carfagno A. K. and Sharpless C. M. (2010) Correlations between dissolved organic matter optical properties and quantum yields of singlet oxygen and hydrogen peroxide. *Environ. Sci. Technol.* **44**, 5824–5829.

Ehrhart J., Mingotaud A.-F. and Violleau F. (2011) Asymmetrical flow field-flow fractionation with multi-angle light scattering and quasi elastic light scattering for characterization of poly(ethyleneglycol-b-ε-caprolactone) block copolymer self-assemblies used as drug carriers for photodynamic therapy. *J. Chromatogr. A* **1218**, 4249–4256.

Fellman J. B., Hood E. and Spencer R. G. M. (2010) Fluorescence spectroscopy opens new windows into dissolved organic matter dynamics in freshwater ecosystems: A review. *Limnol. Oceanogr.* **55**, 2452–2462.

Findlay S. and Sinsabaugh R. L. (2003) *Aquatic ecosystems - interactivity of dissolved organic matter.* Academic Press, Amsterdam, London.

Finlay J., Neff J., Zimov S., Davydova A. and Davydov S. (2006) Snowmelt dominance of dissolved organic carbon in high-latitude watersheds: Implications for characterization and flux of river DOC. *Geophys. Res. Lett.* **33**, L10401.

Florence T. M., Batley G. E. and Benes P. (1980) Chemical speciation in natural waters. *Crit. Rev. Anal. Chem.* **9**, 219–296.

Florence T. M., Morrison G. M. and Stauber J. L. (1992) Determination of trace element speciation and the role of speciation in aquatic toxicity. *Sci. Total Environ.* **125**, 1–13.

Michaelson G. J., Ping C. L., Kling G. W. and Hobbie J. E. (1998) The character and bioactivity of dissolved organic matter at thaw and in the spring runoff waters of the arctic tundra North Slope, Alaska. *J. Geophys. Res.* **103**, 28939–28946.

Gaudet J. M. and Roy A. G. (1995) Effect of bed morphology on flow mixing length at river confluences. *Nature* **373**, 138–139.

Gómez-Gener L., Lupon A., Laudon H. and Sponseller R. A. (2020) Drought alters the biogeochemistry of boreal stream networks. *Nat. Commun.* **11**, 1795.

Gorham E. (1991) Northern Peatlands: Role in the Carbon Cycle and Probable Responses to Climatic Warming. *Ecol. Appl.* **1**, 182–195.

Guéguen C., Burns D. C., McDonald A. and Ring B. (2012) Structural and optical characterization of dissolved organic matter from the lower Athabasca River, Canada. *Chemosphere* **87**, 932–

937.

Guéguen C. and Cuss C. W. (2011) Characterization of aquatic dissolved organic matter by asymmetrical flow field-flow fractionation coupled to UV-Visible diode array and excitation emission matrix fluorescence. *J. Chromatogr. A* **1218**, 4188–4198.

Hassett J. P. (2006) Dissolved natural organic matter as a microreactor. *Science* **311**, 1723–1724.

Hemingway J. D., Spencer R. G.M., Podgorski D. C., Zito P., Sen I. S. and Galy V. V. (2019) Glacier meltwater and monsoon precipitation drive Upper Ganges Basin dissolved organic matter composition. *Geochim. Cosmochim. Acta* **244**, 216–228.

Hewitt L. M., Roy J. W., Rowland S. J., Bickerton G., DeSilva A., Headley J. V., Milestone C. B., Scarlett A. G., Brown S., Spencer C., West C. E., Peru K. M., Grapentine L., Ahad J. M. E., Pakdel H. and Frank R. A. (2020) Advances in distinguishing groundwater influenced by oil sands process-affected water (OSPW) from natural bitumen-influenced groundwaters. *Environ. Sci. Technol.* **54**, 1522–1532.

Holmes R. M., McClelland J. W., Raymond P. A., Frazer B. B., Peterson B. J. and Stieglitz M. (2008) Lability of DOC transported by Alaskan rivers to the Arctic Ocean. *Geophys. Res. Lett.* **35**, L03402.

Hood E., Fellman J., Spencer R. G. M., Hernes P. J., Edwards R., D'Amore D. and Scott D. (2009) Glaciers as a source of ancient and labile organic matter to the marine environment. *Nature* **462**, 1044–1047.

Hood E., Williams M. W. and McKnight D. M. (2005) Sources of dissolved organic matter (DOM) in a Rocky Mountain stream using chemical fractionation and stable isotopes. *Biogeochemistry* **74**, 231–255.

Huguet A., Vacher L., Relexans S., Saubusse S., Froidefond J. M. and Parlanti E. (2009) Properties of fluorescent dissolved organic matter in the Gironde Estuary. *Org. Geochem.* **40**, 706–719.

Hutchins R. H. S., Prairie Y. T. and del Giorgio P. A. (2019) Large-scale landscape drivers of CO_2, CH_4, DOC, and DIC in boreal river networks. *Glob. Biogeochem. Cycle* **33**, 125–142.

Jager D. F., Wilmking M. and Kukkonen J. V. K. (2009) The influence of summer seasonal extremes on dissolved organic carbon export from a boreal peatland catchment: evidence from one dry and one wet growing season. *Sci. Total Environ.* **407**, 1373–1382.

Jiang T., Skyllberg U., Björn E., Green N. W., Tang J., Wang D., Gao J. and Li C. (2017) Characteristics of dissolved organic matter (DOM) and relationship with dissolved mercury in Xiaoqing River-Laizhou Bay estuary, Bohai Sea, China. *Environ. Pollut.* **223**, 19–30.

Keil R. G. and Kirchman D. L. (1991) Contribution of dissolved free amino acids and ammonium to the nitrogen requirements of heterotrophic bacterioplankton. *Mar. Ecol.-Prog. Ser.* **73**, 1–10.

Kellerman A. M., Kothawala D. N., Dittmar T. and Tranvik L. J. (2015) Persistence of dissolved

organic matter in lakes related to its molecular characteristics. *Nat. Geosci.* **8**, 454–457.

Khadka B., Munir T. M. and Strack M. (2016) Dissolved organic carbon in a constructed and natural fens in the Athabasca oil sands region, Alberta, Canada. *Sci. Total Environ.* **557-558**, 579–589.

Kim K. H. and Moon M. H. (2009) Development of a multilane channel system for nongel-based two-dimensional protein separations using isoelectric focusing and asymmetrical flow field-flow fractionation. *Anal. Chem.* **81**, 1715–1721.

Korak J. A., Dotson A. D., Summers R. S. and Rosario-Ortiz F. L. (2014) Critical analysis of commonly used fluorescence metrics to characterize dissolved organic matter. *Water Res.* **49**, 327–338.

Kothawala D. N., Murphy K. R., Stedmon C. A., Weyhenmeyer G. A. and Tranvik L. J. (2013) Inner filter correction of dissolved organic matter fluorescence. *Limnol. Oceanogr. Meth.* **11**, 616–630.

Lambert T., Bouillon S., Darchambeau F., Massicotte P. and Borges A. V. (2016) Shift in the chemical composition of dissolved organic matter in the Congo River network. *Biogeosciences* **13**, 5405–5420.

Latch D. E. and McNeill K. (2006) Microheterogeneity of singlet oxygen distributions in irradiated humic acid solutions. *Science* **311**, 1743–1747.

Lawaetz A. J. and Stedmon C. A. (2009) Fluorescence intensity calibration using the Raman scatter peak of water. *Appl. Spectrosc.* **63**, 936–940.

Lee M.-H., Osburn C. L., Shin K.-H. and Hur J. (2018) New insight into the applicability of spectroscopic indices for dissolved organic matter (DOM) source discrimination in aquatic systems affected by biogeochemical processes. *Water Res.* **147**, 164–176.

Lima A. C. and Wrona F. J. (2019) Multiple threats and stressors to the Athabasca River Basin: What do we know so far? *Sci. Total Environ.* **649**, 640–651.

Lin H. and Guo L. (2020) Variations in Colloidal DOM Composition with Molecular Weight within Individual Water Samples as Characterized by Flow Field-Flow Fractionation and EEM-PARAFAC Analysis. *Environ. Sci. Technol.* **54**, 1657–1667.

Lynch L. M., Sutfin N. A., Fegel T. S., Boot C. M., Covino T. P. and Wallenstein M. D. (2019) River channel connectivity shifts metabolite composition and dissolved organic matter chemistry. *Nat. Commun.* **10**, 459.

Mann P. J., Davydova A., Zimov N., Spencer R. G. M., Davydov S., Bulygina E., Zimov S. and Holmes R. M. (2012) Controls on the composition and lability of dissolved organic matter in Siberia's Kolyma River basin. *J. Geophys. Res.* **117**, G0102.

McKnight D. M., Bencala K. E., Zellweger G. W., Aiken G. R., Feder G. L. and Thorn K. A.

(1992) Sorption of dissolved organic carbon by hydrous aluminum and iron oxides occurring at the confluence of Deer Creek with the Snake River, Summit County, Colorado. *Environ. Sci. Technol.* **26**, 1388–1396.

McKnight D. M., Boyer E. W., Westerhoff P. K., Doran P. T., Kulbe T. and Andersen D. T. (2001) Spectrofluorometric characterization of dissolved organic matter for indication of precursor organic material and aromaticity. *Limnol. Oceanogr.* **46**, 38–48.

Miller M. P. and McKnight D. M. (2010) Comparison of seasonal changes in fluorescent dissolved organic matter among aquatic lake and stream sites in the Green Lakes Valley. *J. Geophys. Res.* **115**, G00F12.

Mitrano D. M., Barber A., Bednar A., Westerhoff P., Higgins C. P. and Ranville J. F. (2012) Silver nanoparticle characterization using single particle ICP-MS (SP-ICP-MS) and asymmetrical flow field flow fractionation ICP-MS (AF4-ICP-MS). *J. Anal. At. Spectrom.* **27**, 1131.

Montaño M. D., Kammer F. von der, Cuss C. W. and Ranville J. F. (2019) Opportunities for examining the natural nanogeochemical environment using recent advances in nanoparticle analysis. *J. Anal. At. Spectrom.* **34**, 1768–1772.

Moreira-Turcq P. F., Seyler P., Guyot J. L. and Etcheber H. (2003) Characteristics of organic matter in the mixing zone of the Rio Negro and Rio Solimões of the Amazon River. *Hydrol. Process.* **17**, 1393–1404.

Murphy K. R., Hambly A., Singh S., Henderson R. K., Baker A., Stuetz R. and Khan S. J. (2011) Organic matter fluorescence in municipal water recycling schemes: toward a unified PARAFAC model. *Environ. Sci. Technol.* **45**, 2909–2916.

Murphy K. R., Stedmon C. A., Graeber D. and Bro R. (2013) Fluorescence spectroscopy and multi-way techniques. PARAFAC. *Anal. Methods* **5**, 6557.

Murphy K. R., Stedmon C. A., Wenig P. and Bro R. (2014) OpenFluor– an online spectral library of auto-fluorescence by organic compounds in the environment. *Anal. Methods* **6**, 658–661.

O'Donnell J. A., Aiken G. R., Kane E. S. and Jones J. B. (2010) Source water controls on the character and origin of dissolved organic matter in streams of the Yukon River basin, Alaska. *J. Geophys. Res.* **115**, G03025.

Oleinikova O. V., Drozdova O. Y., Lapitskiy S. A., Demin V. V., Bychkov A. Y. and Pokrovsky O. S. (2017) Dissolved organic matter degradation by sunlight coagulates organo-mineral colloids and produces low-molecular weight fraction of metals in boreal humic waters. *Geochim. Cosmochim. Acta* **211**, 97–114.

Oliver B. G., Thurman E. M. and Malcolm R. L. (1983) The contribution of humic substances to the acidity of colored natural waters. *Geochim. Cosmochim. Acta* **47**, 2031–2035.

Osburn C. L., Wigdahl C. R., Fritz S. C. and Saros J. E. (2011) Dissolved organic matter composition and photoreactivity in prairie lakes of the U.S. Great Plains. *Limnol. Oceanogr.* **56**,

2371–2390.

Parlanti E., Wörz K., Geoffroy L. and Lamotte M. (2000) Dissolved organic matter fluorescence spectroscopy as a tool to estimate biological activity in a coastal zone submitted to anthropogenic inputs. *Org. Geochem.* **31**, 1765–1781.

Parr T. B., Ohno T., Cronan C. S. and Simon K. S. (2014) comPARAFAC: a library and tools for rapid and quantitative comparison of dissolved organic matter components resolved by Parallel Factor Analysis. *Limnol. Oceanogr. Meth.* **12**, 114–125.

Parsons D. R., Best J. L., Lane S. N., Kostaschuk R. A., Hardy R. J., Orfeo O., Amsler M. L. and Szupiany R. N. (2008) Large river channel confluences. In *River confluences, tributaries and the fluvial network.* John Wiley & Sons, Ltd, pp. 73–91.

Peuravuori J. and Pihlaja K. (1997) Molecular size distribution and spectroscopic properties of aquatic humic substances. *Anal. Chim. Acta* **337**, 133–149.

Podzimek S. (2011) Asymmetric flow field flow fractionation. In *Light scattering, size exclusion chromatography and asymmetric flow field flow fractionation* (ed. S. Podzimek). John Wiley & Sons, Ltd. Hoboken, New Jersey, pp. 259–305.

Poulin B. A., Ryan J. N. and Aiken G. R. (2014) Effects of iron on optical properties of dissolved organic matter. *Environ. Sci. Technol.* **48**, 10098–10106.

Roditi H. A., Fisher N. S. and Sañudo-Wilhelmy S. A. (2000) Uptake of dissolved organic carbon and trace elements by zebra mussels. *Nature* **407**, 78–80.

Rutherford J. C. (1994) *River mixing.* John Wiley & Sons, Ltd, Chichester, England.

Schumacher M., Christl I., Vogt R. D., Barmettler K., Jacobsen C. and Kretzschmar R. (2006) Chemical composition of aquatic dissolved organic matter in five boreal forest catchments sampled in spring and fall seasons. *Biogeochemistry* **80**, 263–275.

Shotyk W. (1988) Review of the inorganic geochemistry of peats and peatland waters. *Earth-Sci. Rev.* **25**, 95–176.

Shotyk W., Bicalho B., Cuss C. W., Donner M. W., Grant-Weaver I., Haas-Neill S., Javed M. B., Krachler M., Noernberg T., Pelletier R. and Zaccone C. (2017) Trace metals in the dissolved fraction (<0.45μm) of the lower Athabasca River: Analytical challenges and environmental implications. *Sci. Total Environ.* **580**, 660–669.

Simon C., Osterholz H., Koschinsky A. and Dittmar T. (2019) Riverine mixing at the molecular scale – An ultrahigh-resolution mass spectrometry study on dissolved organic matter and selected metals in the Amazon confluence zone (Manaus, Brazil). *Org. Geochem.* **129**, 45–62.

Singh S., D'Sa E. J. and Swenson E. M. (2010) Chromophoric dissolved organic matter (CDOM) variability in Barataria Basin using excitation-emission matrix (EEM) fluorescence and parallel factor analysis (PARAFAC). *Sci. Total Environ.* **408**, 3211–3222.

Spencer R. G. M. and Coble P. G. (2014) Sampling design for organic matter fluorescence analysis. In *Aquatic organic matter fluorescence* (eds. Paula G. Coble, Jamie Lead, Andy Baker, Darren M. Reynolds and Robert G. M. Spencer). Cambridge University Press. New York, NY, USA, pp. 125–146.

Spencer R. G.M., Guo W., Raymond P. A., Dittmar T., Hood E., Fellman J. and Stubbins A. (2014) Source and biolability of ancient dissolved organic matter in glacier and lake ecosystems on the Tibetan Plateau. *Geochim. Cosmochim. Acta* **142**, 64–74.

Stedmon C. A. and Bro R. (2008) Characterizing dissolved organic matter fluorescence with parallel factor analysis: a tutorial. *Limnol. Oceanogr. Methods* **6**, 572–579.

Stedmon C. A. and Markager S. (2003) Behaviour of the optical properties of coloured dissolved organic matter under conservative mixing. *Estuar. Coast. Shelf Sci.* **57**, 973–979.

Striegl R. G., Aiken G. R., Dornblaser M. M., Raymond P. A. and Wickland K. P. (2005) A decrease in discharge-normalized DOC export by the Yukon River during summer through autumn. *Geophys. Res. Lett.* **32**, L21413.

Stubbins A., Lapierre J.-F., Berggren M., Prairie Y. T., Dittmar T. and del Giorgio P. A. (2014) What's in an EEM? Molecular signatures associated with dissolved organic fluorescence in boreal Canada. *Environ. Sci. Technol.* **48**, 10598–10606.

Sun C., Shotyk W., Cuss C. W., Donner M. W., Fennell J., Javed M., Noernberg T., Poesch M., Pelletier R., Sinnatamby N., Siddique T. and Martin J. W. (2017) Characterization of Naphthenic Acids and Other Dissolved Organics in Natural Water from the Athabasca Oil Sands Region, Canada. *Environ. Sci. Technol.* **51**, 9524–9532.

Wahlund K. G. and Giddings J. C. (1987) Properties of an asymmetrical flow field-flow fractionation channel having one permeable wall. *Anal. Chem.* **59**, 1332–1339.

Walker S. A., Amon R. M. W. and Stedmon C. A. (2013) Variations in high-latitude riverine fluorescent dissolved organic matter: A comparison of large Arctic rivers. *J. Geophys. Res.-Biogeosci.* **118**, 1689–1702.

Wallis P. M., Hynes H. B. N. and Telang S. A. (1981) The importance of groundwater in the transportation of allochthonous dissolved organic matter to the streams draining a small mountain basin. *Hydrobiologia* **79**, 77–90.

Wang Y., Cuss C. W. and Shotyk W. (2020) Application of asymmetric flow field-flow fractionation to the study of aquatic systems: Coupled methods, challenges, and future needs. *J. Chromatogr. A* **1632**, 461600.

Ward C. P. and Cory R. M. (2015) Chemical composition of dissolved organic matter draining permafrost soils. *Geochim. Cosmochim. Acta* **167**, 63–79.

Weishaar J. L., Aiken G. R., Bergamaschi B. A., Fram M. S., Fujii R. and Mopper K. (2003) Evaluation of specific ultraviolet absorbance as an indicator of the chemical composition and

reactivity of dissolved organic carbon. *Environ. Sci. Technol.* **37**, 4702–4708.

Wetzel R. G. (1992) Gradient-dominated ecosystems: sources and regulatory functions of dissolved organic matter in freshwater ecosystems. *Hydrobiologia* **229**, 181–198.

Wickland K. P., Aiken G. R., Butler K., Dornblaser M. M., Spencer R. G. M. and Striegl R. G. (2012) Biodegradability of dissolved organic carbon in the Yukon River and its tributaries: Seasonality and importance of inorganic nitrogen. *Global Biogeochem. Cycles* **26**, GB0E03.

Wilson H. F. and Xenopoulos M. A. (2009) Effects of agricultural land use on the composition of fluvial dissolved organic matter. *Nat. Geosci.* **2**, 37–41.

Woo M.-K. and Thorne R. (2003) Streamflow in the Mackenzie Basin, Canada. *Arctic* **56**, 328–340.

Worms I. A. M., Chmiel H. E., Traber J., Tofield-Pasche N. and Slaveykova V. I. (2019) Dissolved Organic Matter and Associated Trace Metal Dynamics from River to Lake, Under Ice-Covered and Ice-Free Conditions. *Environ. Sci. Technol.* **53**, 14134–14143.

Yi Y., Birks S. J., Cho S. and Gibson J. J. (2015) Characterization of organic composition in snow and surface waters in the Athabasca Oil Sands Region, using ultrahigh resolution Fourier transform mass spectrometry. *Sci. Total Environ.* **518-519**, 148–158.

Yu Z., Beilman D. W., Frolking S., MacDonald G. M., Roulet N. T., Camill P. and Charman D. J. (2011) Peatlands and Their Role in the Global Carbon Cycle. *Eos Trans. AGU* **92**, 97–98.

Zark M. and Dittmar T. (2018) Universal molecular structures in natural dissolved organic matter. *Nat. Commun.* **9**, 3178.

Zhang M. and He Z. (2015) Characteristics of dissolved organic carbon revealed by ultraviolet‐visible absorbance and fluorescence spectroscopy: the current status and future exploration. In *Labile organic matter—chemical compositions, function, and significance in soil and the environment* (eds. Z. He and F. Wu). Soil Science Society of America, Inc. Madison, WI, USA, pp. 1–21.

Zhou Z., Stolpe B., Guo L. and Shiller A. M. (2016) Colloidal size spectra, composition and estuarine mixing behavior of DOM in river and estuarine waters of the northern Gulf of Mexico. *Geochim. Cosmochim. Acta* **181**, 1–17.

Zsolnay A., Baigar E., Jimenez M., Steinweg B. and Saccomandi F. (1999) Differentiating with fluorescence spectroscopy the sources of dissolved organic matter in soils subjected to drying. *Chemosphere* **38**, 45–50.

2.9 FIGURES

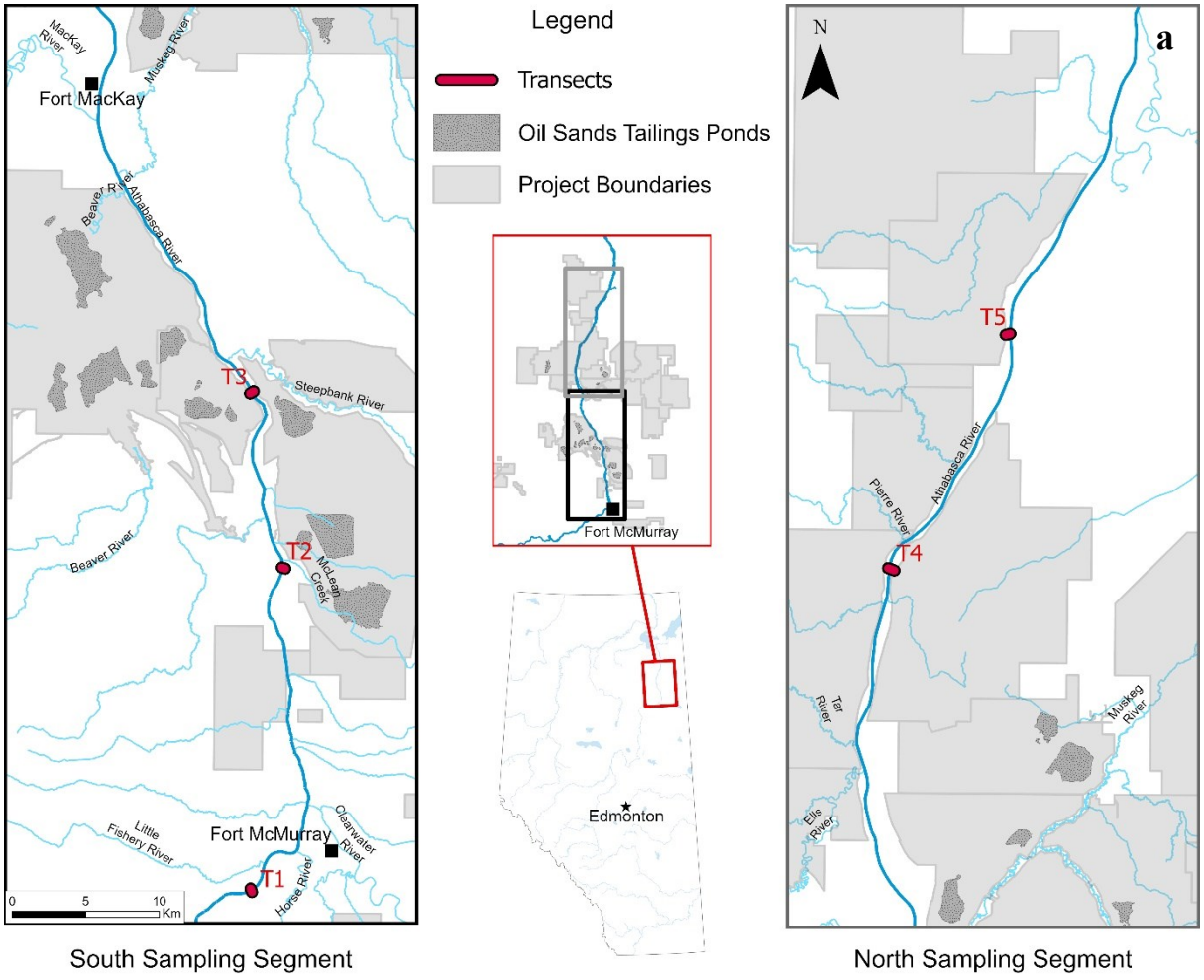
Legend
Transects
Oil Sands Tailings Ponds
Project Boundaries
MacKay River
Muskeg River
Fort MacKay
Beaver River
Athabasca River
T3
Steepbank River
T2
McLean Creek
Beaver River
Little Fishery River
Fort McMurray
Clearwater River
T1
Horse River
0 5 10 Km
Fort McMurray
Edmonton
South Sampling Segment
N
a
T5
Athabasca River
Pierre River
T4
Tar River
Muskeg River
Ells River
North Sampling Segment

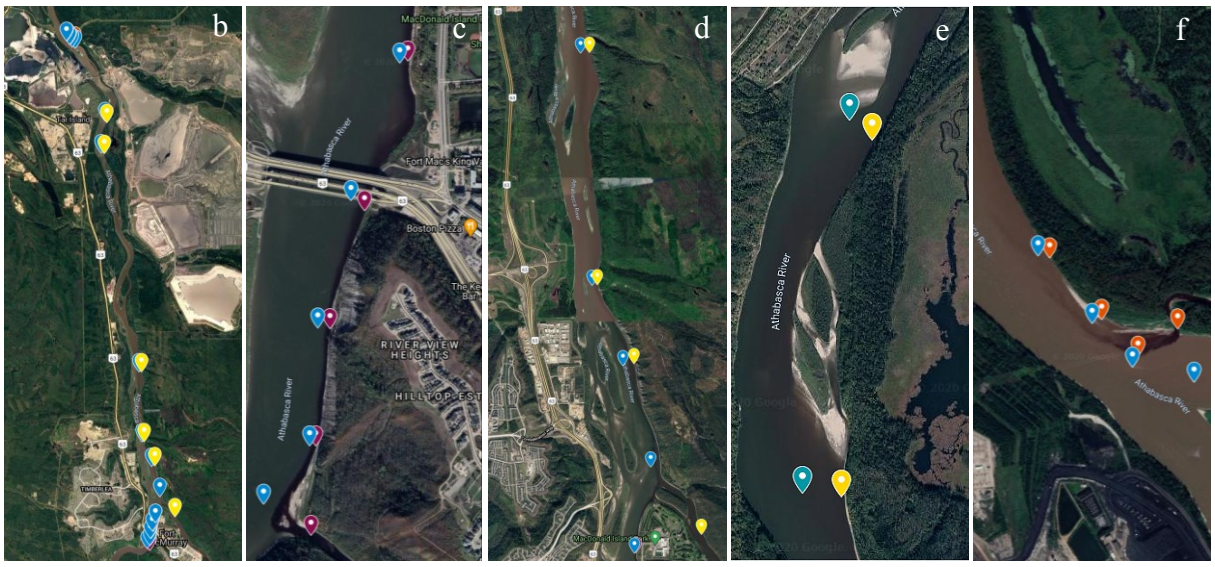
b
c
d
e
f
RIVER VIEW HEIGHTS
HILLTOP EST
Athabasca River

Figure 2-1 Maps of the study area showing sampling sites in the mainstem of the lower Athabasca River (LAR, flowing northwards) (a) and three mixing zones (b–f). Five mainstem transects are marked in red (e.g., T1–T5) and full names for tributaries are also indicated (a). Maps c–f (Not to Scale) show sampling sites in three mixing zones between the LAR and Horse R. (HR) (c), Clearwater R. (d, e), and Steepbank R. (SB) (f) in the spring of 2019. Similar sampling protocol was taken in the fall of 2018. Distinct symbol colors for samples in the tributary side (pink, yellow, and orange for HR, CL, and SB, respectively) are used, while that of the mainstem (blue) is uniform across all mixing zones. Regarding notations, AR-HR01–05 and HR-HR01–05 are used for samples collected from the mainstem and the HR side at five mixing transects of the HR mixing zone along the river, respectively (c). Similarly, AR-CL01–06 and CL-CL01–06 and AR-SB01–04 and SB-SB01–04 refer to sites of the mainstem and the tributary sides of the CL and SB mixing zones along the river, respectively (d–f). Map data ©2020 Google

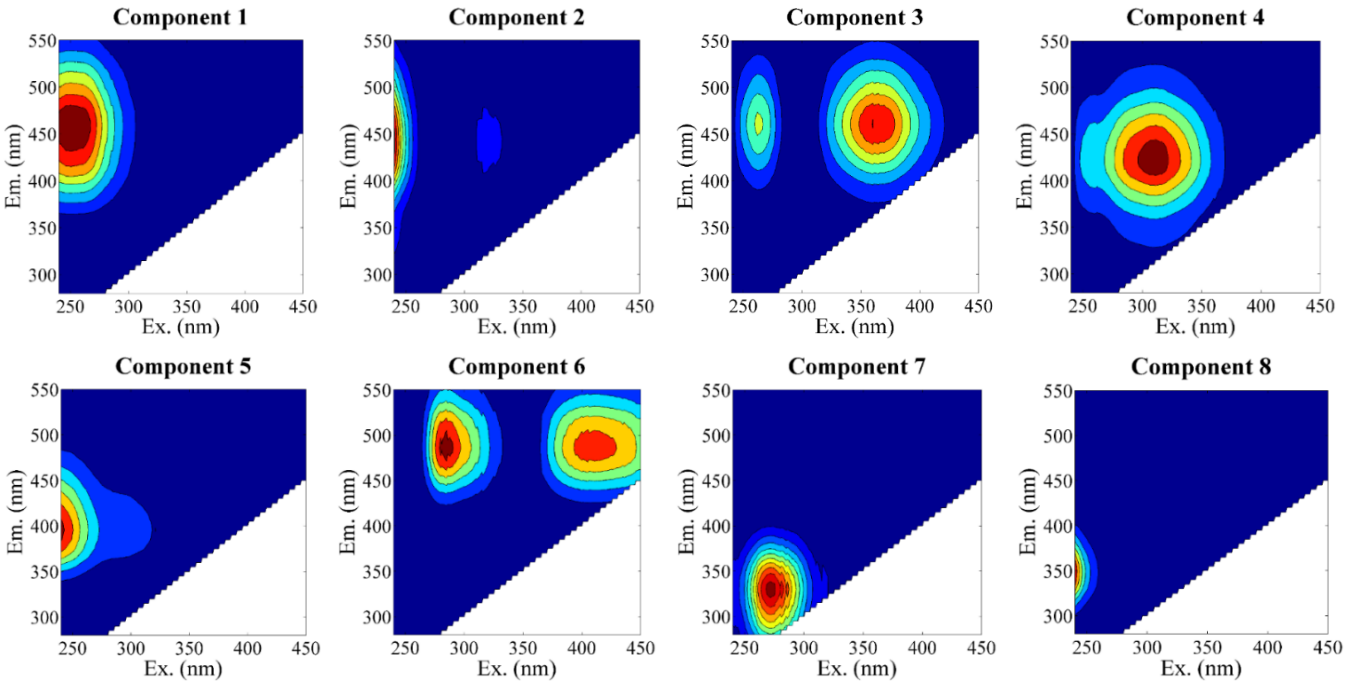

Figure 2-2 Contour plots of 8 PARAFAC-derived fluorescent DOM components (see Figure S2-2 for excitation and emission spectra).

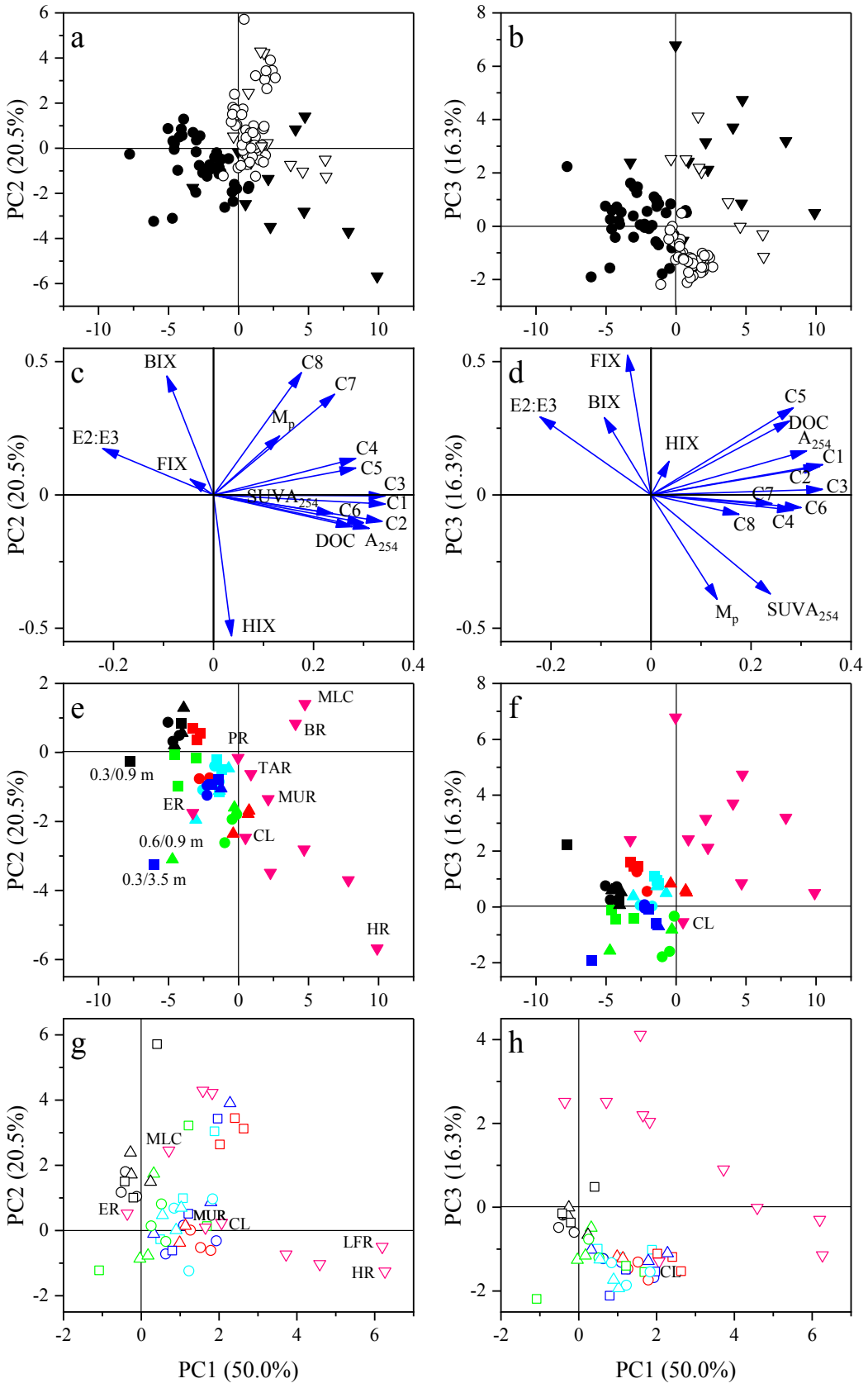
a
b
c
d
e
f
g
h
PC2 (20.5%)
PC3 (16.3%)
PC1 (50.0%)
BIX
E2:E3
FIX
HIX
C8
C7
M_p
C4
C5
C3
$SUVA_{254}$
C1
C6
C2
DOC
A_{254}
MLC
BR
PR
TAR
MUR
ER
CL
0.3/0.9 m
0.6/0.9 m
0.3/3.5 m
HR
LFR

Figure 2-3 Score (a–b and e–h) and loading plots (c–d) of PCA representing DOM quality for samples (*n*=104) from mainstem transects and tributaries of the LAR in the fall (solid, e–f) and spring (open, g–h). In plots a–b, samples from the mainstem (circle) and tributaries (down triangle) are differentiated. Markers are also separated into west (square), middle (circle), east (up triangle), and tributaries (down triangle) for T1 (black), T2 (red), T3 (green), T4 (blue), T5 (cyan) and tributary (pink) samples for plots (e–h).

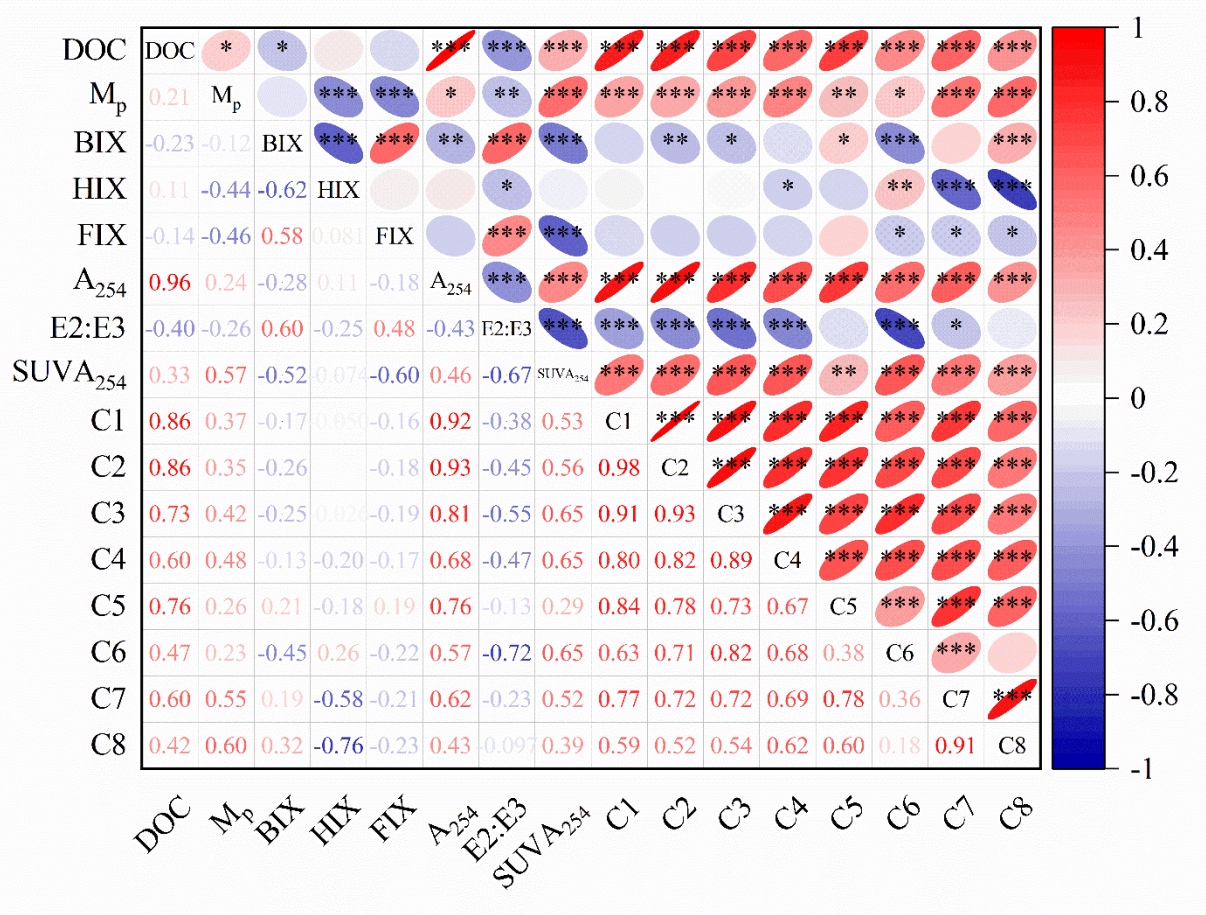

Figure 2-4 Spearman's rank order correlation coefficients between DOM concentration, size, and optical properties for samples (n=104) of 5 mainstem transects (T1–T5) and 10 tributaries (MLC, PR, HR, BR, MKR, TAR, MUR, SB, ER, CL, LFR) of the lower Athabasca River in the fall and spring. Significant correlation coefficients are indicated by: *$p < 0.05$, **$p < 0.01$, ***$p < 0.001$.

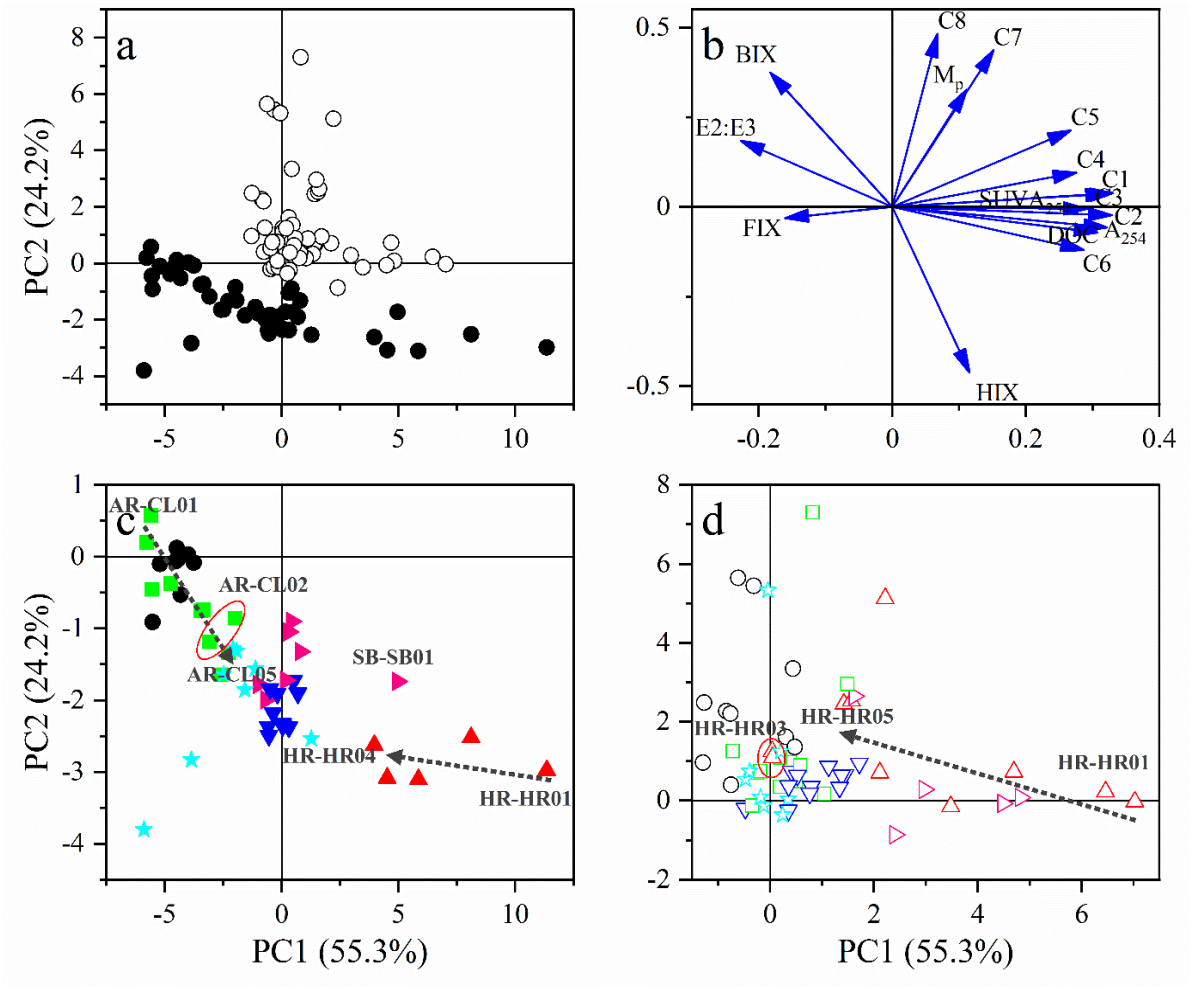

Figure 2-5 Score (a, c, d) and loading plots (b) of PCA representing DOM quality for samples (n=105) from three mixing zones between the lower Athabasca River and Horse River, Clearwater River, and Steepbank River in the fall (solid) and spring (open). Markers are separated for AR-HR (black circle), HR-HR (red up triangle), AR-CL (green square), CL-CL (blue down triangle), AR-SB (cyan star) and SB-SB (pink right triangle) samples across plots (c–d).

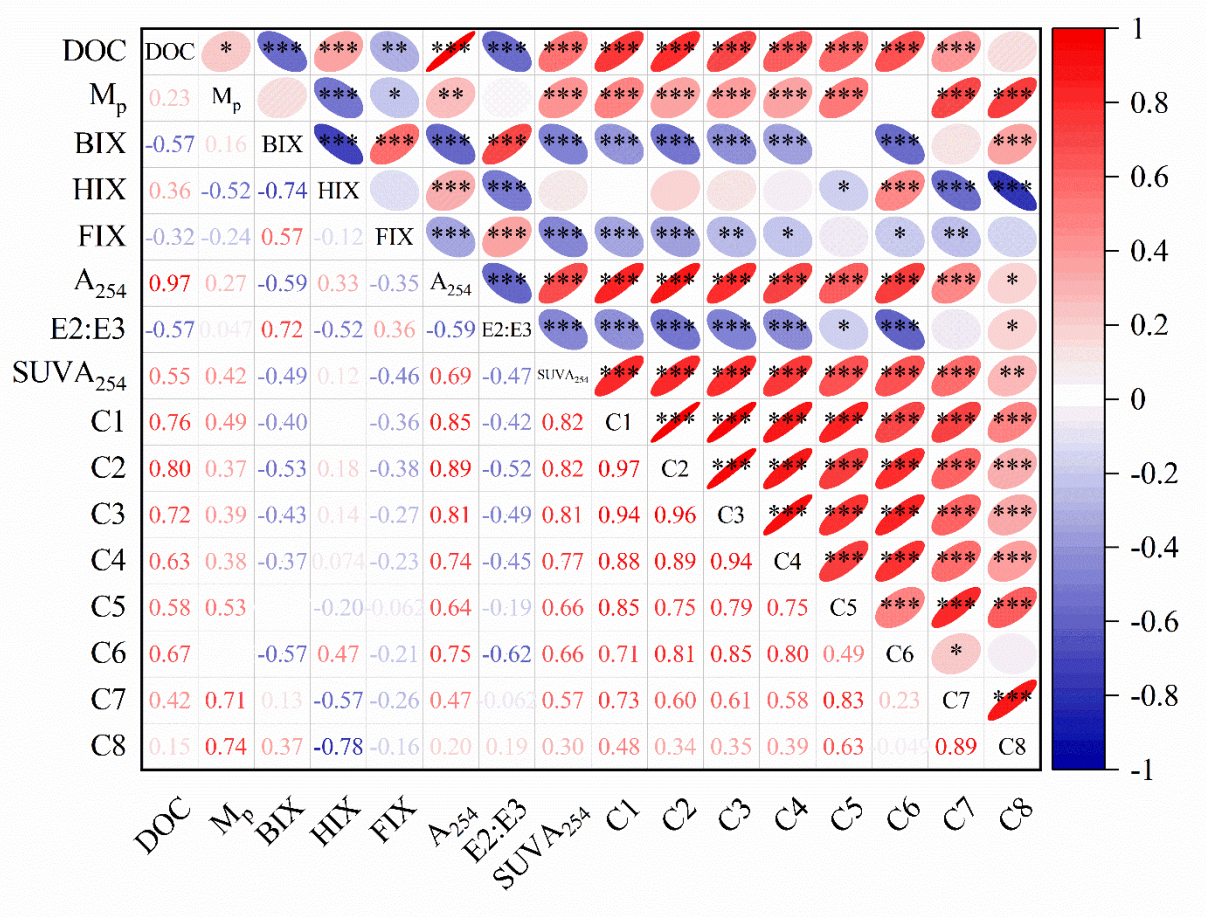

Figure 2-6 Spearman's rank order correlation coefficients between DOM concentration, size, and optical properties for samples (n=105) of 3 mixing zones between the lower Athabasca River and Horse River, Clearwater River, and Steepbank River in the fall and spring, respectively. Significant correlation coefficients are indicated by: *$p < 0.05$, **$p < 0.01$, ***$p < 0.001$.

2.10 TABLES

Table 2-1 Concentrations of DOC and the DOM quality indicators (size and optical properties) in five mainstem transects (T1–T5) of the lower Athabasca River in the fall and spring, respectively. SD denotes standard deviation. The mean values for those indicators are marked in bold. Units: DOC (mg C L^{-1}), M_p (kDa), A_{254} (m^{-1}), and $SUVA_{254}$ (L mg^{-1} C m^{-1}).

Site description		DOC	M_p	BIX	HIX	FIX	A_{254}	E2:E3	$SUVA_{254}$
Fall 2018									
T1 (*n*=8)	**Mean**	**6.6**	**1.05**	**0.56**	**11.9**	**1.5**	**18.1**	**6.6**	**2.76**
	SD	0.2	0.05	0.01	0.9	0.0	0.3	0.4	0.09
	Max	6.8	1.11	0.57	12.8	1.6	18.4	7.0	2.90
	Min	6.3	0.93	0.55	10.4	1.5	17.5	5.9	2.66
T2 (*n*=8)	**Mean**	**9.0**	**1.07**	**0.55**	**15.2**	**1.5**	**26.8**	**6.0**	**2.96**
	SD	1.5	0.05	0.02	1.7	0.0	6.0	0.5	0.18
	Max	11.0	1.13	0.58	17.4	1.5	34.2.	6.7	3.23
	Min	7.5	1.01	0.52	13.3	1.5	21.0	5.2	2.73
T3 (*n*=8)	**Mean**	**8.6**	**1.11**	**0.52**	**15.2**	**1.5**	**26.3**	**5.7**	**3.03**
	SD	0.9	0.04	0.02	1.8	0.0	4.6	0.4	0.30
	Max	9.5	1.18	0.54	17.3	1.5	30.0	6.4	3.30
	Min	7.0	1.04	0.49	12.6	1.4	20.7	5.3	2.41
T4 (*n*=6)	**Mean**	**8.8**	**1.04**	**0.52**	**15.0**	**1.5**	**26.5**	**5.9**	**3.03**
	SD	0.3	0.05	0.02	0.9	0.0	0.4	0.2	0.10
	Max	9.1	1.08	0.54	16.7	1.5	26.9	6.2	3.17
	Min	8.3	0.95	0.48	14.3	1.4	25.9	5.6	2.93
T5 (*n*=9)	**Mean**	**8.9**	**1.10**	**0.54**	**15.2**	**1.5**	**26.5**	**5.9**	**2.98**
	SD	0.2	0.04	0.01	0.6	0.0	0.4	0.3	0.07
	Max	9.1	1.14	0.55	16.6	1.5	27.3	6.4	3.08
	Min	8.7	1.03	0.52	14.5	1.5	25.9	5.4	2.85
Spring 2019									
T1 (*n*=9)	**Mean**	**9.4**	**1.26**	**0.57**	**9.8**	**1.5**	**29.8**	**6.1**	**3.18**
	SD	0.2	0.03	0.02	2.7	0.0	0.2	0.1	0.07
	Max	9.6	1.30	0.62	11.8	1.5	30.2	6.4	3.30
	Min	9.1	1.19	0.55	3.1	1.5	29.5	5.9	3.11
T2 (*n*=8)	**Mean**	**11.9**	**1.33**	**0.53**	**10.6**	**1.5**	**38.6**	**5.6**	**3.25**
	SD	0.7	0.06	0.02	4.1	0.0	2.0	0.2	0.07
	Max	12.8	1.38	0.56	14.5	1.5	40.4	6.0	3.32
	Min	10.9	1.23	0.51	5.1	1.5	35.3	5.4	3.11
T3 (*n*=9)	**Mean**	**10.0**	**1.21**	**0.53**	**11.7**	**1.5**	**32.4**	**5.7**	**3.26**
	SD	0.6	0.05	0.02	3.4	0.0	0.3	0.2	0.19
	Max	10.6	1.26	0.56	14.7	1.5	33.0	6.2	3.56
	Min	9.1	1.10	0.51	5.0	1.4	32.0	5.4	3.06
T4 (*n*=9)	**Mean**	**10.0**	**1.22**	**0.53**	**10.7**	**1.5**	**33.9**	**5.6**	**3.38**
	SD	0.4	0.06	0.02	4.1	0.0	0.3	0.1	0.12
	Max	10.5	1.32	0.57	14.2	1.5	34.2	6.0	3.59
	Min	9.4	1.17	0.51	4.0	1.4	33.4	5.5	3.24
T5 (*n*=9)	**Mean**	**9.6**	**1.25**	**0.53**	**11.6**	**1.5**	**32.7**	**5.7**	**3.40**
	SD	0.4	0.05	0.01	2.8	0.0	0.5	0.2	0.12
	Max	10.4	1.30	0.56	16.0	1.5	33.3	6.3	3.56
	Min	9.2	1.19	0.52	5.7	1.4	31.7	5.6	3.20

Table 2-2 Concentrations of DOC and the DOM quality indicators (size and optical properties) in tributaries (surface water sample) of the lower Athabasca River in the fall and spring, respectively. 95% CI denotes a 95% Confidence Interval. Units: DOC (mg C L^{-1}), M_p (kDa), A_{254} (m^{-1}), and $SUVA_{254}$ (L mg^{-1} C m^{-1}).

Site description	DOC	M_p	95% CI (M_p)	BIX	HIX	FIX	A_{254}	E2:E3	$SUVA_{254}$
Fall 2018 (n=11)									
LFR	23.5	1.10	0.05	0.50	22.0	1.5	70.2	6.0	2.99
HR	33.3	1.08	0.005	0.45	26.6	1.5	135.9	4.7	4.08
CL	11.8	0.99	0.03	0.50	17.1	1.5	38.6	5.4	3.27
MLC	23.0	0.98	0.06	0.59	12.7	1.6	69.4	5.7	3.02
SB	21.1	1.09	0.005	0.49	20.7	1.5	70.4	5.6	3.34
BR	25.3	1.18	0.03	0.57	14.8	1.5	73.3	6.3	2.90
MUR	24.3	1.03	0.06	0.53	17.4	1.5	67.2	6.0	2.77
MKR	32.9	1.01	0.03	0.50	23.0	1.5	115.3	5.2	3.51
ER	16.7	0.98	0.03	0.53	15.6	1.5	45.6	6.7	2.72
TAR	17.2	0.96	0.04	0.54	15.0	1.5	50.7	6.1	2.95
PR	21.0	0.89	0.02	0.59	16.1	1.6	52.8	6.7	2.51
Spring 2019 (n=10)									
LFR	18.4	1.23	0.05	0.50	14.5	1.5	63.4	5.4	3.45
HR	18.7	1.33	0.05	0.49	16.8	1.5	69.6	5.1	3.72
CL	9.3	1.21	0.05	0.52	12.5	1.5	33.0	5.8	3.54
MLC	13.7	1.17	0.05	0.59	10.4	1.5	38.7	6.4	2.83
SB	16.5	1.19	0.04	0.51	16.2	1.5	55.4	5.3	3.36
MUR	17.2	1.20	0.06	0.54	15.0	1.5	50.1	6.3	2.91
MKR	20.7	1.21	0.13	0.52	15.7	1.5	65.3	5.7	3.16
ER	14.6	0.99	0.0007	0.56	12.9	1.5	42.4	6.6	2.91
TAR	14.6	1.08	0.04	0.59	4.8	1.5	44.0	6.4	3.02
PR	14.7	1.07	0.06	0.61	6.1	1.6	38.1	6.3	2.59

Table 2-3 PARAFAC-derived fluorescent DOM components. Numbers in brackets refer to the second peak of excitation.

Components	Ex/Em (nm)	Peak name[1]	General assignment[2]	Molecular association	Sources and reactivity
C1	250/460	A_c	Terrestrial humic-like	Aromatic, intermediate MW[3]	T[2], P+[3,4], Pr[3,4]
C2	< 240 (317)/445	A_c/C	Terrestrial humic-like	High aromaticity, high MW[2,3]	T[2], P-[3]
C3	360 (262)/460	A_c/C	Terrestrial humic-like	High aromaticity, high MW[2,3]	T[2], P-[3]
C4	311/420	C	Terrestrial humic-like	High aromaticity, high MW[2,3]	T[2], P-[3]
C5	< 240 (286)/395	M	Microbial humic-like	Aliphatic[3], low MW[2]	M+[3,5], M-[5]
C6	285 (405)/485	C+	Terrestrial humic-like	High aromaticity, high MW[2]	T[2]
C7	272/330	B/T[3,6]	Tryptophan-like	Aliphatic, low MW[2]	Au[3,6], M+[6], M-[3]
C8	< 240/350	A_T	Tryptophan-like	Aliphatic, low MW[2]	Au, M+[2]

1 Coble et al. (2014). 2 Fellman, Hood and Spencer (2010). 3 Lambert et al. (2016). 4 Chen et al. (2010). 5 Singh, D'Sa and Swenson (2010). 6 Stubbins et al. (2014). Au: autochthonous production; T: terrestrial inputs; M+: microbial degradation; M-: biolabile; P+: photoproduct; Pr: photo-resistant; P-: photosensitive.

2.11 SUPPLEMENTARY INFORMATION

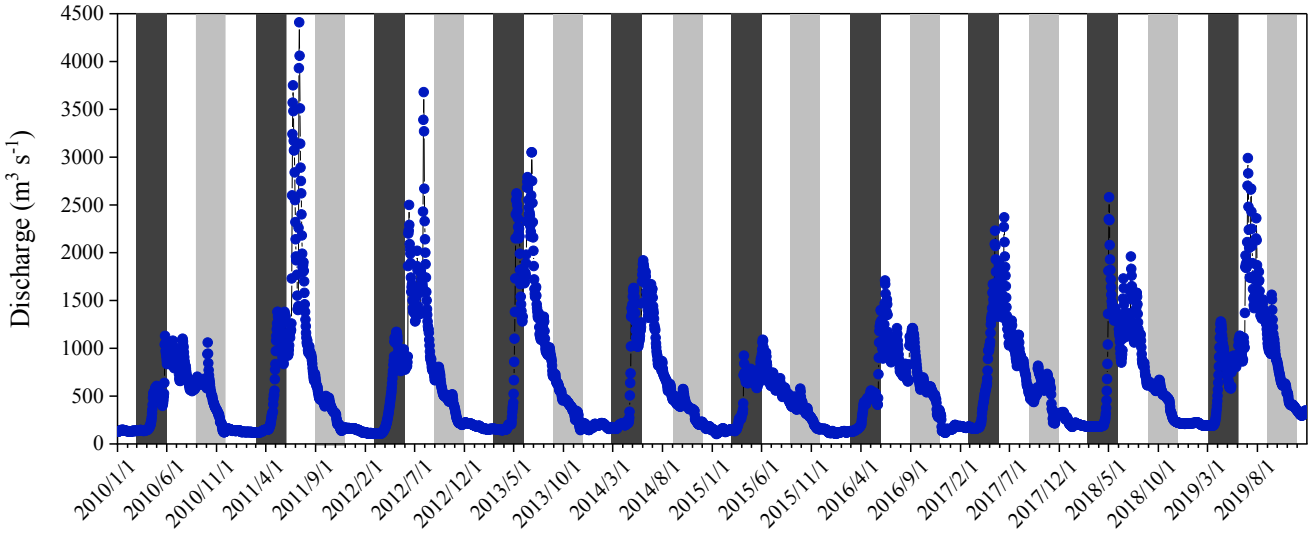

Figure S2-1 Daily flow rate of the lower Athabasca River (LAR) from 2010 to 2019. Deep gray and gray areas denote the high-flow (snowmelt period) and base flow conditions, respectively. Data were derived from the Water Survey of Canada (https://wateroffice.ec.gc.ca/) for the AR station below Fort McMurray (07DA001).

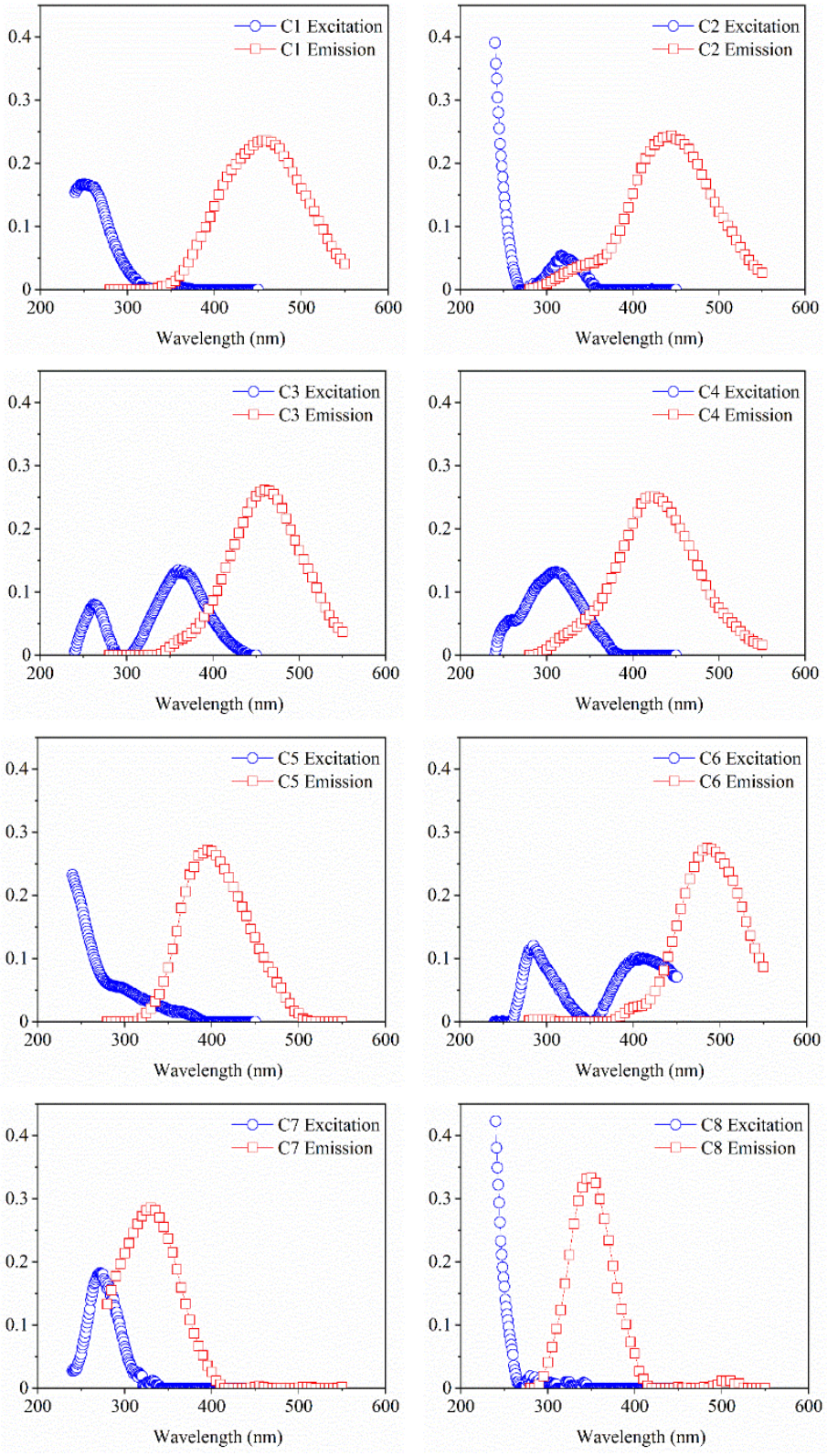

Figure S2-2 Excitation and emission spectra of 8 PARAFAC-derived fluorescent components.

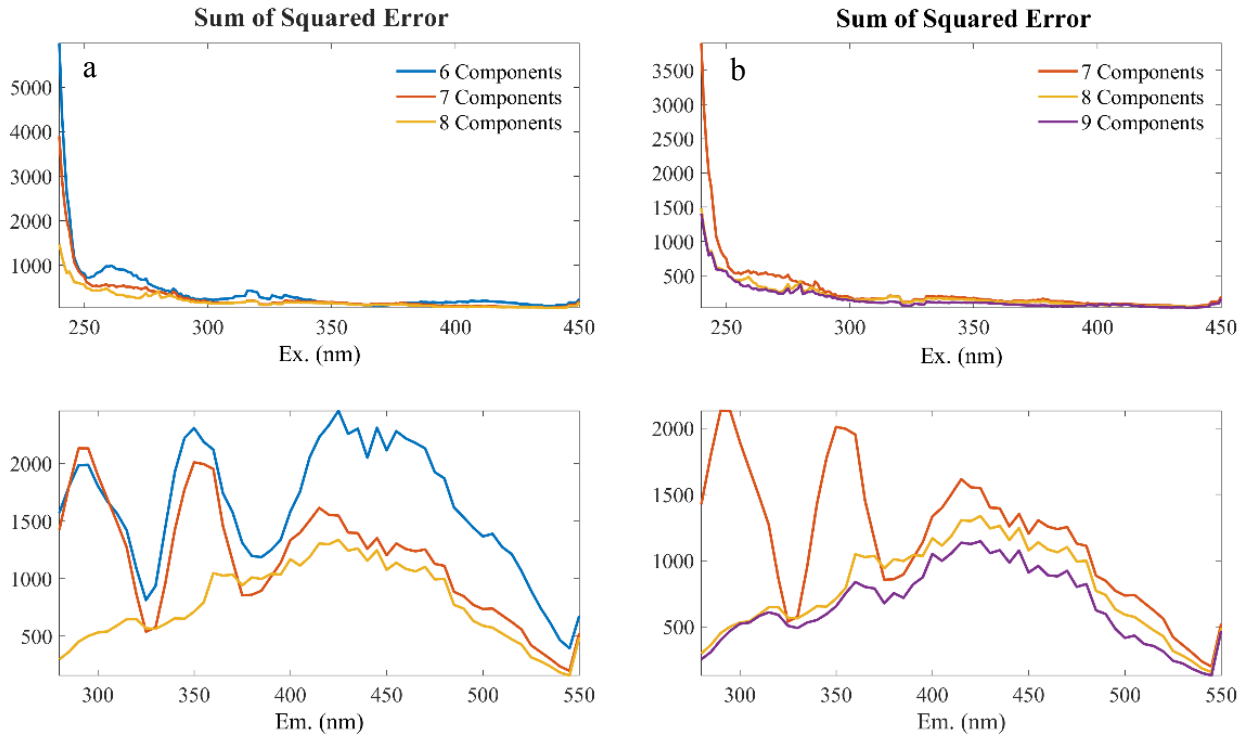

Figure S2-3 The sum of squared residuals in the excitation and emission directions for 6, 7, and 8 component (a) and 7, 8, and 9 component (b) models, respectively. The step from the 8 to 9 component model improved the fit marginally across the entire spectrum, while a large improvement and removal of peak-like features was provided by the step from the 7 to 8 component model, suggesting that 8 component model is adequate.

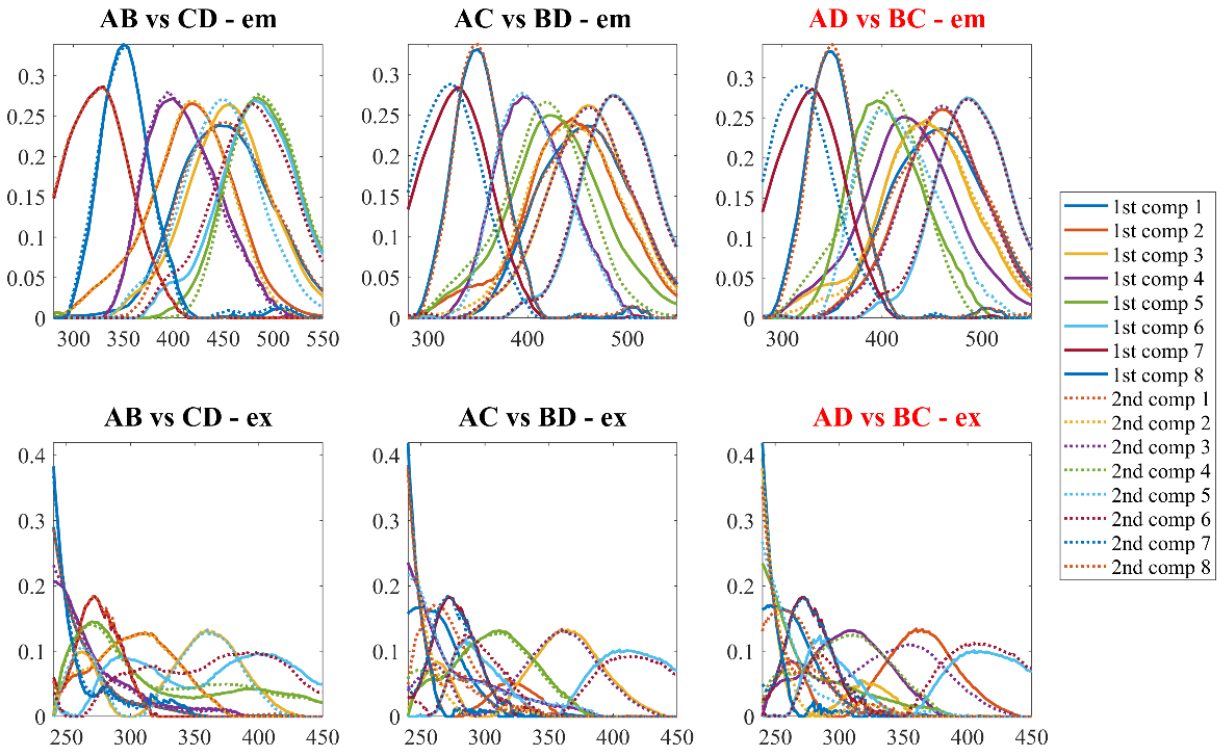

Figure S2-4 Split-half validation for the 8 component PARAFAC model.

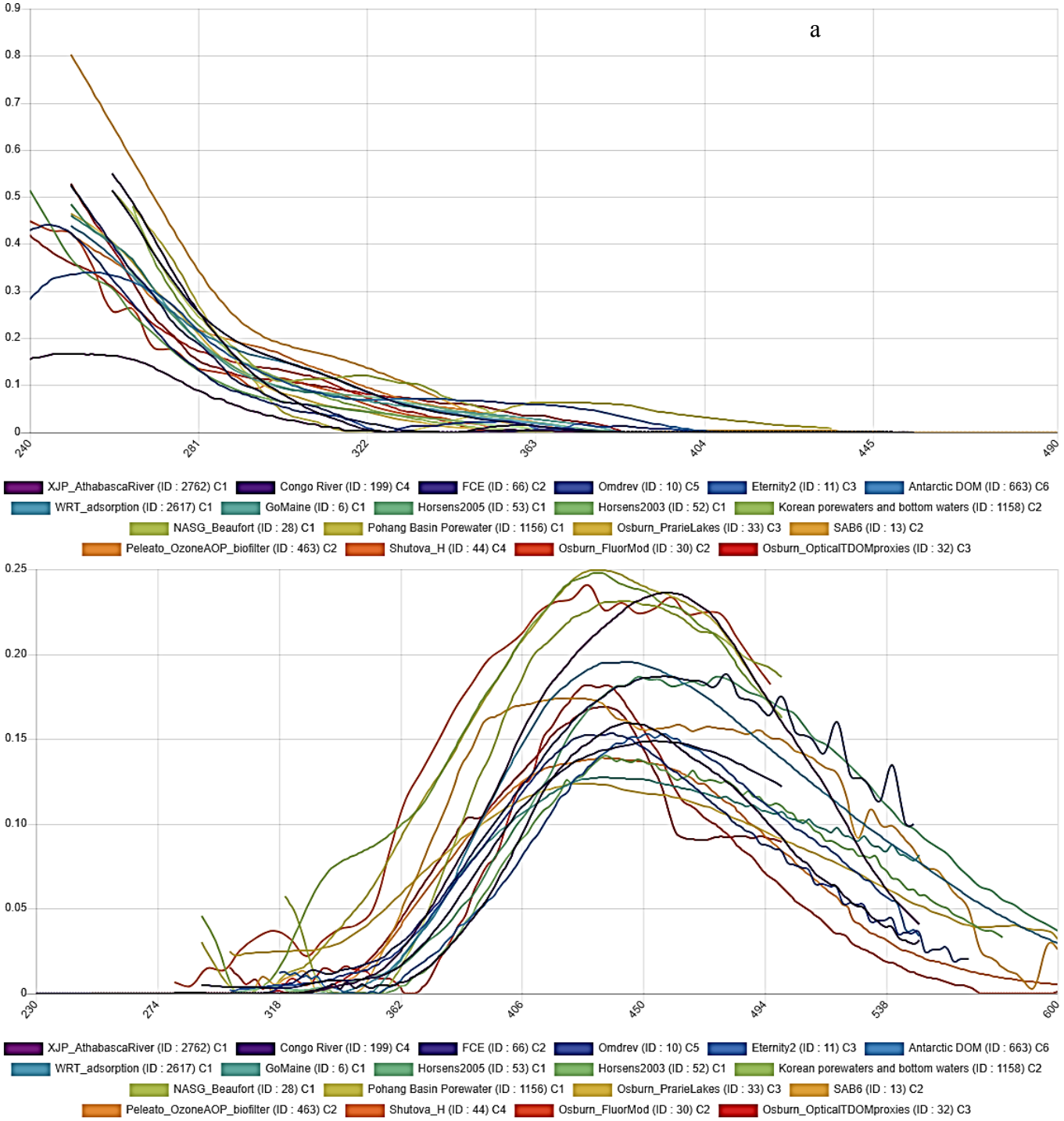
a
0.9
0.8
0.7
0.6
0.5
0.4
0.3
0.2
0.1
0
240
281
322
363
404
445
490
XJP_AthabascaRiver (ID : 2762) C1
Congo River (ID : 199) C4
FCE (ID : 66) C2
Omdrev (ID : 10) C5
Eternity2 (ID : 11) C3
Antarctic DOM (ID : 663) C6
WRT_adsorption (ID : 2617) C1
GoMaine (ID : 6) C1
Horsens2005 (ID : 53) C1
Horsens2003 (ID : 52) C1
Korean porewaters and bottom waters (ID : 1158) C2
NASG_Beaufort (ID : 28) C1
Pohang Basin Porewater (ID : 1156) C1
Osburn_PrarieLakes (ID : 33) C3
SAB6 (ID : 13) C2
Peleato_OzoneAOP_biofilter (ID : 463) C2
Shutova_H (ID : 44) C4
Osburn_FluorMod (ID : 30) C2
Osburn_OpticalTDOMproxies (ID : 32) C3
0.25
0.20
0.15
0.10
0.05
0
230
274
318
362
406
450
494
538
600
XJP_AthabascaRiver (ID : 2762) C1
Congo River (ID : 199) C4
FCE (ID : 66) C2
Omdrev (ID : 10) C5
Eternity2 (ID : 11) C3
Antarctic DOM (ID : 663) C6
WRT_adsorption (ID : 2617) C1
GoMaine (ID : 6) C1
Horsens2005 (ID : 53) C1
Horsens2003 (ID : 52) C1
Korean porewaters and bottom waters (ID : 1158) C2
NASG_Beaufort (ID : 28) C1
Pohang Basin Porewater (ID : 1156) C1
Osburn_PrarieLakes (ID : 33) C3
SAB6 (ID : 13) C2
Peleato_OzoneAOP_biofilter (ID : 463) C2
Shutova_H (ID : 44) C4
Osburn_FluorMod (ID : 30) C2
Osburn_OpticalTDOMproxies (ID : 32) C3

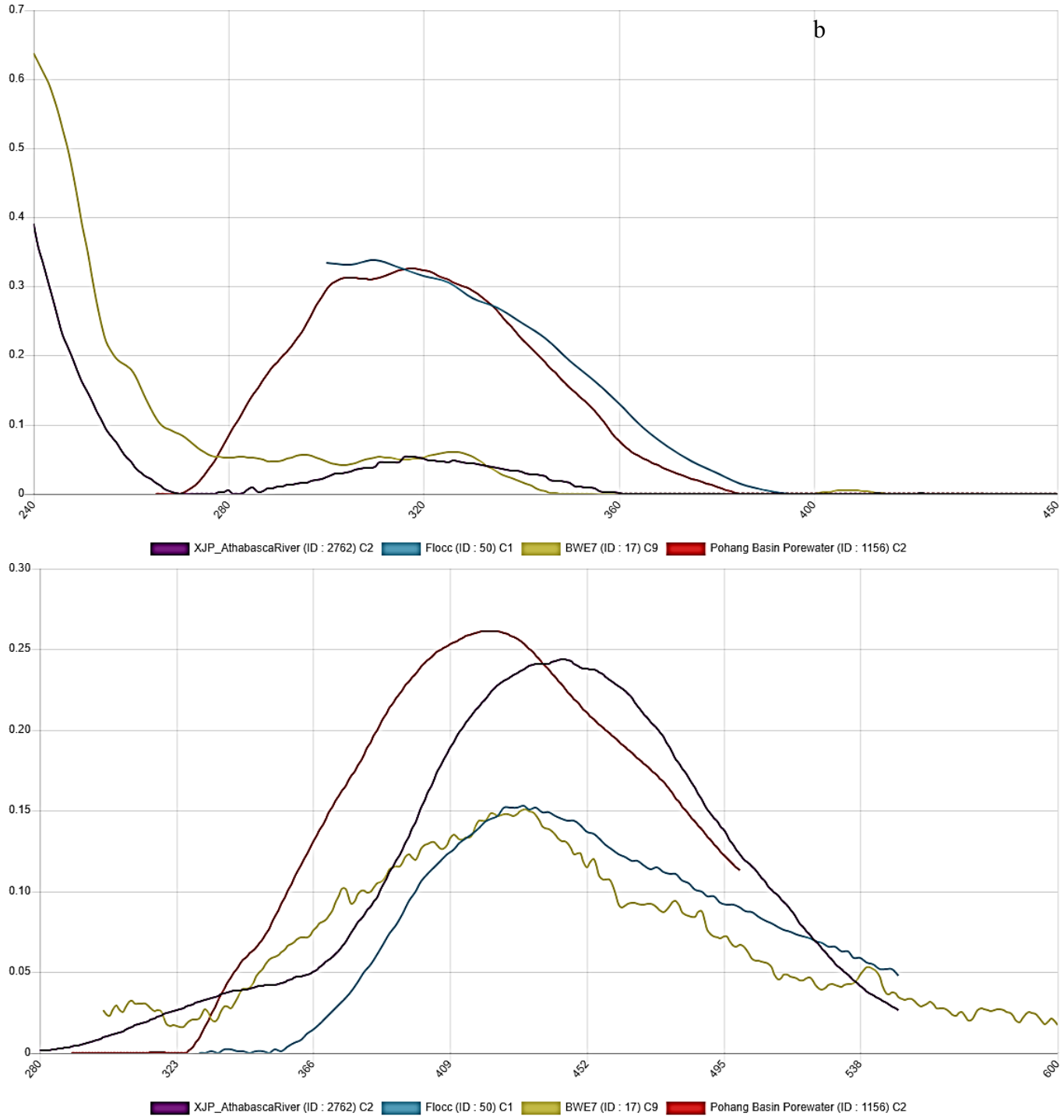
b
0.7
0.6
0.5
0.4
0.3
0.2
0.1
0
240
280
320
360
400
450
XJP_AthabascaRiver (ID : 2762) C2
Flocc (ID : 50) C1
BWE7 (ID : 17) C9
Pohang Basin Porewater (ID : 1156) C2
0.30
0.25
0.20
0.15
0.10
0.05
0
280
323
366
409
452
495
538
600
XJP_AthabascaRiver (ID : 2762) C2
Flocc (ID : 50) C1
BWE7 (ID : 17) C9
Pohang Basin Porewater (ID : 1156) C2

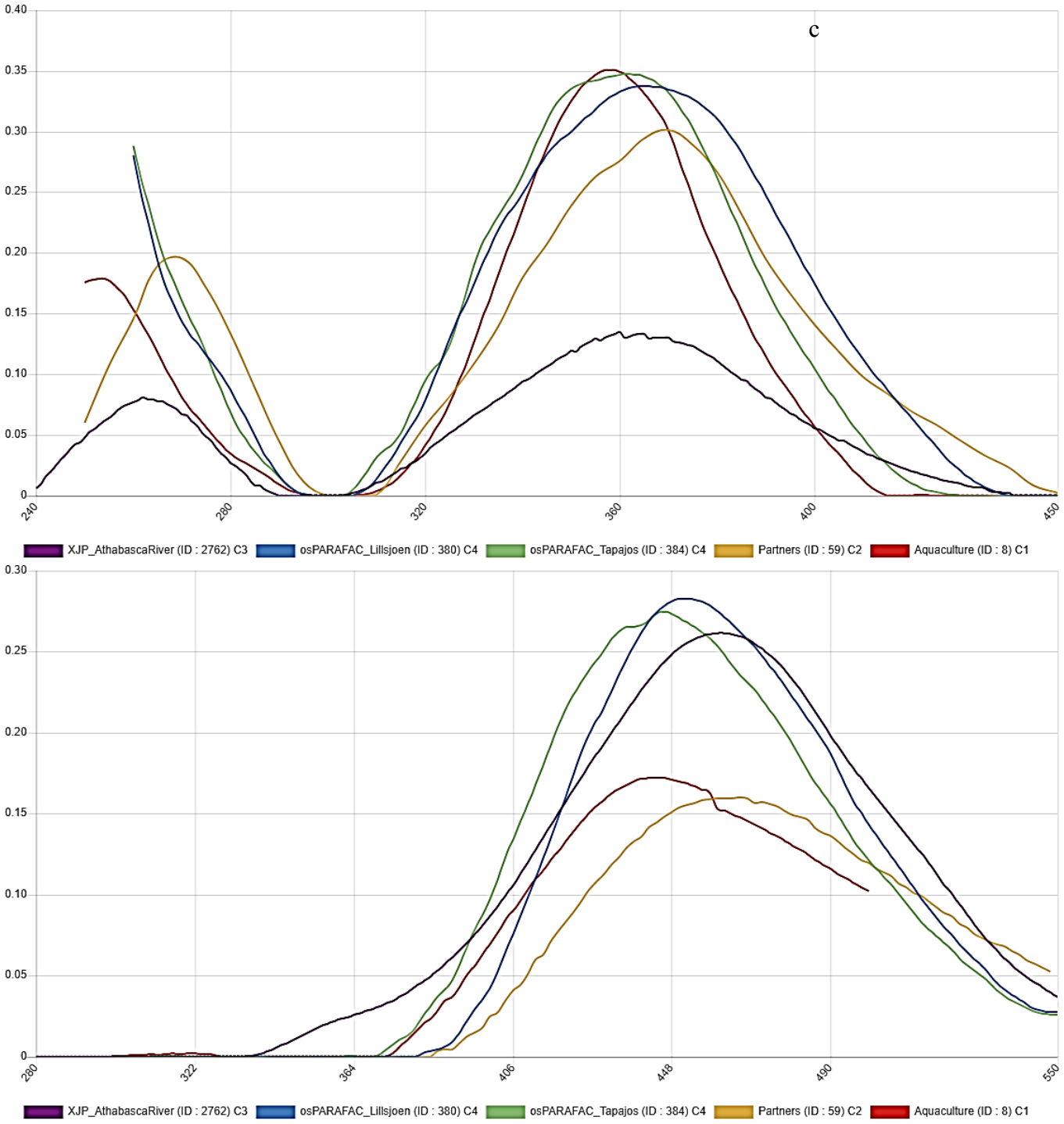
c
0.40
0.35
0.30
0.25
0.20
0.15
0.10
0.05
0
240
280
320
360
400
450
XJP_AthabascaRiver (ID : 2762) C3
osPARAFAC_Lillsjoen (ID : 380) C4
osPARAFAC_Tapajos (ID : 384) C4
Partners (ID : 59) C2
Aquaculture (ID : 8) C1
0.30
0.25
0.20
0.15
0.10
0.05
0
280
322
364
406
448
490
550
XJP_AthabascaRiver (ID : 2762) C3
osPARAFAC_Lillsjoen (ID : 380) C4
osPARAFAC_Tapajos (ID : 384) C4
Partners (ID : 59) C2
Aquaculture (ID : 8) C1

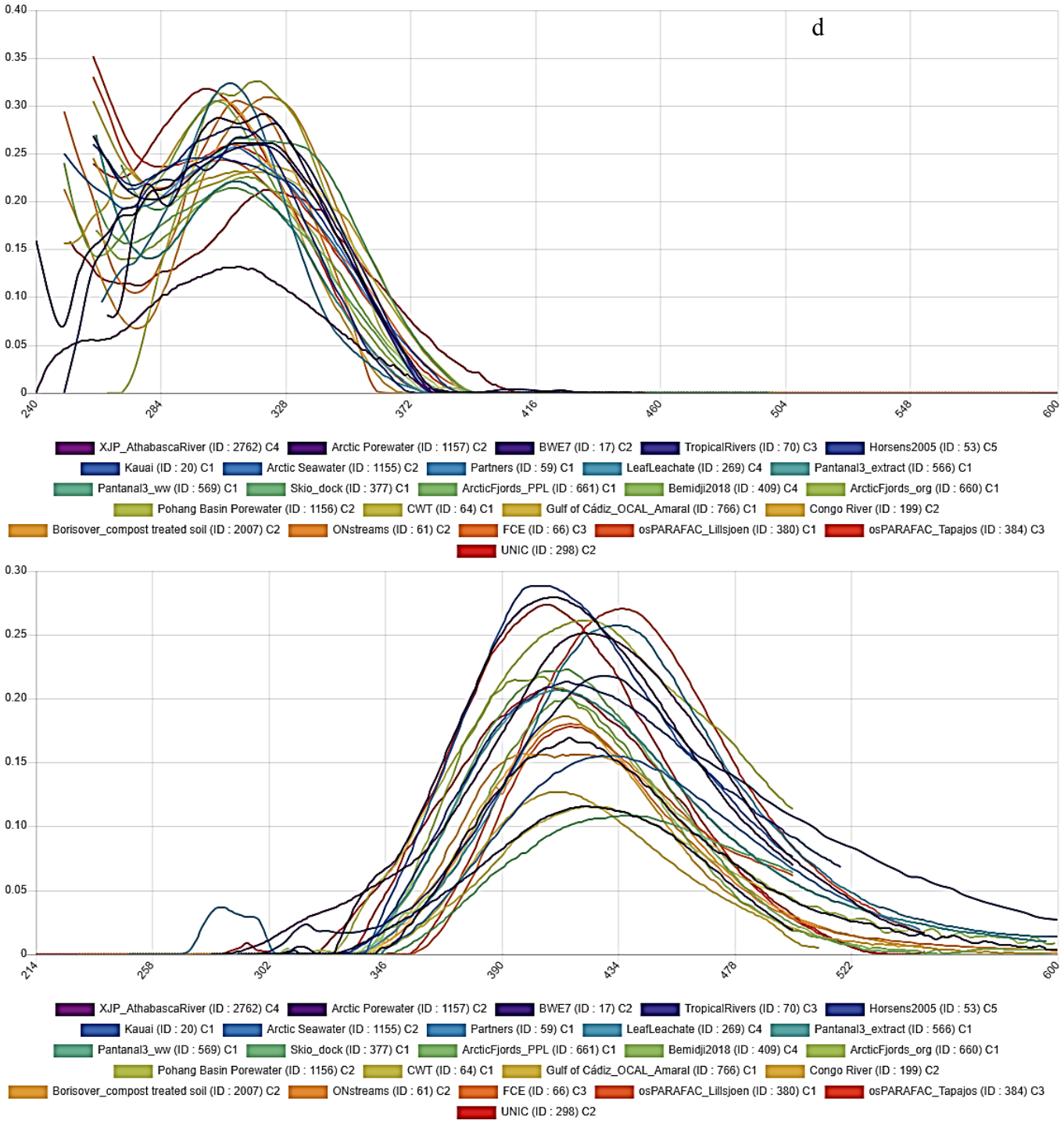
d
0.40
0.35
0.30
0.25
0.20
0.15
0.10
0.05
0
240
284
328
372
416
460
504
548
600
XJP_AthabascaRiver (ID : 2762) C4
Arctic Porewater (ID : 1157) C2
BWE7 (ID : 17) C2
TropicalRivers (ID : 70) C3
Horsens2005 (ID : 53) C5
Kauai (ID : 20) C1
Arctic Seawater (ID : 1155) C2
Partners (ID : 59) C1
LeafLeachate (ID : 269) C4
Pantanal3_extract (ID : 566) C1
Pantanal3_ww (ID : 569) C1
Skio_dock (ID : 377) C1
ArcticFjords_PPL (ID : 661) C1
Bemidji2018 (ID : 409) C4
ArcticFjords_org (ID : 660) C1
Pohang Basin Porewater (ID : 1156) C2
CWT (ID : 64) C1
Gulf of Cádiz_OCAL_Amaral (ID : 766) C1
Congo River (ID : 199) C2
Borisover_compost treated soil (ID : 2007) C2
ONstreams (ID : 61) C2
FCE (ID : 66) C3
osPARAFAC_Lillsjoen (ID : 380) C1
osPARAFAC_Tapajos (ID : 384) C3
UNIC (ID : 298) C2
0.30
0.25
0.20
0.15
0.10
0.05
0
214
258
302
346
390
434
478
522
600
XJP_AthabascaRiver (ID : 2762) C4
Arctic Porewater (ID : 1157) C2
BWE7 (ID : 17) C2
TropicalRivers (ID : 70) C3
Horsens2005 (ID : 53) C5
Kauai (ID : 20) C1
Arctic Seawater (ID : 1155) C2
Partners (ID : 59) C1
LeafLeachate (ID : 269) C4
Pantanal3_extract (ID : 566) C1
Pantanal3_ww (ID : 569) C1
Skio_dock (ID : 377) C1
ArcticFjords_PPL (ID : 661) C1
Bemidji2018 (ID : 409) C4
ArcticFjords_org (ID : 660) C1
Pohang Basin Porewater (ID : 1156) C2
CWT (ID : 64) C1
Gulf of Cádiz_OCAL_Amaral (ID : 766) C1
Congo River (ID : 199) C2
Borisover_compost treated soil (ID : 2007) C2
ONstreams (ID : 61) C2
FCE (ID : 66) C3
osPARAFAC_Lillsjoen (ID : 380) C1
osPARAFAC_Tapajos (ID : 384) C3
UNIC (ID : 298) C2

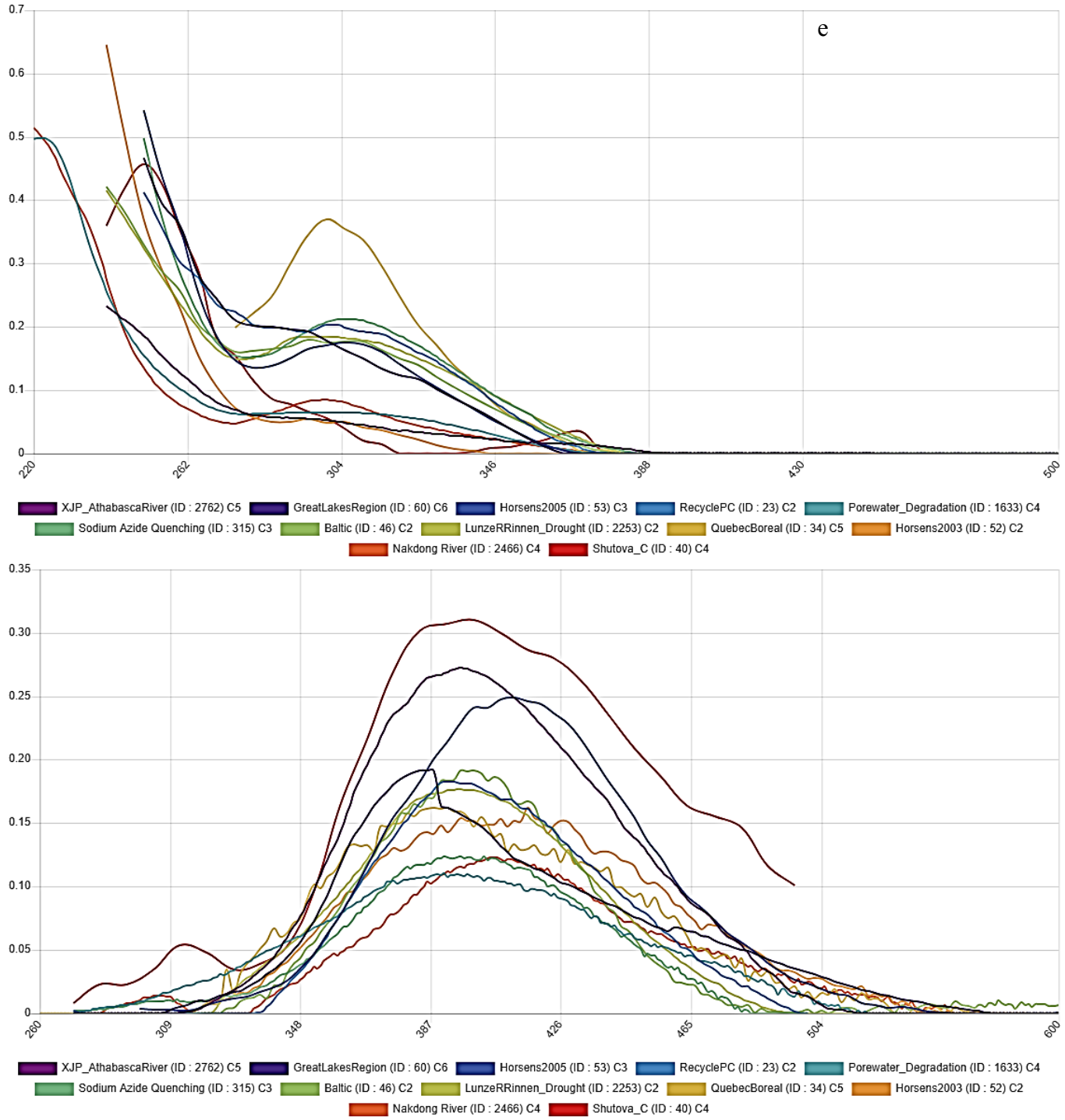
e
0.7
0.6
0.5
0.4
0.3
0.2
0.1
0
220
262
304
346
388
430
500
XJP_AthabascaRiver (ID : 2762) C5
GreatLakesRegion (ID : 60) C6
Horsens2005 (ID : 53) C3
RecyclePC (ID : 23) C2
Porewater_Degradation (ID : 1633) C4
Sodium Azide Quenching (ID : 315) C3
Baltic (ID : 46) C2
LunzeRRinnen_Drought (ID : 2253) C2
QuebecBoreal (ID : 34) C5
Horsens2003 (ID : 52) C2
Nakdong River (ID : 2466) C4
Shutova_C (ID : 40) C4
0.35
0.30
0.25
0.20
0.15
0.10
0.05
0
260
309
348
387
426
465
504
600
XJP_AthabascaRiver (ID : 2762) C5
GreatLakesRegion (ID : 60) C6
Horsens2005 (ID : 53) C3
RecyclePC (ID : 23) C2
Porewater_Degradation (ID : 1633) C4
Sodium Azide Quenching (ID : 315) C3
Baltic (ID : 46) C2
LunzeRRinnen_Drought (ID : 2253) C2
QuebecBoreal (ID : 34) C5
Horsens2003 (ID : 52) C2
Nakdong River (ID : 2466) C4
Shutova_C (ID : 40) C4

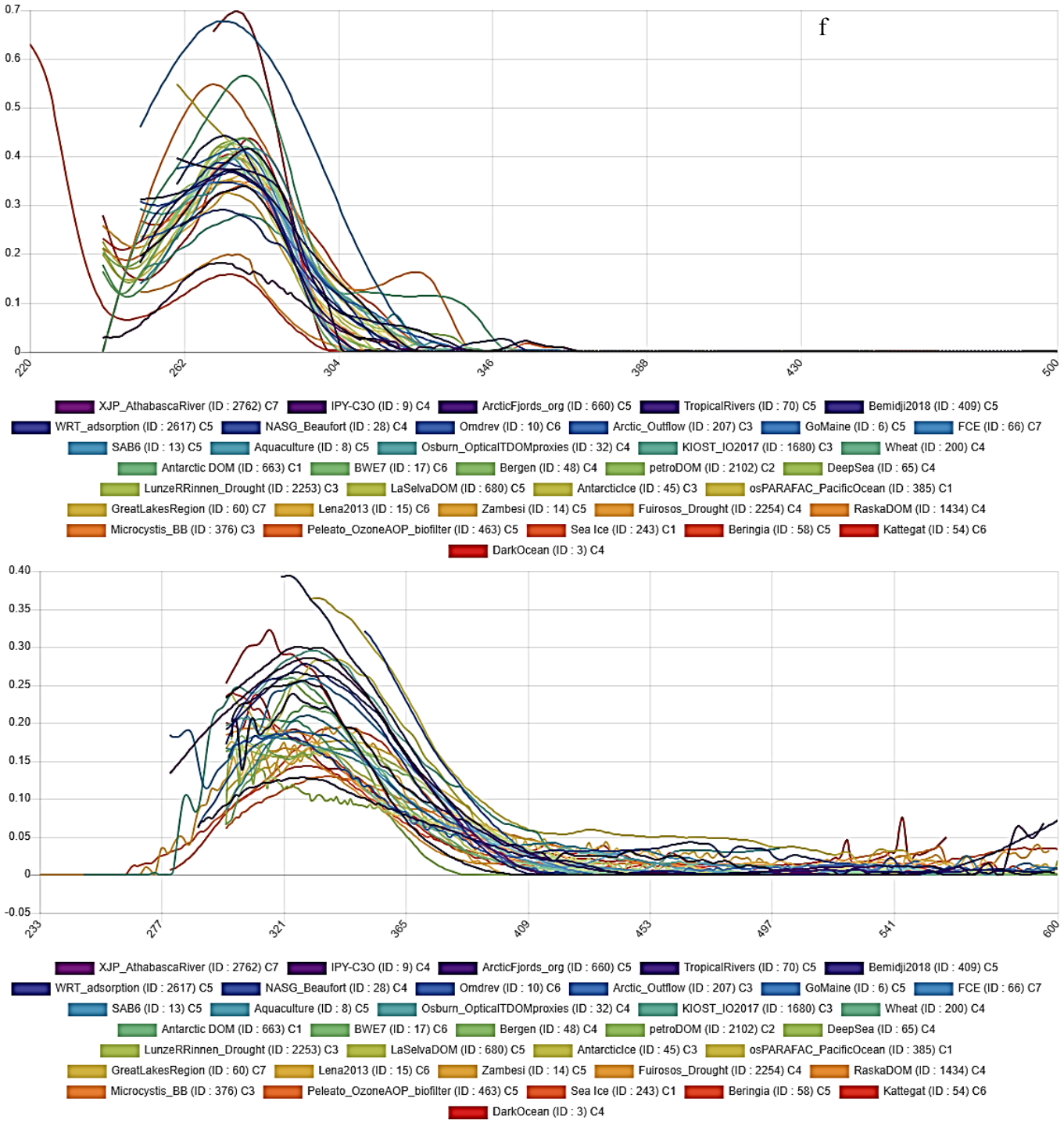
f
0.7
0.6
0.5
0.4
0.3
0.2
0.1
0
220
262
304
346
388
430
500
XJP_AthabascaRiver (ID : 2762) C7
IPY-C3O (ID : 9) C4
ArcticFjords_org (ID : 660) C5
TropicalRivers (ID : 70) C5
Bemidji2018 (ID : 409) C5
WRT_adsorption (ID : 2617) C5
NASG_Beaufort (ID : 28) C4
Omdrev (ID : 10) C6
Arctic_Outflow (ID : 207) C3
GoMaine (ID : 6) C5
FCE (ID : 66) C7
SAB6 (ID : 13) C5
Aquaculture (ID : 8) C5
Osburn_OpticalTDOMproxies (ID : 32) C4
KIOST_IO2017 (ID : 1680) C3
Wheat (ID : 200) C4
Antarctic DOM (ID : 663) C1
BWE7 (ID : 17) C6
Bergen (ID : 48) C4
petroDOM (ID : 2102) C2
DeepSea (ID : 65) C4
LunzeRRinnen_Drought (ID : 2253) C3
LaSelvaDOM (ID : 680) C5
AntarcticIce (ID : 45) C3
osPARAFAC_PacificOcean (ID : 385) C1
GreatLakesRegion (ID : 60) C7
Lena2013 (ID : 15) C6
Zambesi (ID : 14) C5
Fuirosos_Drought (ID : 2254) C4
RaskaDOM (ID : 1434) C4
Microcystis_BB (ID : 376) C3
Peleato_OzoneAOP_biofilter (ID : 463) C5
Sea Ice (ID : 243) C1
Beringia (ID : 58) C5
Kattegat (ID : 54) C6
DarkOcean (ID : 3) C4
0.40
0.35
0.30
0.25
0.20
0.15
0.10
0.05
0
-0.05
233
277
321
365
409
453
497
541
600
XJP_AthabascaRiver (ID : 2762) C7
IPY-C3O (ID : 9) C4
ArcticFjords_org (ID : 660) C5
TropicalRivers (ID : 70) C5
Bemidji2018 (ID : 409) C5
WRT_adsorption (ID : 2617) C5
NASG_Beaufort (ID : 28) C4
Omdrev (ID : 10) C6
Arctic_Outflow (ID : 207) C3
GoMaine (ID : 6) C5
FCE (ID : 66) C7
SAB6 (ID : 13) C5
Aquaculture (ID : 8) C5
Osburn_OpticalTDOMproxies (ID : 32) C4
KIOST_IO2017 (ID : 1680) C3
Wheat (ID : 200) C4
Antarctic DOM (ID : 663) C1
BWE7 (ID : 17) C6
Bergen (ID : 48) C4
petroDOM (ID : 2102) C2
DeepSea (ID : 65) C4
LunzeRRinnen_Drought (ID : 2253) C3
LaSelvaDOM (ID : 680) C5
AntarcticIce (ID : 45) C3
osPARAFAC_PacificOcean (ID : 385) C1
GreatLakesRegion (ID : 60) C7
Lena2013 (ID : 15) C6
Zambesi (ID : 14) C5
Fuirosos_Drought (ID : 2254) C4
RaskaDOM (ID : 1434) C4
Microcystis_BB (ID : 376) C3
Peleato_OzoneAOP_biofilter (ID : 463) C5
Sea Ice (ID : 243) C1
Beringia (ID : 58) C5
Kattegat (ID : 54) C6
DarkOcean (ID : 3) C4

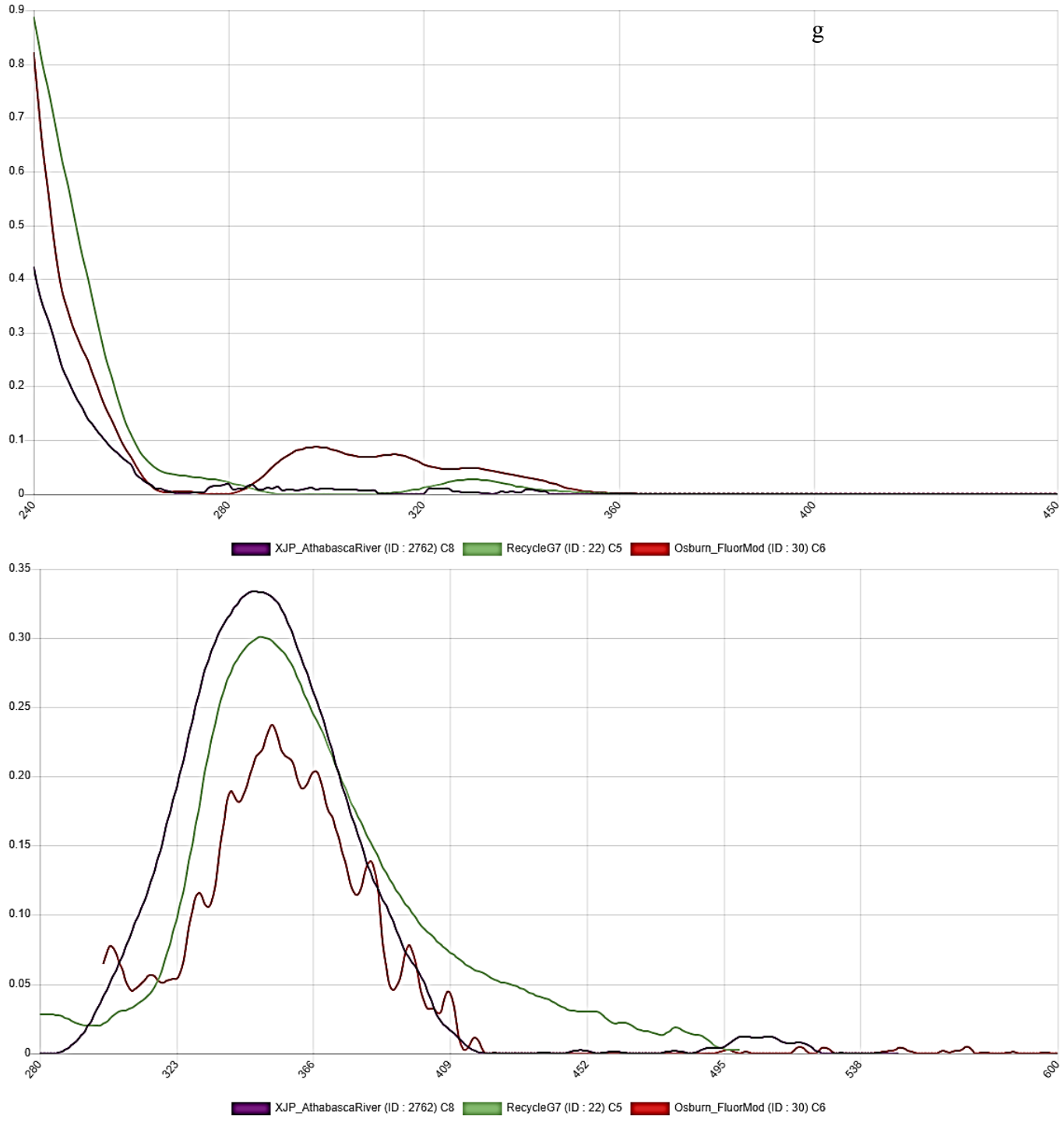

Figure S2-5 Matches for PARAFAC components *(except C6)* between this study and the OpenFluor database (accessed on Aug 7, 2020).

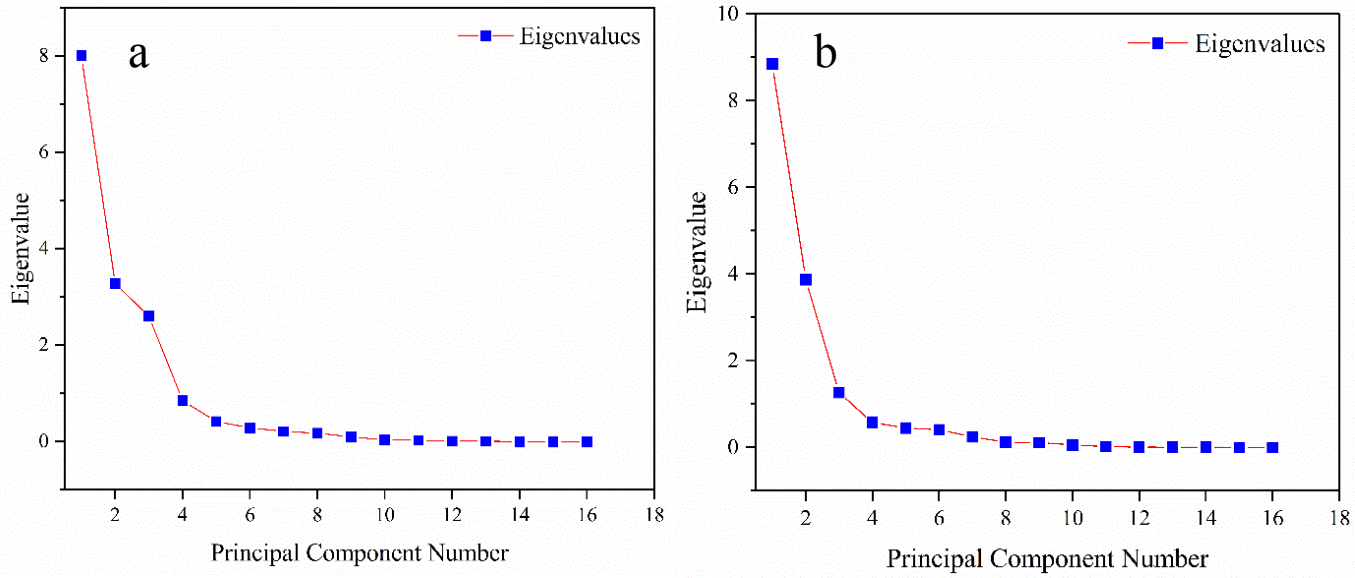

Figure S2-6 Scree plots of two individual PCA analyses for mainstem & TR (a) and mixing zones (b).

Table S2-1 Modified Tucker's Congruence Coefficient (mTCC ≥ 0.95) for the PARAFAC components between the present study and 38 PARAFAC models summarized by *Parr et al. (2014).*

	This_study							
	C1	**C2**	**C3**	**C4**	**C5**	**C6**	**C7**	**C8**
Burrows_2013								
Chen_2010	C2 0.99			C3 0.96	C4 0.95		C7 0.98	
CM_2005							C8 0.96	
Cory_2012			C3 0.95	C1 0.95				
Fellman_2009						C3 0.95	C7/C8 0.97/0.96	
Fellman_2011	C1 0.96				C3 0.95			
Guo_2011							C4 0.98	
Holbrook_2006					C2 0.95			
Hong_2011				C2 0.95				
Jorgensen_2011							C2 0.95	
Kothawala_2012	C3 0.98					C4 0.95		
Kowalczuk_2010	C2 0.97						C5 0.99	
Lapierre_2009		C1 0.97					C8 0.95	
Lu_2013	C5 0.97						C4 0.97	
Lutz_2012								
Massicotte_2011		C1 0.95						
Murphy_2006		C9 0.96		C2 0.99	C4 0.95		C6 0.98	
Murphy_2008			C8 0.95	C1 0.98				
Osburn_2011	C4 0.97						C6 0.96	
Osburn_2012	C3 0.97			C2 0.96			C6 0.97	
Parr_2013	C1 0.97				C8 0.98		C9 0.98	
Singh_2010					C3 0.95			
Singh_2013			C4 0.97	C2 0.96	C2 0.97	C3 0.95	C5 0.99	
Stedmon_2003	C1 0.98			C4 0.95	C2 0.97			
Stedmon_2005	C1 0.98			C5/C6 0.98/0.95	C3 0.98			
Stedmon_2007_EST								
Stedmon_2007_MC					C2 0.97		C5 0.96	
Stedmon_2011_JGR							C3 0.98	
Walker_2009	C2 0.95						C5 0.96	
Williams_2010				C2 0.96				
Yamashita_2010				C1/C3 0.95/0.98			C5 0.99	
Yamashita_2010_DSRI							C4 0.97	
Yamashita_2011				C1 0.97				
Yamashita_2011_Odyn				C1 0.96			C5 0.95	
Yang_2011								
Yang_2012_MC							C3 0.95	
Yang_2013_AG								
Yang_2013_MC					C1 0.95			

3.0 CONCLUSIONS

The functionality of dissolved organic matter (DOM) in natural waters depends on its size and composition. Identifying the sources and associated properties of DOM is vital to understand its effects on downstream ecosystems. The integration of high-resolution sampling allows us to resolve DOM sources and mixing processes in the lower Athabasca River (LAR) using asymmetrical flow field-flow fractionation (AF4) with offline excitation emission matrices (EEMs) measurements and parallel factor (PARAFAC) analysis. We found that inputs of DOM from the major tributaries shifted DOM quality in the LAR. Flowing downstream, DOM tended to be higher in concentrations of dissolved organic carbon (DOC) and degrees of humification and aromaticity. Seasonal variations of DOM as a result of spring freshet were observed, during which times DOM tended to be higher in molecular mass and highly richer in protein-like components relative to humic-like components.

River mixing has great potential to alter DOM quality. In this study, conservative mixing behaviors of DOM at river confluences were observed. Contrasting mixing patterns among mixing zones suggest that both hydrological conditions and river geomorphology affect mixing patterns of DOM between the LAR and its tributaries. Our results demonstrate that DOM could be used as a *quasi*-conservative tracer during mixing at large river confluences. Findings from this study will enhance our ability to determine sources of DOM and to distinguish trends of mixing between the mainstem and the tributaries for DOM-associated trace elements in the boreal zone. They will also provide new insights into the metal-binding properties of DOM exported from terrestrial ecosystems under different hydrological conditions.

BIBLIOGRAPHY

Abdulla H. A. N., Minor E. C. and Hatcher P. G. (2010) Using two-dimensional correlations of ^{13}C NMR and FTIR to investigate changes in the chemical composition of dissolved organic matter along an estuarine transect. *Environ. Sci. Technol.* **44**, 8044–8049.

Ågren A., Buffam I., Berggren M., Bishop K., Jansson M. and Laudon H. (2008) Dissolved organic carbon characteristics in boreal streams in a forest-wetland gradient during the transition between winter and summer. *J. Geophys. Res.* **113**, G03031.

Ahad J. M. E., Pakdel H., Gammon P. R., Mayer B., Savard M. M., Peru K. M. and Headley J. V. (2020) Distinguishing natural from anthropogenic sources of acid extractable organics in groundwater near oil sands tailings ponds. *Environ. Sci. Technol.* **54**, 2790–2799.

Ahrland S., Chatt J. and Davies N. R. (1958) The relative affinities of ligand atoms for acceptor molecules and ions. *Q. Rev. Chem. Soc.* **12**, 265.

Aiken G. R., Hsu-Kim H. and Ryan J. N. (2011) Influence of dissolved organic matter on the environmental fate of metals, nanoparticles, and colloids. *Environ. Sci. Technol.* **45**, 3196–3201.

Aitkenhead-Peterson J. A., McDowell W. H. and Neff J. C. (2003) 2 - Sources, Production, and Regulation of Allochthonous Dissolved Organic Matter Inputs to Surface Waters. In *Aquatic ecosystems* (eds. S. Findlay and R. L. Sinsabaugh). Academic Press. Amsterdam, London, pp. 25–70.

Allen G. H. and Pavelsky T. M. (2018) Global extent of rivers and streams. *Science* **361**, 585–588.

Amon R. M. W. and Benner R. (1996) Bacterial utilization of different size classes of dissolved organic matter. *Limnol. Oceanogr.* **41**, 41–51.

Andersson J.-O. and Nyberg L. (2008) Spatial variation of wetlands and flux of dissolved organic carbon in boreal headwater streams. *Hydrol. Process.* **22**, 1965–1975.

Aucour A.-M., Tao F.-X., Moreira-Turcq P., Seyler P., Sheppard S. and Benedetti M.F. (2003) The Amazon River: behaviour of metals (Fe, Al, Mn) and dissolved organic matter in the initial mixing at the Rio Negro/Solimões confluence. *Chem. Geol.* **197**, 271–285.

Avagyan A., Runkle B. R. K., Hennings N., Haupt H., Virtanen T. and Kutzbach L. (2016) Dissolved organic matter dynamics during the spring snowmelt at a boreal river valley mire complex in Northwest Russia. *Hydrol. Process.* **30**, 1727–1741.

Baalousha M., Kammer F. V. D., Motelica-Heino M., Hilal H. S. and Le Coustumer P. (2006) Size fractionation and characterization of natural colloids by flow-field flow fractionation coupled to multi-angle laser light scattering. *J. Chromatogr. A* **1104**, 272–281.

Backes C. A. and Tipping E. (1987) An Evaluation of the Use of Cation-Exchange Resin for the Determination of Organically-Complexed Al in Natural Acid Waters. *Int. J. Environ. Anal. Chem.* **30**, 135–143.

Barker J. D., Dubnick A., Lyons W. B. and Chin Y.-P. (2013) Changes in dissolved organic matter

(DOM) fluorescence in proglacial Antarctic streams. *Arct. Antarct. Alp. Res.* **45**, 305–317.

Battin T. J. (1998) Dissolved organic matter and its optical properties in a blackwater tributary of the upper Orinoco river, Venezuela. *Org. Geochem.* **28**, 561–569.

Battin T. J., Kaplan L. A., Findlay S., Hopkinson C. S., Marti E., Packman A. I., Newbold J. D. and Sabater F. (2008) Biophysical controls on organic carbon fluxes in fluvial networks. *Nat. Geosci.* **1**, 95–100.

Bauer J. E. and Bianchi T. S. (2011) 5.02 - Dissolved organic carbon cycling and transformation. In *Treatise on estuarine and coastal science* (eds. E. Wolanski and D. S. McLusky). Academic Press. London, Waltham, MA, pp. 7–67.

Bertilsson S. and Jones J. B. (2003) 1 - Supply of dissolved organic matter to aquatic ecosystems: autochthonous sources. In *Aquatic ecosystems* (eds. S. Findlay and R. L. Sinsabaugh). Academic Press. Amsterdam, London, pp. 3–24.

Bonan G. B. and Shugart H. H. (1989) Environmental factors and ecological processes in boreal forests. *Annu. Rev. Ecol. Syst.* **20**, 1–28.

Broder T., Knorr K.-H. and Biester H. (2017) Changes in dissolved organic matter quality in a peatland and forest headwater stream as a function of seasonality and hydrologic conditions. *Hydrol. Earth Syst. Sci.* **21**, 2035–2051.

Burns M. A., Barnard H. R., Gabor R. S., McKnight D. M. and Brooks P. D. (2016) Dissolved organic matter transport reflects hillslope to stream connectivity during snowmelt in a montane catchment. *Water Resour. Res.* **52**, 4905–4923.

Cade-Menun B. J., Bell G., Baker-Ismail S., Fouli Y., Hodder K., McMartin D. W., Perez-Valdivia C. and Wu K. (2013) Nutrient loss from Saskatchewan cropland and pasture in spring snowmelt runoff. *Can. J. Soil. Sci.* **93**, 445–458.

Cao X., Aiken G. R., Spencer R. G.M., Butler K., Mao J. and Schmidt-Rohr K. (2016) Novel insights from NMR spectroscopy into seasonal changes in the composition of dissolved organic matter exported to the Bering Sea by the Yukon River. *Geochim. Cosmochim. Acta* **181**, 72–88.

Chanton J. P., Bauer J. E., Glaser P. A., Siegel D. I., Kelley C. A., Tyler S. C., Romanowicz E. H. and Lazrus A. (1995) Radiocarbon evidence for the substrates supporting methane formation within northern Minnesota peatlands. *Geochim. Cosmochim. Acta* **59**, 3663–3668.

Chanton J. P., Glaser P. H., Chasar L. S., Burdige D. J., Hines M. E., Siegel D. I., Tremblay L. B. and Cooper W. T. (2008) Radiocarbon evidence for the importance of surface vegetation on fermentation and methanogenesis in contrasting types of boreal peatlands. *Glob. Biogeochem. Cycle* **22**, GB4022.

Chen M., Price R. M., Yamashita Y. and Jaffé R. (2010) Comparative study of dissolved organic matter from groundwater and surface water in the Florida coastal Everglades using multi-dimensional spectrofluorometry combined with multivariate statistics. *Appl. Geochem.* **25**, 872–

880.

Chow A. T., Dai J., Conner W. H., Hitchcock D. R. and Wang J.-J. (2013) Dissolved organic matter and nutrient dynamics of a coastal freshwater forested wetland in Winyah Bay, South Carolina. *Biogeochemistry* **112**, 571–587.

Coble P., Spencer R. G. M., Andy Baker and Reynolds D. M. (2014) Aquatic Organic Matter Fluorescence. In *Aquatic organic matter fluorescence* (eds. Paula G. Coble, Jamie Lead, Andy Baker, Darren M. Reynolds and Robert G. M. Spencer). Cambridge University Press. New York, NY, USA, pp. 75–122.

Cuss C. W., Donner M. W., Grant-Weaver I., Noernberg T., Pelletier R., Sinnatamby R. N. and Shotyk W. (2018) Measuring the distribution of trace elements amongst dissolved colloidal species as a fingerprint for the contribution of tributaries to large boreal rivers. *Sci. Total Environ.* **642**, 1242–1251.

Cuss C. W., Donner M. W., Noernberg T., Pelletier R. and Shotyk W. (2019) EEM-PARAFAC-SOM for assessing variation in the quality of dissolved organic matter: simultaneous detection of differences by source and season. *Environ. Chem.* **16**, 360–374.

Cuss C. W., Ghotbizadeh M., Grant-Weaver I., Javed M. B., Noernberg T. and Shotyk W. (2020a) Delayed mixing of iron-laden tributaries in large boreal rivers: implications for iron transport, water quality and monitoring. *J. Hydrol.*, 125747.

Cuss C. W., Glover C. N., Javed M. B., Nagel A. and Shotyk W. (2020b) Geochemical and biological controls on the ecological relevance of total, dissolved, and colloidal forms of trace elements in large boreal rivers: review and case studies. *Environ. Rev.* **28**, 138–163.

Cuss C. W., Grant-Weaver I. and Shotyk W. (2017) AF4-ICPMS with the 300 Da membrane to resolve metal-bearing “colloids” < 1 kDa: optimization, fractogram deconvolution, and advanced quality control. *Anal. Chem.* **89**, 8027–8035.

Cuss C. W. and Guéguen C. (2012a) Determination of relative molecular weights of fluorescent components in dissolved organic matter using asymmetrical flow field-flow fractionation and parallel factor analysis. *Anal. Chim. Acta* **733**, 98–102.

Cuss C. W. and Guéguen C. (2012b) Impacts of microbial activity on the optical and copper-binding properties of leaf-litter leachate. *Front. Microbiol.* **3**, 166.

Cuss C. W. and Guéguen C. (2015) Relationships between molecular weight and fluorescence properties for size-fractionated dissolved organic matter from fresh and aged sources. *Water Res.* **68**, 487–497.

D’Andrilli J., Chanton J. P., Glaser P. H. and Cooper W. T. (2010) Characterization of dissolved organic matter in northern peatland soil porewaters by ultra high resolution mass spectrometry. *Org. Geochem.* **41**, 791–799.

Dalrymple R. M., Carfagno A. K. and Sharpless C. M. (2010) Correlations between dissolved

organic matter optical properties and quantum yields of singlet oxygen and hydrogen peroxide. *Environ. Sci. Technol.* **44**, 5824–5829.

DeAngelis D. L. (2019) The boreal forest ecosystem. In *Encyclopedia of ecology* (eds. B. D. Fath and S. E. Jørgensen). Elsevier. Amsterdam, pp. 479–483.

Dillon P. J. and Molot L. A. (1997) Effect of landscape form on export of dissolved organic carbon, iron, and phosphorus from forested stream catchments. *Water Resour. Res.* **33**, 2591–2600.

Dittmar T. and Stubbins A. (2014) 12.6 - Dissolved organic matter in aquatic systems. In *Treatise on geochemistry* (eds. H. D. Holland and K. K. Turekian). Elsevier Ltd. Amsterdam, Netherlands, Oxford, England, Waltham, Massachusetts, pp. 125–156.

Ehrhart J., Mingotaud A.-F. and Violleau F. (2011) Asymmetrical flow field-flow fractionation with multi-angle light scattering and quasi elastic light scattering for characterization of poly(ethyleneglycol-b-ε-caprolactone) block copolymer self-assemblies used as drug carriers for photodynamic therapy. *J. Chromatogr. A* **1218**, 4249–4256.

Fellman J. B., Hood E., Edwards R. T. and Jones J. B. (2009) Uptake of allochthonous dissolved organic matter from soil and salmon in coastal temperate rainforest streams. *Ecosystems* **12**, 747–759.

Fellman J. B., Hood E. and Spencer R. G. M. (2010) Fluorescence spectroscopy opens new windows into dissolved organic matter dynamics in freshwater ecosystems: A review. *Limnol. Oceanogr.* **55**, 2452–2462.

Findlay S. and Sinsabaugh R. L. (2003) *Aquatic ecosystems - interactivity of dissolved organic matter.* Academic Press, Amsterdam, London.

Finlay J., Neff J., Zimov S., Davydova A. and Davydov S. (2006) Snowmelt dominance of dissolved organic carbon in high-latitude watersheds: Implications for characterization and flux of river DOC. *Geophys. Res. Lett.* **33**, L10401.

Fischer H., Sachse A., Steinberg C. E. W. and Pusch M. (2002) Differential retention and utilization of dissolved organic carbon by bacteria in river sediments. *Limnol. Oceanogr.* **47**, 1702–1711.

Florence T. M. (1986) Electrochemical approaches to trace element speciation in waters. A review. *Analyst* **111**, 489–505.

Florence T. M., Batley G. E. and Benes P. (1980) Chemical speciation in natural waters. *Crit. Rev. Anal. Chem.* **9**, 219–296.

Florence T. M., Morrison G. M. and Stauber J. L. (1992) Determination of trace element speciation and the role of speciation in aquatic toxicity. *Science of The Total Environment* **125**, 1–13.

Foreman C. M. and Covert J. S. (2003) 14 - Linkages between Dissolved Organic Matter Composition and Bacterial Community Structure. In *Aquatic ecosystems* (eds. S. Findlay and R.

L. Sinsabaugh). Academic Press. Amsterdam, London, pp. 343–362.

Franke D., Hamilton M. W. and Ziegler S. E. (2012) Variation in the photochemical lability of dissolved organic matter in a large boreal watershed. *Aquat. Sci.* **74**, 751–768.

Michaelson G. J., Ping C. L., Kling G. W. and Hobbie J. E. (1998) The character and bioactivity of dissolved organic matter at thaw and in the spring runoff waters of the arctic tundra North Slope, Alaska. *J. Geophys. Res.* **103**, 28939–28946.

Gao H. and Zepp R. G. (1998) Factors Influencing Photoreactions of Dissolved Organic Matter in a Coastal River of the Southeastern United States. *Environ. Sci. Technol.* **32**, 2940–2946.

Gaudet J. M. and Roy A. G. (1995) Effect of bed morphology on flow mixing length at river confluences. *Nature* **373**, 138–139.

Giddings J. C. (1966) A new separation concept based on a coupling of concentration and flow nonuniformities. *Sep. Sci.* **1**, 123–125.

Giddings J. C. (1993) Field-flow fractionation: analysis of macromolecular, colloidal, and particulate materials. *Science* **260**, 1456–1465.

Giddings J. C., Yang F. J. and Myers M. N. (1976a) Flow-field-flow fractionation: a versatile new separation method. *Science* **193**, 1244–1245.

Giddings J. C., Yang F. J. and Myers M. N. (1976b) Theoretical and experimental characterization of flow field-flow fractionation. *Anal. Chem.* **48**, 1126–1132.

Gómez-Gener L., Lupon A., Laudon H. and Sponseller R. A. (2020) Drought alters the biogeochemistry of boreal stream networks. *Nat. Commun.* **11**, 1795.

Gorham E. (1991) Northern Peatlands: Role in the Carbon Cycle and Probable Responses to Climatic Warming. *Ecol. Appl.* **1**, 182–195.

Guéguen C., Burns D. C., McDonald A. and Ring B. (2012) Structural and optical characterization of dissolved organic matter from the lower Athabasca River, Canada. *Chemosphere* **87**, 932–937.

Guéguen C. and Cuss C. W. (2011) Characterization of aquatic dissolved organic matter by asymmetrical flow field-flow fractionation coupled to UV-Visible diode array and excitation emission matrix fluorescence. *J. Chromatogr. A* **1218**, 4188–4198.

Hansen A. M., Kraus T. E. C., Pellerin B. A., Fleck J. A., Downing B. D. and Bergamaschi B. A. (2016) Optical properties of dissolved organic matter (DOM): Effects of biological and photolytic degradation. *Limnol. Oceanogr.* **61**, 1015–1032.

Hassellöv M. (2005) Relative molar mass distributions of chromophoric colloidal organic matter in coastal seawater determined by Flow Field-Flow Fractionation with UV absorbance and fluorescence detection. *Mar. Chem.* **94**, 111–123.

Hassett J. P. (2006) Dissolved natural organic matter as a microreactor. *Science* **311**, 1723–1724.

Hemingway J. D., Spencer R. G.M., Podgorski D. C., Zito P., Sen I. S. and Galy V. V. (2019) Glacier meltwater and monsoon precipitation drive Upper Ganges Basin dissolved organic matter composition. *Geochim. Cosmochim. Acta* **244**, 216–228.

Hertkorn N., Harir M., Koch B. P., Michalke B. and Schmitt-Kopplin P. (2013) High-field NMR spectroscopy and FTICR mass spectrometry: powerful discovery tools for the molecular level characterization of marine dissolved organic matter. *Biogeosciences* **10**, 1583–1624.

Hewitt L. M., Roy J. W., Rowland S. J., Bickerton G., DeSilva A., Headley J. V., Milestone C. B., Scarlett A. G., Brown S., Spencer C., West C. E., Peru K. M., Grapentine L., Ahad J. M. E., Pakdel H. and Frank R. A. (2020) Advances in distinguishing groundwater influenced by oil sands process-affected water (OSPW) from natural bitumen-influenced groundwaters. *Environ. Sci. Technol.* **54**, 1522–1532.

Holmes R. M., McClelland J. W., Raymond P. A., Frazer B. B., Peterson B. J. and Stieglitz M. (2008) Lability of DOC transported by Alaskan rivers to the Arctic Ocean. *Geophys. Res. Lett.* **35**, L03402.

Hood E., Fellman J., Spencer R. G. M., Hernes P. J., Edwards R., D'Amore D. and Scott D. (2009) Glaciers as a source of ancient and labile organic matter to the marine environment. *Nature* **462**, 1044–1047.

Hood E., Williams M. W. and McKnight D. M. (2005) Sources of dissolved organic matter (DOM) in a Rocky Mountain stream using chemical fractionation and stable isotopes. *Biogeochemistry* **74**, 231–255.

Huguet A., Vacher L., Relexans S., Saubusse S., Froidefond J. M. and Parlanti E. (2009) Properties of fluorescent dissolved organic matter in the Gironde Estuary. *Org. Geochem.* **40**, 706–719.

Hutchins R. H. S., Prairie Y. T. and del Giorgio P. A. (2019b) Large-scale landscape drivers of CO_2, CH_4, DOC, and DIC in boreal river networks. *Glob. Biogeochem. Cycle* **33**, 125–142.

Irving H. and Williams R. J. P. (1948) Order of Stability of Metal Complexes. *Nature* **162**, 746–747.

Jager D. F., Wilmking M. and Kukkonen J. V. K. (2009) The influence of summer seasonal extremes on dissolved organic carbon export from a boreal peatland catchment: evidence from one dry and one wet growing season. *Sci. Total Environ.* **407**, 1373–1382.

Jiang T., Skyllberg U., Björn E., Green N. W., Tang J., Wang D., Gao J. and Li C. (2017) Characteristics of dissolved organic matter (DOM) and relationship with dissolved mercury in Xiaoqing River-Laizhou Bay estuary, Bohai Sea, China. *Environ. Pollut.* **223**, 19–30.

Kammer F. V. D., Baborowski M. and Friese K. (2005) Field-flow fractionation coupled to multi-angle laser light scattering detectors: Applicability and analytical benefits for the analysis of environmental colloids. *Anal. Chim. Acta* **552**, 166–174.

Karlsson T. and Persson P. (2010) Coordination chemistry and hydrolysis of Fe(III) in a peat humic acid studied by X-ray absorption spectroscopy. *Geochim. Cosmochim. Acta* **74**, 30–40.

Keil R. G. and Kirchman D. L. (1991) Contribution of dissolved free amino acids and ammonium to the nitrogen requirements of heterotrophic bacterioplankton. *Mar. Ecol.-Prog. Ser.* **73**, 1–10.

Kellerman A. M., Kothawala D. N., Dittmar T. and Tranvik L. J. (2015) Persistence of dissolved organic matter in lakes related to its molecular characteristics. *Nat. Geosci.* **8**, 454–457.

Khadka B., Munir T. M. and Strack M. (2016) Dissolved organic carbon in a constructed and natural fens in the Athabasca oil sands region, Alberta, Canada. *Sci. Total Environ.* **557-558**, 579–589.

Kikuchi T., Fujii M., Terao K., Jiwei R., Lee Y. P. and Yoshimura C. (2017) Correlations between aromaticity of dissolved organic matter and trace metal concentrations in natural and effluent waters: A case study in the Sagami River Basin, Japan. *Sci. Total Environ.* **576**, 36–45.

Kim K. H. and Moon M. H. (2009) Development of a multilane channel system for nongel-based two-dimensional protein separations using isoelectric focusing and asymmetrical flow field-flow fractionation. *Anal. Chem.* **81**, 1715–1721.

Korak J. A., Dotson A. D., Summers R. S. and Rosario-Ortiz F. L. (2014) Critical analysis of commonly used fluorescence metrics to characterize dissolved organic matter. *Water Res.* **49**, 327–338.

Kothawala D. N., Ji X., Laudon H., Ågren A. M., Futter M. N., Köhler S. J. and Tranvik L. J. (2015) The relative influence of land cover, hydrology, and in‐stream processing on the composition of dissolved organic matter in boreal streams. *J. Geophys. Res.-Biogeosci.* **120**, 1491–1505.

Kothawala D. N., Murphy K. R., Stedmon C. A., Weyhenmeyer G. A. and Tranvik L. J. (2013) Inner filter correction of dissolved organic matter fluorescence. *Limnol. Oceanogr. Meth.* **11**, 616–630.

Lambert T., Bouillon S., Darchambeau F., Massicotte P. and Borges A. V. (2016) Shift in the chemical composition of dissolved organic matter in the Congo River network. *Biogeosciences* **13**, 5405–5420.

Lapierre J.-F., Guillemette F., Berggren M. and del Giorgio P. A. (2013) Increases in terrestrially derived carbon stimulate organic carbon processing and CO_2 emissions in boreal aquatic ecosystems. *Nat. Commun.* **4**, 2972.

Latch D. E. and McNeill K. (2006) Microheterogeneity of singlet oxygen distributions in irradiated humic acid solutions. *Science* **311**, 1743–1747.

Laudon H., Buttle J., Carey S. K., McDonnell J., McGuire K., Seibert J., Shanley J., Soulsby C. and Tetzlaff D. (2012) Cross-regional prediction of long-term trajectory of stream water DOC response to climate change. *Geophys. Res. Lett.* **39**, L18404.

Lawaetz A. J. and Stedmon C. A. (2009) Fluorescence intensity calibration using the Raman scatter peak of water. *Appl. Spectrosc.* **63**, 936–940.

Lee M.-H., Osburn C. L., Shin K.-H. and Hur J. (2018) New insight into the applicability of spectroscopic indices for dissolved organic matter (DOM) source discrimination in aquatic systems affected by biogeochemical processes. *Water Res.* **147**, 164–176.

Lima A. C. and Wrona F. J. (2019) Multiple threats and stressors to the Athabasca River Basin: What do we know so far? *Sci. Total Environ.* **649**, 640–651.

Lin H. and Guo L. (2020) Variations in colloidal DOM composition with molecular weight within individual water samples as characterized by flow field-flow fractionation and EEM-PARAFAC analysis. *Environ. Sci. Technol.* **54**, 1657–1667.

Lynch L. M., Sutfin N. A., Fegel T. S., Boot C. M., Covino T. P. and Wallenstein M. D. (2019) River channel connectivity shifts metabolite composition and dissolved organic matter chemistry. *Nat. Commun.* **10**, 459.

Mann P. J., Davydova A., Zimov N., Spencer R. G. M., Davydov S., Bulygina E., Zimov S. and Holmes R. M. (2012) Controls on the composition and lability of dissolved organic matter in Siberia's Kolyma River basin. *J. Geophys. Res.* **117**, G0102.

Manskaya S. M. and Drozdova T. V. (1968) *Geochemistry of Organic Substances.* Elsevier Science, Burlington.

McCallister S. L., Ishikawa N. F. and Kothawala D. N. (2018) Biogeochemical tools for characterizing organic carbon in inland aquatic ecosystems. *Limnol. Oceanogr. Lett.* **3**, 444–457.

McKnight D. M., Bencala K. E., Zellweger G. W., Aiken G. R., Feder G. L. and Thorn K. A. (1992) Sorption of dissolved organic carbon by hydrous aluminum and iron oxides occurring at the confluence of Deer Creek with the Snake River, Summit County, Colorado. *Environ. Sci. Technol.* **26**, 1388–1396.

McKnight D. M., Boyer E. W., Westerhoff P. K., Doran P. T., Kulbe T. and Andersen D. T. (2001) Spectrofluorometric characterization of dissolved organic matter for indication of precursor organic material and aromaticity. *Limnol. Oceanogr.* **46**, 38–48.

Miller M. P. and McKnight D. M. (2010) Comparison of seasonal changes in fluorescent dissolved organic matter among aquatic lake and stream sites in the Green Lakes Valley. *J. Geophys. Res.* **115**, G00F12.

Miller W. L. (1998) Effects of UV Radiation on Aquatic Humus: Photochemical Principles and Experimental Considerations. In *Aquatic Humic Substances* (eds. D. O. Hessen and L. J. Tranvik). Springer Berlin Heidelberg. Berlin, Heidelberg, pp. 125–143.

Minor E. C., Swenson M. M., Mattson B. M. and Oyler A. R. (2014) Structural characterization of dissolved organic matter: a review of current techniques for isolation and analysis. *Environ. Sci.-Process Impacts* **16**, 2064–2079.

Mitrano D. M., Barber A., Bednar A., Westerhoff P., Higgins C. P. and Ranville J. F. (2012) Silver nanoparticle characterization using single particle ICP-MS (SP-ICP-MS) and asymmetrical flow field flow fractionation ICP-MS (AF4-ICP-MS). *J. Anal. At. Spectrom.* **27**, 1131.

Montaño M. D., Kammer F. von der, Cuss C. W. and Ranville J. F. (2019) Opportunities for examining the natural nanogeochemical environment using recent advances in nanoparticle analysis. *J. Anal. At. Spectrom.* **34**, 1768–1772.

Moody C. S. and Worrall F. (2017) Modeling rates of DOC degradation using DOM composition and hydroclimatic variables. *J. Geophys. Res.-Biogeosci.* **122**, 1175–1191.

Moore T. R. (2003) Dissolved organic carbon in a northern boreal landscape. *Global Biogeochem. Cycles* **17**, 1109.

Mopper K., Stubbins A., Ritchie J. D., Bialk H. M. and Hatcher P. G. (2007) Advanced instrumental approaches for characterization of marine dissolved organic matter: extraction techniques, mass spectrometry, and nuclear magnetic resonance spectroscopy. *Chem. Rev.* **107**, 419–442.

Moreira-Turcq P. F., Seyler P., Guyot J. L. and Etcheber H. (2003) Characteristics of organic matter in the mixing zone of the Rio Negro and Rio Solimões of the Amazon River. *Hydrol. Process.* **17**, 1393–1404.

Murphy K. R., Hambly A., Singh S., Henderson R. K., Baker A., Stuetz R. and Khan S. J. (2011) Organic matter fluorescence in municipal water recycling schemes: toward a unified PARAFAC model. *Environ. Sci. Technol.* **45**, 2909–2916.

Murphy K. R., Stedmon C. A., Graeber D. and Bro R. (2013) Fluorescence spectroscopy and multi-way techniques. PARAFAC. *Anal. Methods* **5**, 6557.

Murphy K. R., Stedmon C. A., Wenig P. and Bro R. (2014) OpenFluor– an online spectral library of auto-fluorescence by organic compounds in the environment. *Anal. Methods* **6**, 658–661.

Nieboer E. and Richardson D. H.S. (1980) The replacement of the nondescript term ‘heavy metals’ by a biologically and chemically significant classification of metal ions. *Environ. Pollut. Series B, Chemical and Physical* **1**, 3–26.

Nikolaou A. D. and Lekkas T. D. (2001) The role of natural organic matter during formation of chlorination by-products: a review. *Acta Hydrochim. Hydrobiol.* **29**, 63–77.

O’Donnell J. A., Aiken G. R., Kane E. S. and Jones J. B. (2010) Source water controls on the character and origin of dissolved organic matter in streams of the Yukon River basin, Alaska. *J. Geophys. Res.* **115**, G03025.

Oleinikova O. V., Drozdova O. Y., Lapitskiy S. A., Demin V. V., Bychkov A. Y. and Pokrovsky O. S. (2017) Dissolved organic matter degradation by sunlight coagulates organo-mineral colloids and produces low-molecular weight fraction of metals in boreal humic waters. *Geochim. Cosmochim. Acta* **211**, 97–114.

Oliver B. G., Thurman E. M. and Malcolm R. L. (1983) The contribution of humic substances to the acidity of colored natural waters. *Geochim. Cosmochim. Acta* **47**, 2031–2035.

Osburn C. L., Wigdahl C. R., Fritz S. C. and Saros J. E. (2011) Dissolved organic matter composition and photoreactivity in prairie lakes of the U.S. Great Plains. *Limnol. Oceanogr.* **56**, 2371–2390.

Paquin P. R., Gorsuch J. W., Apte S., Batley G. E., Bowles K. C., Campbell P. G.C., Delos C. G., Di Toro D. M., Dwyer R. L., Galvez F., Gensemer R. W., Goss G. G., Hogstrand C., Janssen C. R., McGeer J. C., Naddy R. B., Playle R. C., Santore R. C., Schneider U., Stubblefield W. A., Wood C. M. and Wu K. B. (2002) The biotic ligand model: a historical overview. *Comp. Biochem. Physiol. C-Pharmacol. Toxicol. Endocrinol.* **133**, 3–35.

Parlanti E., Wörz K., Geoffroy L. and Lamotte M. (2000) Dissolved organic matter fluorescence spectroscopy as a tool to estimate biological activity in a coastal zone submitted to anthropogenic inputs. *Org. Geochem.* **31**, 1765–1781.

Parr T. B., Ohno T., Cronan C. S. and Simon K. S. (2014) comPARAFAC: a library and tools for rapid and quantitative comparison of dissolved organic matter components resolved by Parallel Factor Analysis. *Limnol. Oceanogr. Meth.* **12**, 114–125.

Parsons D. R., Best J. L., Lane S. N., Kostaschuk R. A., Hardy R. J., Orfeo O., Amsler M. L. and Szupiany R. N. (2008) Large River Channel Confluences. In *River confluences, tributaries, and the fluvial network* (eds. S. P. Rice, A. G. Roy and B. L. Rhoads). John Wiley & Sons, Ltd. Hoboken, N.J., pp. 73–91.

Paul A., Stösser R., Zehl A., Zwirnmann E., Vogt R. D. and Steinberg C. E. W. (2006) Nature and abundance of organic radicals in natural organic matter: effect of pH and irradiation. *Environ. Sci. Technol.* **40**, 5897–5903.

Pearson R. G. (1968a) Hard and soft acids and bases, HSAB, part 1: Fundamental principles. *J. Chem. Educ.* **45**, 581–587.

Pearson R. G. (1968b) Hard and soft acids and bases, HSAB, part II: Underlying theories. *J. Chem. Educ.* **45**, 643–648.

Perdue E. M. and Ritchie J. D. (2014) 7.8 - Dissolved organic matter in freshwaters. In *Treatise on geochemistry* (eds. H. D. Holland and K. K. Turekian). Elsevier Ltd. Amsterdam, Netherlands, Oxford, England, Waltham, Massachusetts, pp. 237–272.

Peuravuori J. and Pihlaja K. (1997) Molecular size distribution and spectroscopic properties of aquatic humic substances. *Anal. Chim. Acta* **337**, 133–149.

Plante A. F., Fernández J. M. and Leifeld J. (2009) Application of thermal analysis techniques in soil science. *Geoderma* **153**, 1–10.

Podzimek S. (2011) Asymmetric flow field flow fractionation. In *Light scattering, size exclusion chromatography and asymmetric flow field flow fractionation* (ed. S. Podzimek). John Wiley &

Sons, Ltd. Hoboken, New Jersey, pp. 259–305.

Poulin B. A., Ryan J. N. and Aiken G. R. (2014) Effects of iron on optical properties of dissolved organic matter. *Environ. Sci. Technol.* **48**, 10098–10106.

Roditi H. A., Fisher N. S. and Sañudo-Wilhelmy S. A. (2000) Uptake of dissolved organic carbon and trace elements by zebra mussels. *Nature* **407**, 78–80.

Rutherford J. C. (1994) *River mixing.* John Wiley & Sons, Ltd, Chichester, England.

Schimpf M. E., Caldwell K. and Giddings J. C. (2000) *Field-flow fractionation handbook.* Wiley-Interscience, New York, Chichester.

Schnitzer M. and Khan S. U. (1978) *Soil Organic Matter.* Elsevier Science, Amsterdam.

Schumacher M., Christl I., Vogt R. D., Barmettler K., Jacobsen C. and Kretzschmar R. (2006) Chemical composition of aquatic dissolved organic matter in five boreal forest catchments sampled in spring and fall seasons. *Biogeochemistry* **80**, 263–275.

Shotyk W. (1988) Review of the inorganic geochemistry of peats and peatland waters. *Earth-Sci. Rev.* **25**, 95–176.

Shotyk W., Bicalho B., Cuss C. W., Donner M. W., Grant-Weaver I., Haas-Neill S., Javed M. B., Krachler M., Noernberg T., Pelletier R. and Zaccone C. (2017) Trace metals in the dissolved fraction (<0.45μm) of the lower Athabasca River: Analytical challenges and environmental implications. *Sci. Total Environ.* **580**, 660–669.

Simon C., Osterholz H., Koschinsky A. and Dittmar T. (2019) Riverine mixing at the molecular scale – An ultrahigh-resolution mass spectrometry study on dissolved organic matter and selected metals in the Amazon confluence zone (Manaus, Brazil). *Org. Geochem.* **129**, 45–62.

Simpson A. J., Tseng L.-H., Simpson M. J., Spraul M., Braumann U., Kingery W. L., Kelleher B. P. and Hayes M. H. B. (2004) The application of LC-NMR and LC-SPE-NMR to compositional studies of natural organic matter. *Analyst* **129**, 1216–1222.

Singh S., D'Sa E. J. and Swenson E. M. (2010) Chromophoric dissolved organic matter (CDOM) variability in Barataria Basin using excitation-emission matrix (EEM) fluorescence and parallel factor analysis (PARAFAC). *Sci. Total Environ.* **408**, 3211–3222.

Spencer R. G. M., Aiken G. R., Butler K. D., Dornblaser M. M., Striegl R. G. and Hernes P. J. (2009) Utilizing chromophoric dissolved organic matter measurements to derive export and reactivity of dissolved organic carbon exported to the Arctic Ocean: A case study of the Yukon River, Alaska. *Geophys. Res. Lett.* **36**, L06401.

Spencer R. G. M. and Coble P. G. (2014) Sampling design for organic matter fluorescence analysis. In *Aquatic organic matter fluorescence* (eds. Paula G. Coble, Jamie Lead, Andy Baker, Darren M. Reynolds and Robert G. M. Spencer). Cambridge University Press. New York, NY, USA, pp. 125–146.

Spencer R. G.M., Guo W., Raymond P. A., Dittmar T., Hood E., Fellman J. and Stubbins A. (2014) Source and biolability of ancient dissolved organic matter in glacier and lake ecosystems on the Tibetan Plateau. *Geochim. Cosmochim. Acta* **142**, 64–74.

Stedmon C. A. and Bro R. (2008) Characterizing dissolved organic matter fluorescence with parallel factor analysis: a tutorial. *Limnol. Oceanogr. Methods* **6**, 572–579.

Stedmon C. A. and Markager S. (2003) Behaviour of the optical properties of coloured dissolved organic matter under conservative mixing. *Estuar. Coast. Shelf Sci.* **57**, 973–979.

Stolpe B., Guo L., Shiller A. M. and Hassellöv M. (2010) Size and composition of colloidal organic matter and trace elements in the Mississippi River, Pearl River and the northern Gulf of Mexico, as characterized by flow field-flow fractionation. *Mar. Chem.* **118**, 119–128.

Striegl R. G., Aiken G. R., Dornblaser M. M., Raymond P. A. and Wickland K. P. (2005) A decrease in discharge-normalized DOC export by the Yukon River during summer through autumn. *Geophys. Res. Lett.* **32**, L21413.

Stubbins A., Lapierre J.-F., Berggren M., Prairie Y. T., Dittmar T. and del Giorgio P. A. (2014) What's in an EEM? Molecular signatures associated with dissolved organic fluorescence in boreal Canada. *Environ. Sci. Technol.* **48**, 10598–10606.

Sun C., Shotyk W., Cuss C. W., Donner M. W., Fennell J., Javed M., Noernberg T., Poesch M., Pelletier R., Sinnatamby N., Siddique T. and Martin J. W. (2017) Characterization of Naphthenic Acids and Other Dissolved Organics in Natural Water from the Athabasca Oil Sands Region, Canada. *Environ. Sci. Technol.* **51**, 9524–9532.

Tfaily M. M., Wilson R. M., Cooper W. T., Kostka J. E., Hanson P. and Chanton J. P. (2018) Vertical Stratification of Peat Pore Water Dissolved Organic Matter Composition in a Peat Bog in Northern Minnesota. *J. Geophys. Res. Biogeosci.* **123**, 479–494.

Thurman E. M. (1985) *Organic geochemistry of natural waters.* Springer Netherlands, Dordrecht.

Urbansky E. T. and Magnuson M. L. (2002) Analyzing drinking water for disinfection byproducts. *Anal. Chem.* **74**, 260A-267A.

Wahlund K. G. and Giddings J. C. (1987) Properties of an asymmetrical flow field-flow fractionation channel having one permeable wall. *Anal. Chem.* **59**, 1332–1339.

Wahlund K. G., Winegarner H. S., Caldwell K. D. and Giddings J. C. (1986) Improved flow field-flow fractionation system applied to water-soluble polymers: programming, outlet stream splitting, and flow optimization. *Anal. Chem.* **58**, 573–578.

Walker S. A., Amon R. M. W. and Stedmon C. A. (2013) Variations in high-latitude riverine fluorescent dissolved organic matter: A comparison of large Arctic rivers. *J. Geophys. Res.-Biogeosci.* **118**, 1689–1702.

Wallis P. M., Hynes H. B. N. and Telang S. A. (1981) The importance of groundwater in the

transportation of allochthonous dissolved organic matter to the streams draining a small mountain basin. *Hydrobiologia* **79**, 77–90.

Wang Y., Cuss C. W. and Shotyk W. (2020) Application of asymmetric flow field-flow fractionation to the study of aquatic systems: Coupled methods, challenges, and future needs. *J. Chromatogr. A* **1632**, 461600.

Ward C. P. and Cory R. M. (2015) Chemical composition of dissolved organic matter draining permafrost soils. *Geochim. Cosmochim. Acta* **167**, 63–79.

Warren L. A. and Haack E. A. (2001) Biogeochemical controls on metal behaviour in freshwater environments. *Earth-Sci. Rev.* **54**, 261–320.

Weishaar J. L., Aiken G. R., Bergamaschi B. A., Fram M. S., Fujii R. and Mopper K. (2003) Evaluation of specific ultraviolet absorbance as an indicator of the chemical composition and reactivity of dissolved organic carbon. *Environ. Sci. Technol.* **37**, 4702–4708.

Wetzel R. G. (1992) Gradient-dominated ecosystems: sources and regulatory functions of dissolved organic matter in freshwater ecosystems. *Hydrobiologia* **229**, 181–198.

Wickland K. P., Aiken G. R., Butler K., Dornblaser M. M., Spencer R. G. M. and Striegl R. G. (2012) Biodegradability of dissolved organic carbon in the Yukon River and its tributaries: Seasonality and importance of inorganic nitrogen. *Global Biogeochem. Cycles* **26**, GB0E03.

Wilson H. F. and Xenopoulos M. A. (2009) Effects of agricultural land use on the composition of fluvial dissolved organic matter. *Nat. Geosci.* **2**, 37–41.

Wittgren B., Borgström J., Piculell L. and Wahlund K.-G. (1998) Conformational change and aggregation of κ-carrageenan studied by flow field-flow fractionation and multiangle light scattering. *Biopolymers* **45**, 85–96.

Woo M.-K. and Thorne R. (2003) Streamflow in the Mackenzie Basin, Canada. *Arctic* **56**, 328–340.

Worms I. A. M., Chmiel H. E., Traber J., Tofield-Pasche N. and Slaveykova V. I. (2019) Dissolved organic matter and associated trace metal dynamics from river to lake, under ice-covered and ice-free conditions. *Environ. Sci. Technol.* **53**, 14134–14143.

Yamashita Y. and Jaffé R. (2008) Characterizing the interactions between trace metals and dissolved organic matter using excitation-emission matrix and parallel factor analysis. *Environ. Sci. Technol.* **42**, 7374–7379.

Yi Y., Birks S. J., Cho S. and Gibson J. J. (2015) Characterization of organic composition in snow and surface waters in the Athabasca Oil Sands Region, using ultrahigh resolution Fourier transform mass spectrometry. *Sci. Total Environ.* **518-519**, 148–158.

Yoon J.-H. and Chen T.-C. (2006) Maintenance of the boreal forest rainbelts during northern summer. *J. Climate* **19**, 1437–1449.

Yu Z., Beilman D. W., Frolking S., MacDonald G. M., Roulet N. T., Camill P. and Charman D. J. (2011) Peatlands and Their Role in the Global Carbon Cycle. *Eos Trans. AGU* **92**, 97–98.

Zark M. and Dittmar T. (2018) Universal molecular structures in natural dissolved organic matter. *Nat. Commun.* **9**, 3178.

Zhang H. and Lyden D. (2019) Asymmetric-flow field-flow fractionation technology for exomere and small extracellular vesicle separation and characterization. *Nat. Protoc.* **14**, 1027–1053.

Zhang M. and He Z. (2015) Characteristics of dissolved organic carbon revealed by ultraviolet‐visible absorbance and fluorescence spectroscopy: the current status and future exploration. In *Labile organic matter—chemical compositions, function, and significance in soil and the environment* (eds. Z. He and F. Wu). Soil Science Society of America, Inc. Madison, WI, USA, pp. 1–21.

Zhang Y., Shotyk W., Zaccone C., Noernberg T., Pelletier R., Bicalho B., Froese D. G., Davies L. and Martin J. W. (2016) Airborne petcoke dust is a major source of polycyclic aromatic hydrocarbons in the Athabasca oil sands region. *Environ. Sci. Technol.* **50**, 1711–1720.

Zhou Z., Stolpe B., Guo L. and Shiller A. M. (2016) Colloidal size spectra, composition and estuarine mixing behavior of DOM in river and estuarine waters of the northern Gulf of Mexico. *Geochim. Cosmochim. Acta* **181**, 1–17.

Zsolnay A., Baigar E., Jimenez M., Steinweg B. and Saccomandi F. (1999) Differentiating with fluorescence spectroscopy the sources of dissolved organic matter in soils subjected to drying. *Chemosphere* **38**, 45–50.

APPENDICES

Appendix I: field data summary, 2018 fall

Sample Number	Date	Weather	River Name	Nickname	Location
480	2018/9/25	Sunny Light breeze	Athabasca	A17 - west	N 56.99874° W 111.45676°
468	2018/9/25	Cloudy Light breeze	Athabasca	A17 - west	N 56.99874° W 111.45676°
475	2018/9/25	Sunny/Cloudy Light breeze	Athabasca	A17 - west	N 56.99874° W 111.45676°
471	2018/9/25	Cloudy	Athabasca	A17 - middle	N 56.99963° W 111.45493°
476	2018/9/25	Cloudy	Athabasca	A17 - middle	N 56.99963° W 111.45493°
479	2018/9/25	Cloudy	Athabasca	A17 - middle	N 56.99963° W 111.45493°
467	2018/9/25	Cloudy Light breeze	Athabasca	A17 - east	N 57.00005° W 111.45273°
470	2018/9/25	Cloudy	Athabasca	A17 - east	N 57.00005° W 111.45273°
451	2018/9/26	Cloudy Breezy	Steepbank	SB01-SB	
481	2018/9/26	Cloudy Breezy	Athabasca	AR01-SB	N 57.01773° W 111.48048°
466	2018/9/26	Cloudy Breezy/windy	Athabasca	AR01-SB	N 57.01773° W 111.48048°
473	2018/9/26	Cloudy Breezy	Athabasca	AR02-SB	N 57.01843° W 111.48303°
443	2018/9/26	Cloudy Breezy	Athabasca	AR02-SB	N 57.01843° W 111.48303°
469	2018/9/26	Sunny/Cloudy Windy	Athabasca	AR03-SB	N 57.01969° W 111.48603°
442	2018/9/26	Cloudy Windy	Athabasca	AR03-SB	N 57.01969° W 111.48603°
474	2018/9/26	Cloudy Rainy	Athabasca	AR04-SB	N 57.02192° W 111.48968°
438	2018/9/26	Cloudy Windy	Athabasca	AR04-SB	N 57.02192° W 111.48968°
444	2018/9/26	Cloudy/Light rain Windy	Steepbank	SB04-SB	N 57.02242° W 111.48871°
448	2018/9/26	Cloudy Windy	Steepbank	SB04-SB	N 57.02242° W 111.48871°
440	2018/9/26	Cloudy Windy	Steepbank	SB03-SB	N 57.02008° W 111.48531°
446	2018/9/26	Cloudy Windy	Steepbank	SB03-SB	N 57.02008° W 111.48531°
439	2018/9/26	Cloudy Breezy	Steepbank	SB02-SB	N 57.01874° W 111.48264°
445	2018/9/26	Cloudy	Steepbank	SB02-SB	N 57.01874° W 111.48264°
463	2018/9/27	Cloudy Light breeze	Athabasca	A9 - west	N 57.43055° W 111.64511°
457	2018/9/27	Cloudy Breezy	Athabasca	A9 - west	N 57.43055° W 111.64511°
452	2018/9/27	Cloudy Breezy	Athabasca	A9 - west	N 57.43055° W 111.64511°
453	2018/9/27	Cloudy Windy	Athabasca	A9 - middle	N 57.43015° W 111.64195°
455	2018/9/27	Cloudy Windy	Athabasca	A9 - middle	N 57.43015° W 111.64195°
478	2018/9/27	Cloudy Breezy	Athabasca	A9 - east	N 57.42913° W 111.63788°
449	2018/9/27	Partially cloudy Breezy	Tar		N 57.32224° W 111.68301°
458	2018/9/27	Sunny Windy	Ells		
405	2018/9/28	Sunny Light breeze	Athabasca	WWTP upstream west	N 56.69728° W 111.45253°
459	2018/9/28	Sunny Breezy	Athabasca	WWTP upstream west	N 56.69728° W 111.45253°

460	2018/9/28	Sunny Breezy	Athabasca	WWTP upstream middle	N 56.69624° W 111.45145°
465	2018/9/28	Sunny Breezy	Athabasca	WWTP upstream middle	N 56.69624° W 111.45145°
432	2018/9/28	Sunny Breezy	Athabasca	WWTP upstream middle	N 56.69624° W 111.45145°
485	2018/9/28	Sunny Breezy	Athabasca	WWTP upstream east	N 56.69510° W 111.45097°
482	2018/9/28	Sunny Breezy	Athabasca	WWTP upstream east	N 56.69510° W 111.45097°
456	2018/9/28	Sunny/Cloudy Breezy	Athabasca	WWTP upstream east	N 56.69510° W 111.45097°
483	2018/9/28	Sunny Breezy	Little Fishery		N 56.713505° W 111.439750°
472	2018/9/28	Sunny/Cloudy Breezy	Clearwater	CL01-CL	N 56.73907° W 111.37091°
462	2018/9/28	Sunny/Cloudy Breezy	Clearwater	CL01-CL	N 56.73907° W 111.37091°
431	2018/9/28	Cloudy Breezy	Athabasca	AR01-CL	N 56.75095° W 111.38748°
437	2018/9/28	Cloudy Windy	Athabasca	AR01-CL	N 56.75095° W 111.38748°
430	2018/9/29	Cloudy/Flurries Slight breeze	MacKay		
450	2018/9/29	Cloudy/Snow	Muskeg		
436	2018/9/30	Sunny Breezy	Athabasca	AR02-CL	N 56.78896° W 111.40866°
484	2018/9/30	Sunny Breezy	Athabasca	AR02-CL	N 56.78896° W 111.40866°
406	2018/9/30	Sunny Light breeze	Clearwater	CL02-CL	N 56.78812° W 111.40484°
464	2018/9/30	Sunny Light breeze	Clearwater	CL02-CL	N 56.78812° W 111.40484°
461	2018/9/30	Sunny Light breeze	Athabasca	AR03-CL	N 56.82568° W 111.41066°
477	2018/9/30	Sunny Breezy	Athabasca	AR03-CL	N 56.82568° W 111.41066°
454	2018/9/30	Cloudy Light breeze	Clearwater	CL03-CL	N 56.82572° W 111.40795°
434	2018/9/30	Cloudy Light breeze	Clearwater	CL03-CL	N 56.82572° W 111.40795°
447	2018/9/30	Sunny Breezy	Clearwater	CL04-CL	N 56.85838° W 111.42497°
428	2018/9/30	Sunny Breezy	Clearwater	CL04-CL	N 56.65838° W 111.42497°
433	2018/9/30	Sunny Windy	Athabasca	AR04-CL	N 56.85786° W 111.42779°
429	2018/9/30	Sunny Windy	Athabasca	AR04-CL	N 56.85786° W 111.42779°
	2018/9/30	Sunny Windy	Clearwater	CW09 - downstream	N 56.67824° W 111.18350°
	2018/9/30	Sunny Windy	Clearwater	CW09 - upstream	N 56.67683° W 111.15408°
421	2018/10/1	Cloudy Clam	Athabasca	A5 - west	N 57.57334° W 111.51402°
425	2018/10/1	Partially sunny and clouds	Athabasca	A5 - west	N 57.57334° W 111.51402°
404	2018/10/1	Partially sunny and clouds	Athabasca	A5 - west	N 57.57334° W 111.51402°
435	2018/10/1	Partially sunny and clouds	Athabasca	A5 - middle	N 57.57307° W 111.51172°
427	2018/10/1	Partially sunny and clouds	Athabasca	A5 - middle	N 57.57307° W 111.51172°

420	2018/10/1	Sunny/Cloudy	Athabasca	A5 - middle	N 57.57307°
					W 111.51172°
416	2018/10/1	Cloudy	Athabasca	A5 - east	N 57.57405°
		Breezy			W 111.50876°
418	2018/10/1	Cloudy	Athabasca	A5 - east	N 57.57405°
		Windy			W 111.50876°
417	2018/10/1	Cloudy	Athabasca	A5 - east	N 57.57405°
		Windy			W 111.50876°
401	2018/10/1	Cloudy/Light snow	Pierre		
423	2018/10/1	Cloudy	Beaver Creek		
		Windy			
403	2018/10/2	Cloudy	Horse	HR01-HR	
		Breezy			
407	2018/10/2	Cloudy	Athabasca	AR01-HR	N 56.72013°
		Breezy			W 111.40139°
411	2018/10/2	Cloudy	Athabasca	AR01-HR	N 56.72013°
		Windy			W 111.40139°
413	2018/10/2	Sunny	Athabasca	AR02-HR	N 56.72632°
		Windy/Gusty			W 111.39791°
402	2018/10/2	Partially cloudy	Athabasca	AR02-HR	N 56.72632°
		Windy			W 111.39791°
409	2018/10/2	Sunny	Horse	HR02-HR	N 56.72641°
		Windy			W 111.39713°
408	2018/10/2	Partially cloudy	Horse	HR02-HR	N 56.72641°
		Windy			W 111.39713°
415	2018/10/2	Cloudy	Athabasca	AR03-HR	N 56.73091°
		Windy			W 111.39571°
426	2018/10/2	Partially cloudy	Athabasca	AR03-HR	N 56.73091°
		Windy			W 111.39571°
414	2018/10/2	Sunny	Horse	HR03-HR	N 56.73054°
		Windy			W 111.39487°
410	2018/10/2	Sunny	Athabasca	AR04-HR	N 56.73576°
		Windy			W 111.39260°
400	2018/10/2	Cloudy	Athabasca	AR04-HR	N 56.73576°
		Windy			W 111.39260°
412	2018/10/2	Cloudy	Horse	HR04-HR	N 56.73565°
		Windy			W 111.39207°
424	2018/10/3	Cloudy	Athabasca	Upstream of Mclean Creek - west	N 56.89309°
		Breezy			W 111.42003°
285	2018/10/3	Cloudy	Athabasca	Upstream of Mclean Creek - west	N 56.89309°
		Breezy			W 111.42003°
286	2018/10/3	Cloudy	Athabasca	Upstream of Mclean Creek - west	N 56.89309°
		Breezy			W 111.42003°
267	2018/10/3	Cloudy	Athabasca	Upstream of Mclean Creek - middle	N 56.89307°
		Breezy			W 111.41909°
289	2018/10/3	Cloudy	Athabasca	Upstream of Mclean Creek - middle	N 56.89307°
		Calm			W 111.41909°
259	2018/10/3	Cloudy	Athabasca	Upstream of Mclean Creek - east	N 56.89240°
		Little breeze			W 111.41623°
284	2018/10/3	Cloudy	Athabasca	Upstream of Mclean Creek - east	N 56.89240°
		Little breeze			W 111.41623°
283	2018/10/3	Cloudy	Athabasca	Upstream of Mclean Creek - east	N 56.89240°
		Little breeze			W 111.41623°
308	2018/10/3	Cloudy	Mclean Creek		
		Little breeze			
288	2018/10/3	Cloudy Calm	Athabasca	AR05-CL	N 56.95571°
					W 111.45156°
309	2018/10/3	Cloudy	Athabasca	AR05-CL	N 56.95571°
		Light breeze			W 111.45156°
310	2018/10/3	Cloudy	Clearwater	CL05-CL	N 56.95555°
		Calm			W 111.44798°
277	2018/10/3	Cloudy	Clearwater	CL05-CL	N 56.95555°
		Calm			W 111.44798°

Note: WWTP, Upstream of Mclean Creek, A17, A9, and A5 refer to T1-T5.

Appendix II: field data summary, 2019 spring

No.	Sample ID	Date	Weather	River Name	Nickname	Location
1	507	May. 14, 2019	Cloudy	Athabasca	Fort McMurray upstream west	N 56.69724° W 111.45261°
2	504	May. 14, 2019	Cloudy	Athabasca	Fort McMurray upstream west	N 56.69724° W 111.45261°
3	501	May. 14, 2019	Cloudy	Athabasca	Fort McMurray upstream west	N 56.69724° W 111.45261°
4	506	May. 14, 2019	Cloudy	Athabasca	Upstream Fort McMurray middle UPM-1	N 56.69625° W 111.45123°
5	539	May. 14, 2019	Cloudy	Athabasca	Upstream Fort McMurray middle UPM-1	N 56.69625° W 111.45123°
6	502	May. 14, 2019	Cloudy	Athabasca	Upstream Fort McMurray middle UPM-1	N 56.69625° W 111.45123°
7	505	May. 14, 2019	Partly cloudy	Athabasca	Upstream Fort McMurray east	N 56.69511° W 111.45100°
8	503	May. 14, 2019	Sunny A little wind	Athabasca	Upstream Fort McMurray east	N 56.69511° W 111.45100°
9	531	May. 14, 2019	Sunny A little wind	Athabasca	Upstream Fort McMurray east	N 56.69511° W 111.45100°
10	530	May. 14, 2019	Sunny A little wind	Little Fishery Creek	Little Fishery Creek	
11	525	May. 15, 2019	Sunny A little wind	Horse river	Horse river site (HR-1)	N 56.71918° W 111.39835°
12	508	May. 15, 2019	Sunny A little wind	Horse river	Horse river site (HR-1)	N 56.71918° W 111.39835°
13	526	May. 15, 2019	Sunny Windy	Athabasca	Horse river-AR mixing transect 1 (AR-1)	N 56.72026° W 111.40138°
14	500	May. 15, 2019	Sunny Windy	Athabasca	Horse river-AR mixing transect 1 (AR-1)	N 56.72026° W 111.40138°
15	524	May. 15, 2019	Sunny Windy	Athabasca	Horse river mixing - AR2	N 56.72228° W 111.39847°
16	527	May. 15, 2019	Sunny Windy	Athabasca	Horse river mixing - AR2	N 56.72228° W 111.39847°
17	532	May. 15, 2019	Sunny Windy	Horse river	Horse river mixing - HR2	N 56.72229° W 111.39764°
18	523	May. 15, 2019	Sunny Windy	Horse river	Horse river mixing - HR2	N 56.72229° W 111.39764°
19	536	May. 15, 2019	Sunny Windy	Athabasca	Horse river mixing - AR3	N 56.72639° W 111.39792°
20	533	May. 15, 2019	Sunny Windy	Athabasca	Horse river mixing - AR3	N 56.72639° W 111.39792°
21	537	May. 15, 2019	Sunny Windy	Horse river	Horse river mixing transect HR-3	N 56.72637° W 111.39718°
22	521	May. 15, 2019	Sunny Windy	Horse river	Horse river mixing transect HR-3	N 56.72637° W 111.39718°
23	509	May. 16, 2019	Sunny	Athabasca	Horse river mixing transect AR-4	N 56.73080° W 111.39584°
24	538	May. 16, 2019	Sunny	Athabasca	Horse river mixing transect AR-4	N 56.73080° W 111.39584°
25	522	May. 16, 2019	Sunny	Horse river	Horse river mixing transect HR-4	N 56.73045° W 111.39491°
26	529	May. 16, 2019	Sunny	Horse river	Horse river mixing transect HR-4	N 56.73045° W 111.39491°
27	534	May. 16, 2019	Sunny	Athabasca	Horse river mixing transect AR-5	N 56.73560° W 111.39274°
28	513	May. 16, 2019	Sunny	Athabasca	Horse river mixing transect AR-5	N 56.73560° W 111.39274°
29	520	May. 16, 2019	Sunny	Horse river	Horse river mixing transect HR-5	N 56.73566° W 111.39224°
30	514	May. 16, 2019	Sunny	Horse river	Horse river mixing transect HR-5	N 56.73566° W 111.39224°
31	535	May. 16, 2019	Sunny Gentle wind	Athabasca	Clearwater mixing transect AR-1	N 56.75110° W 111.38743°
32	566	May. 16, 2019	Sunny Gentle wind	Athabasca	Clearwater mixing transect AR-1	N 56.75110° W 111.38743°
33	565	May. 16, 2019	Sunny Gentle wind	Athabasca	Clearwater mixing transect AR-2	N 56.76939° W 111.39648°
34	518	May. 16, 2019	Sunny	Athabasca	Clearwater mixing transect AR-2	N 56.76939° W 111.39648°
35	510	May. 16, 2019	Sunny Gentle wind	Clearwater	Clearwater mixing transect CL-2	N 56.76973° W 111.39298°
36	568	May. 16, 2019	Sunny Gentle wind	Clearwater	Clearwater mixing transect CL-2	N 56.76973° W 111.39298°
37	511	May. 16, 2019	Sunny Gentle wind	Clearwater	Clearwater mixing transect CL-1	N 56.73900° W 111.37083°

38	516	May. 16, 2019	Sunny Gentle wind	Clearwater	Clearwater mixing transect CL-1	N 56.73900° W 111.37083°
39	567	May. 17, 2019	Sunny Windy	Athabasca	Clearwater mixing transect AR-3	N 56.78388° W 111.40673°
40	561	May. 17, 2019	Sunny Very windy	Athabasca	Clearwater mixing transect AR-3	N 56.78388° W 111.40673°
41	569	May. 17, 2019	Sunny Gentle wind	Clearwater	Clearwater mixing transect CL-3	N 56.78397° W 111.40492°
42	560	May. 17, 2019	Sunny Windy	Clearwater	Clearwater mixing transect CL-3	N 56.78397° W 111.40492°
43	563	May. 17, 2019	Sunny Very windy	Athabasca	Clearwater mixing transect AR-4	N 56.82565° W 111.41055°
44	562	May. 17, 2019	Sunny Windy	Athabasca	Clearwater mixing transect AR-4	N 56.82565° W 111.41055°
45	557	May. 17, 2019	Sunny Windy	Clearwater	Clearwater mixing transect CL-4	N 56.82575° W 111.40760°
46	558	May. 17, 2019	Sunny Windy	Clearwater	Clearwater mixing transect CL-4	N 56.82575° W 111.40760°
47	556	May. 17, 2019	Sunny Very windy	Athabasca	Clearwater mixing transect AR-5	N 56.95569° W 111.45177°
48	555	May. 17, 2019	Sunny Very windy	Athabasca	Clearwater mixing transect AR-5	N 56.95569° W 111.45177°
49	559	May. 17, 2019	Sunny Very windy	Clearwater	Clearwater mixing transect CL-5	N 56.95552° W 111.44807°
50	564	May. 17, 2019	Sunny Very windy	Clearwater	Clearwater mixing transect CL-5	N 56.95552° W 111.44807°
51	579	May. 18, 2019	sunny	AR	Upstream McLean Creek-West	N 56.85711° W 111.43108°
52	575	May. 18, 2019	sunny	AR	Upstream McLean Creek-West	N 56.85711° W 111.43108°
53	570	May. 18, 2019	sunny	AR	Upstream McLean Creek-West	N 56.85711° W 111.43108°
54	583	May. 18, 2019	sunny	AR	Upstream McLean Creek-middle	N 56.85743° W 111.42947°
55	573	May. 18, 2019	sunny	AR	Upstream McLean Creek-middle	N 56.85743° W 111.42947°
56	572	May. 18, 2019	Sunny A little wind	AR	Upstream McLean Creek-middle	N 56.85743° W 111.42947°
57	574	May. 18, 2019	Sunny Windy	AR	Upstream McLean Creek-east	N 56.85792° W 111.42319°
58	582	May. 18, 2019	Sunny Windy	AR	Upstream McLean Creek-east	N 56.85792° W 111.42319°
59	554	May. 18, 2019	Sunny	McLean Creek	McLean Creek	N 56.89753° W 111.41645°
60	551	May. 18, 2019	Sunny A little wind	Athabasca	Clearwater mixing transect AR-6	N 56.97498° W 111.44727°
61	553	May. 18, 2019	Sunny	Athabasca	Clearwater mixing transect AR-6	N 56.97498° W 111.44727°
62	550	May. 18, 2019	Sunny	Clearwater	Clearwater mixing transect CL-6	N 56.97392° W 111.44511°
63	547	May. 18, 2019	Sunny	Clearwater	Clearwater mixing transect CL-6	N 56.97392° W 111.44511°
64	Sed AR-1	May. 18, 2019	Sunny Gentle wind		AR1-Clearwater mixing transect Sed-1	N 56.74862° W 111.39638°
65	CLR-Sed1	May. 18, 2019	Sunny		Clearwater sediment 2	N 56.70404° W 111.33632°
66	584	May. 25, 2019	Sunny Windy	Athabasca	Downstream A9 west	N 57.43058° W 111.64530°
67	581	May. 25, 2019	Sunny Windy	Athabasca	Downstream A9 west	N 57.43058° W 111.64530°
68	578	May. 25, 2019	Sunny Windy	Athabasca	Downstream A9 west	N 57.43058° W 111.64530°
69	544	May. 25, 2019	Sunny Windy	Athabasca	Downstream A9 transect middle	N 57.43020° W 111.64169°
70	552	May. 25, 2019	Sunny Windy	Athabasca	Downstream A9 transect middle	N 57.43020° W 111.64169°
71	577	May. 25, 2019	Sunny Windy	Athabasca	Downstream A9 transect middle	N 57.43020° W 111.64169°
72	571	May. 25, 2019	Sunny Windy	Athabasca	Downstream A9 transect east	N 57.42876° W 111.63834°
73	540	May. 25, 2019	Sunny Windy	Athabasca	Downstream A9 transect east	N 57.42876° W 111.63834°
74	546	May. 25, 2019	Sunny Windy	Athabasca	Downstream A9 transect east	N 57.42876° W 111.63834°

75	545	May. 25, 2019	Sunny A little wind	Tar river		
76	548	May. 25, 2019	Sunny Gentle wind	Ells river		
77	585	May. 25, 2019	Sunny A little wind	Mackay river		
78	597	May. 26, 2019	Sunny Windy	Athabasca	A17 transect west	N 56.99895° W 111.45674°
79	541	May. 26, 2019	Sunny Windy	Athabasca	A17 transect west	N 56.99895° W 111.45674°
80	543	May. 26, 2019	Sunny Windy	Athabasca	A17 transect west	N 56.99895° W 111.45674°
81	542	May. 26, 2019	Sunny Windy	Athabasca	A17 transect middle	N 56.99960° W 111.45511°
82	596	May. 26, 2019	Sunny Windy	Athabasca	A17 transect middle	N 56.99960° W 111.45511°
83	595	May. 26, 2019	Sunny Windy	Athabasca	A17 transect middle	N 56.99960° W 111.45511°
84	580	May. 26, 2019	Sunny Gentle wind	Athabasca	A17 transect east	N 57.00008° W 111.45266°
85	593	May. 26, 2019	Sunny Gentle wind	Athabasca	A17 transect east	N 57.00008° W 111.45266°
86	594	May. 26, 2019	Sunny Gentle wind	Athabasca	A17 transect east	N 57.00008° W 111.45266°
87	599	May. 26, 2019	Sunny	Steepbank river	Steepbank river mixing transect SB-1	
88	588	May. 26, 2019	Sunny Gentle wind	Athabasca	Steepbank river mixing transect AR-1	N 57.01804° W 111.47942°
89	598	May. 26, 2019	Sunny Gentle wind	Athabasca	Steepbank river mixing transect AR-1	N 57.01804° W 111.47942°
90	589	May. 26, 2019	Sunny A little wind	Athabasca	Steepbank river mixing transect AR-2	N 57.01855° W 111.48331°
91	586	May. 26, 2019	Sunny A little wind	Athabasca	Steepbank river mixing transect AR-2	N 57.01855° W 111.48331°
92	587	May. 26, 2019	Sunny Windy	Athabasca	Steepbank river mixing transect AR-3	N 57.02003° W 111.48581°
93	591	May. 26, 2019	Sunny Windy	Athabasca	Steepbank river mixing transect AR-3	N 57.02003° W 111.48581°
94	592	May. 26, 2019	Sunny Windy	Athabasca	Steepbank river mixing transect AR-4	N 57.02236° W 111.48923°
95	549	May. 26, 2019	Sunny Windy	Athabasca	Steepbank river mixing transect AR-4	N 57.02236° W 111.48923°
96	590	May. 26, 2019	Sunny	Steepbank river	Steepbank river mixing transect SB-4	N 57.02227° W 111.48847°
97	528	May. 26, 2019	Sunny Gentle wind	Steepbank river	Steepbank river mixing transect SB-4	N 57.02227° W 111.48847°
98	519	May. 26, 2019	Sunny Gentle wind	Steepbank river	Steepbank river mixing transect SB-3	N 57.02017° W 111.48521°
99	515	May. 26, 2019	Sunny Gentle wind	Steepbank river	Steepbank river mixing transect SB-2	N 57.01892° W 111.48296°
100	576	May. 27, 2019	Sunny Gentle wind	Athabasca	A5 transect west	N 57.57321° W 111.51399°
101	512	May. 27, 2019	Sunny Gentle wind	Athabasca	A5 transect west	N 57.57321° W 111.51399°
102	517	May. 27, 2019	Sunny Gentle wind	Athabasca	A5 transect west	N 57.57321° W 111.51399°
103	600	May. 27, 2019	Sunny Gentle wind	Athabasca	A5 transect middle	N 57.57309° W 111.51162°
104	601	May. 27, 2019	Sunny Gentle wind	Athabasca	A5 transect middle	N 57.57309° W 111.51162°
105	602	May. 27, 2019	Sunny Windy	Athabasca	A5 transect middle	N 57.57309° W 111.51162°
106	603	May. 27, 2019	Sunny Gentle wind	Athabasca	A5 transect east	N 57.57337° W 111.50471°
107	604	May. 27, 2019	Sunny Gentle wind	Athabasca	A5 transect east	N 57.57337° W 111.50471°
108	605	May. 27, 2019	Sunny Gentle wind	Athabasca	A5 transect east	N 57.57337° W 111.50471°
109	606	May. 27, 2019	Sunny	Pierre river		
110	607	May. 27, 2019	Sunny	Muskeg river		

Appendix III: original DOM dataset

Sample ID	Year	Season	River	Nickname	Location	Sample Depth (m)	Total Depth (m)	DOC (C mg/L)	*Mp* (Da)	95% CI (Mp)	BIX	HIX	FIX	A_{254} (m^{-1})	E2:E3	$SUVA_{254}$ (L/mg-C/m)	COMP1	COMP2	COMP3	COMP4	COMP5	COMP6	COMP7	COMP8
259	2018	Fall	AR	Upstream MLC	East	0.3	2.8	10.6	1005.25	37.03	0.53	16.56	1.52	34.22	5.34	3.23	0.58	0.57	0.34	0.28	0.26	0.13	0.05	0.01
267	2018	Fall	AR	Upstream MLC	Middle	0.3	1	8.1	1132.95	9.00	0.54	15.24	1.52	23.82	6.11	2.94	0.43	0.44	0.28	0.23	0.21	0.11	0.04	0.00
277	2018	Fall	CL	CL05-CL	Mixing	1.2	1.6	10.1	1086.97	28.40	0.53	17.05	1.52	32.77	5.10	3.24	0.56	0.56	0.33	0.28	0.26	0.13	0.04	0.00
283	2018	Fall	AR	Upstream MLC	East	2.2	2.8	11.0	1025.96	20.01	0.52	17.37	1.52	33.60	5.49	3.05	0.53	0.53	0.31	0.26	0.24	0.12	0.04	0.00
284	2018	Fall	AR	Upstream MLC	East	1.2	2.8	10.7	1065.08	43.95	0.53	17.00	1.53	34.06	5.22	3.18	0.58	0.56	0.33	0.28	0.27	0.13	0.05	0.00
285	2018	Fall	AR	Upstream MLC	West	1.8	3.7	7.7	1134.23	5.54	0.57	13.62	1.54	21.01	6.72	2.73	0.40	0.37	0.26	0.23	0.23	0.10	0.04	0.01
286	2018	Fall	AR	Upstream MLC	West	3.4	3.7	7.5	1062.20	15.48	0.58	13.33	1.54	21.37	6.10	2.85	0.41	0.37	0.27	0.23	0.25	0.10	0.05	0.02
288	2018	Fall	AR	AR05-CL	Mixing	0.3	1.7	8.7	1120.85	45.55	0.54	15.79	1.53	26.63	6.09	3.06	0.47	0.47	0.29	0.25	0.23	0.12	0.04	0.00
289	2018	Fall	AR	Upstream MLC	Middle	0.7	1	8.5	1073.40	32.80	0.54	15.26	1.53	24.01	6.32	2.82	0.41	0.40	0.26	0.22	0.20	0.11	0.04	0.00
308	2018	Fall	MLC	MLC	N/A	0.1	0.2	23.0	981.03	56.62	0.59	12.72	1.58	69.38	5.69	3.02	1.19	1.04	0.43	0.29	0.97	0.14	0.15	0.32
309	2018	Fall	AR	AR05-CL	Mixing	1.3	1.7	9.1	1042.70	38.01	0.54	15.88	1.52	27.02	6.18	2.97	0.46	0.46	0.29	0.24	0.23	0.12	0.04	0.00
310	2018	Fall	CL	CL05-CL	Mixing	0.3	1.6	10.2	1012.89	19.67	0.53	16.79	1.52	32.39	5.54	3.18	0.55	0.55	0.33	0.27	0.25	0.13	0.04	0.00
400	2018	Fall	AR	AR04-HR	Mixing	1.3	1.7	7.5	1094.65	37.19	0.56	13.83	1.52	21.86	6.42	2.91	0.39	0.38	0.25	0.22	0.21	0.10	0.04	0.01
401	2018	Fall	PR	PR	N/A	0.1	0.2	21.0	891.89	16.58	0.59	16.13	1.64	52.81	6.71	2.51	0.71	0.71	0.32	0.26	0.54	0.10	0.06	0.01
402	2018	Fall	AR	AR02-HR	Mixing	1.9	2.3	7.3	1156.35	30.37	0.58	12.93	1.53	20.37	5.82	2.79	0.40	0.37	0.26	0.23	0.24	0.10	0.05	0.02
403	2018	Fall	HR	HR01-HR	Mixing	0.3	0.8	33.3	1081.74	4.94	0.45	26.60	1.45	135.95	4.66	4.08	2.77	3.36	0.51	0.23	0.95	0.17	0.19	0.01
404	2018	Fall	AR	A5	West	1.8	2.3	9.1	1067.54	60.40	0.54	15.51	1.53	27.27	5.81	3.00	0.48	0.46	0.29	0.25	0.24	0.11	0.04	0.00
405	2018	Fall	AR	Upstream FMM	West	0.3	0.9	6.5	929.72	9.16	0.57	12.47	1.56	17.53	6.95	2.70	0.21	0.23	0.15	0.14	0.14	0.05	0.02	0.00
406	2018	Fall	CL	CL02-CL	Mixing	0.3	2.1	11.6	967.22	18.49	0.53	16.35	1.53	37.75	5.55	3.25	0.63	0.62	0.35	0.29	0.28	0.13	0.06	0.01
407	2018	Fall	AR	AR01-HR	Mixing	0.3	2.7	6.8	1101.86	37.40	0.56	13.45	1.52	19.88	6.98	2.92	0.41	0.40	0.27	0.23	0.22	0.11	0.05	0.01
408	2018	Fall	HR	HR02-HR	Mixing	2.1	2.5	19.9	1192.10	65.68	0.47	22.92	1.48	79.19	4.86	3.98	1.36	1.40	0.47	0.35	0.41	0.19	0.09	0.01
409	2018	Fall	HR	HR02-HR	Mixing	0.3	2.5	19.8	1147.53	33.81	0.47	22.14	1.48	72.60	4.87	3.67	1.10	1.15	0.41	0.31	0.34	0.16	0.08	0.00
410	2018	Fall	AR	AR04-HR	Mixing	0.3	1.7	7.7	1101.50	5.10	0.57	12.92	1.53	21.15	6.62	2.75	0.39	0.44	0.25	0.22	0.23	0.10	0.05	0.02
411	2018	Fall	AR	AR01-HR	Mixing	2.4	2.7	6.7	1104.63	45.09	0.57	13.06	1.54	19.97	6.00	2.98	0.42	0.39	0.28	0.24	0.24	0.11	0.05	0.01
412	2018	Fall	HR	HR04-HR	Mixing	0.5	0.8	14.5	1195.96	34.43	0.49	19.79	1.49	53.74	5.00	3.71	0.84	0.85	0.39	0.30	0.27	0.16	0.06	0.00
413	2018	Fall	AR	AR02-HR	Mixing	0.3	2.3	7.3	1077.41	15.45	0.56	13.15	1.53	19.81	6.02	2.71	0.34	0.33	0.22	0.20	0.19	0.09	0.04	0.00
414	2018	Fall	HR	HR03-HR	Mixing	0.6	0.9	16.6	1142.96	0.20	0.48	21.44	1.47	58.63	4.97	3.53	0.90	0.92	0.39	0.30	0.27	0.17	0.06	0.00
415	2018	Fall	AR	AR03-HR	Mixing	0.3	2.6	7.6	1041.94	10.17	0.58	12.73	1.53	20.16	6.37	2.65	0.37	0.34	0.24	0.21	0.22	0.09	0.05	0.01
416	2018	Fall	AR	A5	East	0.3	2.8	9.1	1114.53	5.30	0.52	16.62	1.52	26.64	5.87	2.93	0.38	0.40	0.24	0.21	0.17	0.10	0.03	0.00
417	2018	Fall	AR	A5	East	2.4	2.8	8.7	1041.44	0.11	0.54	15.39	1.52	26.80	5.87	3.08	0.48	0.46	0.29	0.25	0.24	0.11	0.04	0.00
418	2018	Fall	AR	A5	East	1.2	2.8	8.8	1136.05	29.79	0.55	14.79	1.53	26.49	5.40	3.01	0.49	0.46	0.30	0.26	0.26	0.12	0.05	0.01
420	2018	Fall	AR	A5	Middle	1.2	1.7	8.7	1028.91	0.10	0.54	15.16	1.53	26.59	5.97	3.06	0.48	0.46	0.29	0.25	0.24	0.12	0.05	0.00
421	2018	Fall	AR	A5	West	0.3	2.3	9.0	1127.36	45.73	0.55	14.73	1.54	26.70	5.62	2.97	0.47	0.45	0.29	0.25	0.25	0.11	0.05	0.01
423	2018	Fall	BC	BC	N/A	0.1	0.2	25.3	1178.85	31.01	0.57	14.80	1.52	73.31	6.28	2.90	1.24	1.16	0.37	0.25	0.95	0.13	0.13	0.18
424	2018	Fall	AR	Upstream MLC	West	0.3	3.7	7.8	1042.40	0.11	0.57	13.30	1.53	22.08	6.33	2.83	0.40	0.38	0.26	0.23	0.23	0.10	0.05	0.01
425	2018	Fall	AR	A5	West	1.2	2.3	8.9	1139.08	29.88	0.55	14.76	1.53	25.88	6.36	2.91	0.47	0.49	0.29	0.25	0.24	0.12	0.05	0.01
426	2018	Fall	AR	AR03-HR	Mixing	2.1	2.6	7.3	1123.84	5.41	0.58	12.74	1.55	20.31	5.71	2.78	0.38	0.34	0.25	0.22	0.23	0.10	0.05	0.02
427	2018	Fall	AR	A5	Middle	0.8	1.7	8.8	1114.01	8.87	0.54	14.47	1.49	26.52	6.10	3.01	0.47	0.43	0.27	0.24	0.21	0.11	0.05	0.02
428	2018	Fall	CL	CL04-CL	Mixing	1.1	1.4	11.1	1072.21	8.57	0.52	17.69	1.51	33.76	5.70	3.04	0.56	0.56	0.32	0.27	0.23	0.13	0.04	0.00
429	2018	Fall	AR	AR04-CL	Mixing	2.2	2.5	8.4	1103.71	5.12	0.53	14.11	1.48	24.08	6.55	2.87	0.43	0.44	0.26	0.22	0.19	0.10	0.05	0.01
430	2018	Fall	MKR	MKR	N/A	0.15	0.3	32.9	1010.75	26.25	0.50	22.98	1.52	115.35	5.24	3.51	2.19	2.46	0.49	0.25	1.02	0.15	0.15	0.01
431	2018	Fall	AR	AR01-CL	Mixing	0.3	1.5	6.6	1118.46	8.90	0.56	12.08	1.49	18.00	5.85	2.73	0.33	0.31	0.21	0.19	0.17	0.08	0.05	0.01
432	2018	Fall	AR	Upstream FMM	Middle	1.6	1.9	6.6	1066.25	15.47	0.56	12.26	1.52	18.38	6.28	2.78	0.36	0.33	0.22	0.20	0.18	0.09	0.05	0.01
433	2018	Fall	AR	AR04-CL	Mixing	0.3	2.5	8.3	1077.64	32.86	0.54	13.47	1.49	24.23	6.08	2.92	0.43	0.41	0.25	0.22	0.19	0.10	0.05	0.01
434	2018	Fall	CL	CL03-CL	Mixing	2.1	2.4	10.8	1036.66	32.26	0.53	16.44	1.52	33.80	5.17	3.13	0.55	0.54	0.32	0.27	0.24	0.12	0.05	0.00
435	2018	Fall	AR	A5	Middle	0.3	1.7	9.1	1131.00	29.65	0.52	15.37	1.48	25.97	6.39	2.85	0.43	0.45	0.25	0.22	0.17	0.10	0.04	0.00
436	2018	Fall	AR	AR02-CL	Mixing	0.3	1.7	8.5	1150.30	46.38	0.55	14.70	1.53	25.39	5.45	2.99	0.47	0.45	0.30	0.25	0.24	0.12	0.05	0.01
437	2018	Fall	AR	AR01-CL	Mixing	1	1.5	6.7	1042.70	38.01	0.58	11.87	1.53	18.22	6.54	2.72	0.35	0.32	0.23	0.21	0.21	0.09	0.05	0.02
438	2018	Fall	AR	AR04-SB	Mixing	3	3.3	8.6	1107.86	45.18	0.52	15.15	1.47	28.06	5.24	3.26	0.49	0.49	0.29	0.25	0.21	0.12	0.05	0.01
439	2018	Fall	SB	SB02-SB	Mixing	0.3	1.9	14.3	1131.83	8.99	0.53	17.20	1.52	42.95	5.54	3.00	0.67	0.63	0.34	0.28	0.28	0.13	0.06	0.02
440	2018	Fall	SB	SB03-SB	Mixing	0.3	1.2	10.8	1064.83	38.59	0.53	16.48	1.52	33.60	5.14	3.11	0.58	0.56	0.34	0.28	0.26	0.13	0.05	0.01
442	2018	Fall	AR	AR03-SB	Mixing	5	5.2	8.9	1080.82	32.90	0.53	14.27	1.47	27.03	5.42	3.04	0.47	0.46	0.27	0.24	0.20	0.11	0.05	0.01
443	2018	Fall	AR	AR02-SB	Mixing	3.9	4.4	8.6	1087.21	4.98	0.53	14.56	1.48	26.16	5.70	3.04	0.46	0.51	0.27	0.23	0.19	0.11	0.05	0.01
444	2018	Fall	SB	SB04-SB	Mixing	0.3	1	10.4	1076.15	60.77	0.54	15.54	1.53	33.77	5.66	3.25	0.62	0.59	0.36	0.29	0.29	0.14	0.06	0.02
445	2018	Fall	SB	SB02-SB	Mixing	1.5	1.9	10.3	1058.49	38.42	0.51	16.38	1.47	31.98	5.42	3.10	0.54	0.52	0.30	0.25	0.21	0.12	0.05	0.01
446	2018	Fall	SB	SB03-SB	Mixing	0.7	1.2	10.4	1139.08	29.88	0.52	15.25	1.47	34.61	5.44	3.33	0.59	0.56	0.31	0.27	0.24	0.13	0.06	0.03
447	2018	Fall	CL	CL04-CL	Mixing	0.3	1.4	11.0	1031.27	58.83	0.51	16.40	1.47	35.29	5.42	3.21	0.57	0.55	0.30	0.26	0.23	0.12	0.05	0.01
448	2018	Fall	SB	SB04-SB	Mixing	0.7	1	10.7	1052.09	0.12	0.51	16.09	1.46	33.61	5.79	3.14	0.53	0.51	0.29	0.24	0.20	0.12	0.05	0.01
449	2018	Fall	TAR	TAR	N/A	0.2	0.5	17.2	963.36	35.91	0.54	15.03	1.49	50.69	6.13	2.95	0.75	0.67	0.29	0.26	0.46	0.11	0.07	0.03
450	2018	Fall	MUR	MUR	N/A	0.15	0.3	24.3	1034.45	58.97	0.53	17.44	1.51	67.21	6.03	2.77	0.94	0.89	0.33	0.25	0.49	0.11	0.08	0.04
451	2018	Fall	SB	SB01-SB	Mixing	0.2	0.3	21.1	1089.87	5.00	0.49	20.70	1.48	70.43	5.59	3.34	1.15	1.11	0.40	0.30	0.44	0.15	0.08	0.03
452	2018	Fall	AR	A9	West	3	3.5	9.0	1064.95	32.68	0.53	14.78	1.47	26.59	6.11	2.95	0.46	0.44	0.26	0.23	0.20	0.11	0.05	0.01
453	2018	Fall	AR	A9	Middle	0.2	0.6	8.8	1036.07	20.27	0.52	14.58	1.47	25.88	6.20	2.94	0.44	0.43	0.26	0.22	0.19	0.11	0.04	0.01
454	2018	Fall	CL	CL03-CL	Mixing	0.3	2.4	10.7	1098.53	8.76	0.51	16.08	1.47	33.44	5.20	3.13	0.54	0.52	0.29	0.25	0.21	0.12	0.05	0.01
455	2018	Fall	AR	A9	Middle	0.4	0.6	9.1	949.97	9.34	0.53	14.59	1.47	26.69	5.65	2.93	0.43	0.41	0.25	0.22	0.19	0.10	0.04	0.01
456	2018	Fall	AR	Upstream FMM	East	0.9	1.3	6.7	1028.91	0.10	0.55	12.75	1.49	18.39	6.67	2.74	0.35	0.33	0.22	0.19	0.17	0.09	0.04	0.01
457	2018	Fall	AR	A9	West	1.5	3.5	8.7	1069.69	60.49	0.54	14.32	1.47	26.93	5.69	3.10	0.47	0.44	0.27	0.23	0.20	0.11	0.05	0.02
458	2018	Fall	ER	ER	N/A	0.1	0.3	16.7	978.26	25.33	0.53	15.61	1.48	45.46	6.72	2.72	0.46	0.43	0.18	0.17	0.27	0.07	0.04	0.00

459	2018	Fall	AR	Upstream FMM	West	0.6	0.9	6.7	1041.88	32.34	0.57	11.00	1.49	17.90	5.90	2.67	0.35	0.33	0.22	0.20	0.19	0.09	0.05	0.03
460	2018	Fall	AR	Upstream FMM	Middle	0.3	1.9	6.6	1114.53	5.30	0.55	12.81	1.49	17.98	6.80	2.72	0.34	0.33	0.22	0.19	0.16	0.09	0.04	0.01
461	2018	Fall	AR	AR03-CL	Mixing	0.3	1.3	6.8	1096.02	44.84	0.56	12.19	1.50	19.30	5.74	2.84	0.37	0.34	0.22	0.21	0.20	0.09	0.05	0.01
462	2018	Fall	CL	CL01-CL	Mixing	1.5	1.8	12.1	963.92	31.14	0.50	16.82	1.46	38.52	5.45	3.18	0.59	0.58	0.30	0.26	0.22	0.12	0.05	0.01
463	2018	Fall	AR	A9	West	0.3	3.5	8.6	1042.94	59.34	0.48	16.72	1.43	26.43	6.09	3.07	0.24	0.29	0.14	0.13	0.07	0.06	0.02	0.00
464	2018	Fall	CL	CL02-CL	Mixing	1.8	2.1	11.6	1046.18	8.39	0.51	16.75	1.47	38.44	5.27	3.31	0.61	0.59	0.31	0.27	0.24	0.12	0.05	0.01
465	2018	Fall	AR	Upstream FMM	Middle	0.9	1.9	6.8	1052.16	38.26	0.57	11.74	1.48	18.07	6.93	2.66	0.33	0.30	0.21	0.19	0.18	0.08	0.04	0.02
466	2018	Fall	AR	AR01-SB	Mixing	3	3.4	9.2	1077.37	4.90	0.51	15.40	1.46	28.29	5.49	3.07	0.48	0.48	0.28	0.24	0.19	0.11	0.05	0.01
467	2018	Fall	AR	A17	East	0.3	0.9	9.5	1056.10	10.30	0.52	15.51	1.47	30.03	5.40	3.16	0.53	0.51	0.30	0.26	0.21	0.12	0.05	0.01
468	2018	Fall	AR	A17	West	2.5	5.4	7.0	1041.65	37.98	0.54	12.62	1.47	20.94	6.27	2.99	0.40	0.39	0.25	0.22	0.18	0.10	0.05	0.02
469	2018	Fall	AR	AR03-SB	Mixing	0.3	5.2	8.5	1140.10	29.90	0.51	15.51	1.49	28.02	5.18	3.30	0.34	0.37	0.20	0.18	0.14	0.08	0.03	0.00
470	2018	Fall	AR	A17	East	0.6	0.9	9.2	1085.55	15.43	0.49	16.89	1.46	29.94	5.80	3.25	0.28	0.33	0.16	0.15	0.10	0.06	0.02	0.00
471	2018	Fall	AR	A17	Middle	0.3	1.9	9.3	1103.20	5.16	0.49	17.27	1.45	29.40	5.37	3.16	0.48	0.51	0.28	0.23	0.14	0.12	0.04	0.00
472	2018	Fall	CL	CL01-CL	Mixing	0.3	1.8	11.8	987.06	34.02	0.50	17.10	1.46	38.64	5.35	3.27	0.60	0.59	0.31	0.26	0.22	0.12	0.05	0.01
473	2018	Fall	AR	AR02-SB	Mixing	0.3	4.4	9.1	1052.09	0.12	0.53	14.87	1.47	27.31	5.50	3.00	0.44	0.43	0.26	0.22	0.18	0.11	0.04	0.01
474	2018	Fall	AR	AR04-SB	Mixing	0.3	3.3	6.9	1074.10	4.88	0.50	16.65	1.46	27.94	5.41	4.05	0.61	0.63	0.36	0.30	0.20	0.15	0.05	0.00
475	2018	Fall	AR	A17	West	5	5.4	8.6	1179.88	31.04	0.54	12.67	1.48	20.69	5.89	2.41	0.32	0.31	0.20	0.17	0.15	0.08	0.04	0.01
476	2018	Fall	AR	A17	Middle	0.8	1.9	8.9	1128.48	8.97	0.51	16.05	1.47	29.40	5.28	3.30	0.50	0.51	0.29	0.24	0.18	0.12	0.04	0.01
477	2018	Fall	AR	AR03-CL	Mixing	0.8	1.3	6.5	1107.31	5.21	0.57	11.02	1.52	18.64	7.21	2.87	0.36	0.36	0.24	0.21	0.18	0.10	0.06	0.02
478	2018	Fall	AR	A9	East	0.1	0.3	8.3	1082.83	4.95	0.52	14.78	1.47	26.29	5.88	3.17	0.48	0.47	0.28	0.24	0.21	0.11	0.05	0.01
479	2018	Fall	AR	A17	Middle	1.6	1.9	9.2	1116.23	8.88	0.52	16.49	1.51	29.15	5.34	3.17	0.52	0.53	0.32	0.27	0.22	0.13	0.04	0.00
480	2018	Fall	AR	A17	West	0.3	5.4	7.4	1130.71	8.98	0.52	14.33	1.48	20.67	6.43	2.79	0.34	0.35	0.21	0.19	0.14	0.09	0.03	0.00
481	2018	Fall	AR	AR01-SB	Mixing	0.3	3.4	8.7	1079.55	4.92	0.48	16.36	1.45	28.36	5.71	3.26	0.24	0.30	0.15	0.13	0.08	0.05	0.02	0.00
482	2018	Fall	AR	Upstream FMM	East	0.6	1.3	6.3	1071.92	4.86	0.57	10.36	1.50	18.17	6.80	2.88	0.37	0.36	0.24	0.21	0.18	0.10	0.06	0.03
483	2018	Fall	LFC	LFC	N/A	0.2	0.3	23.5	1103.55	45.06	0.50	22.00	1.49	70.22	6.02	2.99	0.99	0.98	0.33	0.25	0.41	0.12	0.05	0.00
484	2018	Fall	AR	AR02-CL	Mixing	1.4	1.7	8.2	1087.20	32.99	0.53	14.78	1.47	24.75	6.36	3.02	0.44	0.46	0.26	0.22	0.17	0.11	0.04	0.01
485	2018	Fall	AR	Upstream FMM	East	0.3	1.3	6.3	1065.39	60.31	0.56	12.07	1.48	18.25	6.56	2.90	0.36	0.34	0.23	0.20	0.18	0.09	0.05	0.02
500	2019	Spring	AR	AR01-HR	Mixing	3.1	3.4	9.4	1272.35	4.98	0.57	9.42	1.50	30.35	6.14	3.23	0.60	0.53	0.31	0.27	0.30	0.11	0.13	0.12
501	2019	Spring	AR	Upstream FMM	West	0.9	1.2	9.6	1273.49	4.98	0.62	3.12	1.50	29.86	6.36	3.11	0.58	0.52	0.29	0.26	0.37	0.10	0.48	0.70
502	2019	Spring	AR	Upstream FMM	Middle	1.8	2.4	9.4	1271.21	4.98	0.57	10.14	1.49	29.48	6.17	3.14	0.56	0.50	0.29	0.26	0.30	0.10	0.10	0.08
503	2019	Spring	AR	Upstream FMM	East	1	1.6	9.4	1256.44	4.97	0.57	8.55	1.49	29.70	6.18	3.16	0.56	0.49	0.29	0.25	0.32	0.10	0.13	0.14
504	2019	Spring	AR	Upstream FMM	West	0.6	1.2	9.2	1257.57	4.97	0.55	11.72	1.49	29.59	5.98	3.22	0.57	0.51	0.30	0.26	0.30	0.10	0.09	0.05
505	2019	Spring	AR	Upstream FMM	East	0.3	1.6	9.1	1259.84	4.97	0.56	10.55	1.48	30.04	5.98	3.30	0.59	0.52	0.30	0.27	0.32	0.10	0.10	0.08
506	2019	Spring	AR	Upstream FMM	Middle	0.3	2.1	9.5	1299.82	5.00	0.56	11.76	1.48	29.67	6.14	3.12	0.55	0.49	0.29	0.25	0.28	0.10	0.08	0.05
507	2019	Spring	AR	Upstream FMM	West	0.3	1.2	9.5	1251.90	4.97	0.56	10.68	1.49	29.57	5.99	3.11	0.55	0.49	0.29	0.25	0.31	0.10	0.10	0.07
508	2019	Spring	HR	HR01-HR	Mixing	0.6	0.9	18.0	1317.12	5.00	0.50	17.80	1.47	69.46	5.08	3.86	1.31	1.29	0.45	0.35	0.57	0.15	0.12	0.05
509	2019	Spring	AR	AR04-HR	Mixing	0.3	3.1	9.4	1354.33	5.02	0.56	6.99	1.48	31.69	5.92	3.37	0.64	0.58	0.34	0.28	0.33	0.12	0.20	0.26
510	2019	Spring	CL	CL02-CL	Mixing	0.3	2.5	9.6	1195.85	4.93	0.51	12.32	1.47	33.13	5.42	3.45	0.67	0.64	0.35	0.30	0.28	0.12	0.10	0.07
511	2019	Spring	CL	CL01-CL	Mixing	0.3	1.8	9.3	1211.86	51.52	0.52	12.45	1.48	32.95	5.75	3.54	0.69	0.65	0.36	0.31	0.30	0.13	0.10	0.08
512	2019	Spring	AR	A5	West	1.3	2.7	9.8	1199.36	43.46	0.56	5.68	1.47	33.32	5.61	3.40	0.66	0.59	0.34	0.28	0.33	0.12	0.27	0.38
513	2019	Spring	AR	AR05-HR	Mixing	1.9	2.2	10.1	1397.06	54.28	0.53	13.87	1.46	31.85	5.78	3.15	0.56	0.51	0.30	0.24	0.23	0.11	0.06	0.03
514	2019	Spring	HR	HR05-HR	Mixing	1.4	1.7	10.3	1411.29	54.46	0.55	9.31	1.50	35.77	5.54	3.47	0.70	0.64	0.35	0.29	0.33	0.12	0.15	0.16
515	2019	Spring	SB	SB02-SB	Mixing	0.3	0.7	15.5	1191.95	43.27	0.51	17.11	1.47	55.55	5.49	3.58	0.80	0.73	0.33	0.26	0.34	0.11	0.07	0.04
516	2019	Spring	CL	CL01-CL	Mixing	1.5	1.8	9.5	1281.89	52.65	0.52	11.99	1.47	32.91	5.31	3.46	0.66	0.63	0.35	0.30	0.28	0.12	0.10	0.07
517	2019	Spring	AR	A5	West	2.4	2.7	10.0	1197.24	43.41	0.54	10.27	1.46	33.03	5.58	3.30	0.63	0.56	0.33	0.27	0.26	0.12	0.12	0.13
518	2019	Spring	AR	AR02-CL	Mixing	2.1	2.4	10.0	1387.60	54.15	0.54	12.75	1.47	33.21	5.62	3.32	0.62	0.57	0.33	0.27	0.28	0.11	0.09	0.05
519	2019	Spring	SB	SB03-SB	Mixing	0.3	0.6	15.6	1189.83	43.22	0.51	16.13	1.48	55.19	5.42	3.54	1.08	0.97	0.42	0.34	0.48	0.14	0.10	0.07
520	2019	Spring	HR	HR05-HR	Mixing	0.3	1.7	10.4	1405.36	54.38	0.55	9.60	1.46	34.84	5.76	3.35	0.71	0.63	0.37	0.29	0.33	0.13	0.15	0.16
521	2019	Spring	HR	HR03-HR	Mixing	2.4	2.6	9.7	1381.70	54.07	0.54	12.65	1.48	31.76	6.03	3.27	0.63	0.57	0.32	0.28	0.31	0.11	0.08	0.04
522	2019	Spring	HR	HR04-HR	Mixing	0.3	1.4	10.9	1412.48	54.48	0.52	14.04	1.47	37.46	5.53	3.44	0.74	0.69	0.37	0.30	0.31	0.13	0.09	0.05
523	2019	Spring	HR	HR02-HR	Mixing	0.8	1.1	15.4	1353.54	53.69	0.51	16.20	1.47	52.39	5.25	3.40	0.89	0.84	0.37	0.30	0.38	0.12	0.09	0.03
524	2019	Spring	AR	AR02-HR	Mixing	0.3	2.6	9.7	1300.23	52.92	0.55	12.23	1.49	30.82	5.91	3.18	0.55	0.49	0.29	0.25	0.29	0.10	0.08	0.04
525	2019	Spring	HR	HR01-HR	Mixing	0.3	0.9	18.7	1332.57	53.39	0.49	16.80	1.47	69.64	5.12	3.72	1.26	1.22	0.43	0.33	0.50	0.14	0.13	0.08
526	2019	Spring	AR	AR01-HR	Mixing	0.3	3.4	9.6	1256.12	45.32	0.62	3.52	1.48	31.22	5.91	3.25	0.62	0.53	0.31	0.27	0.43	0.10	0.43	0.63
527	2019	Spring	AR	AR02-HR	Mixing	2.3	2.6	9.6	1217.12	45.34	0.57	9.08	1.49	30.73	5.98	3.20	0.59	0.52	0.31	0.27	0.34	0.11	0.13	0.14
528	2019	Spring	SB	SB04-SB	Mixing	0.8	1.1	13.9	1224.92	44.13	0.53	7.27	1.48	43.74	5.63	3.15	0.76	0.69	0.34	0.28	0.38	0.11	0.23	0.31
529	2019	Spring	HR	HR04-HR	Mixing	1.1	1.4	10.7	1273.61	45.29	0.58	4.07	1.47	38.04	6.03	3.55	0.78	0.72	0.37	0.31	0.42	0.13	0.47	0.72
530	2019	Spring	LFC	LFC	N/A	0.1	0.45	18.4	1232.23	45.33	0.50	14.52	1.48	63.43	5.35	3.45	1.24	1.17	0.47	0.34	0.42	0.16	0.16	0.17
531	2019	Spring	AR	Upstream FMM	East	1.2	1.6	9.5	1186.08	45.32	0.57	9.88	1.48	29.97	6.02	3.15	0.57	0.50	0.29	0.26	0.32	0.10	0.11	0.09
532	2019	Spring	HR	HR02-HR	Mixing	0.3	1.1	15.3	1244.15	45.33	0.51	13.68	1.46	55.33	5.30	3.62	1.01	0.96	0.40	0.33	0.43	0.13	0.13	0.11
533	2019	Spring	AR	AR03-HR	Mixing	2.2	2.6	9.7	1225.74	45.34	0.62	3.07	1.48	31.02	6.01	3.20	0.61	0.53	0.30	0.26	0.40	0.10	0.49	0.73
534	2019	Spring	AR	AR05-HR	Mixing	0.3048	2.2	9.6	1286.80	45.27	0.55	10.85	1.49	32.00	5.76	3.33	0.64	0.58	0.34	0.28	0.31	0.12	0.11	0.10
535	2019	Spring	AR	AR01-CL	Mixing	0.3	2	10.1	1283.49	45.27	0.54	11.58	1.47	32.92	5.68	3.26	0.62	0.57	0.33	0.27	0.27	0.12	0.10	0.08
536	2019	Spring	AR	AR03-HR	Mixing	0.3	2.6	9.4	1226.82	45.34	0.58	8.49	1.48	30.58	6.09	3.25	0.57	0.49	0.29	0.25	0.30	0.10	0.14	0.15
537	2019	Spring	HR	HR03-HR	Mixing	0.3	2.6	9.9	1245.10	47.33	0.55	12.03	1.48	32.56	5.84	3.29	0.63	0.57	0.32	0.28	0.32	0.11	0.09	0.06
538	2019	Spring	AR	AR04-HR	Mixing	2.8	3.1	9.5	1294.20	48.52	0.55	11.28	1.47	31.92	5.66	3.36	0.64	0.57	0.34	0.28	0.29	0.12	0.10	0.09
539	2019	Spring	AR	Upstream FMM	Middle	0.9	2.1	9.2	1244.02	47.31	0.55	11.38	1.48	30.23	5.92	3.29	0.57	0.51	0.30	0.26	0.30	0.10	0.09	0.05
540	2019	Spring	AR	A9	East	0.6	1.2	9.5	1222.78	44.07	0.53	10.83	1.47	34.08	5.95	3.59	0.68	0.63	0.35	0.29	0.29	0.12	0.12	0.11
541	2019	Spring	AR	A17	West	2.9	5.9	9.1	1196.18	43.38	0.52	12.18	1.47	32.43	5.61	3.56	0.66	0.62	0.35	0.29	0.26	0.13	0.10	0.07

542	2019	Spring	AR	A17	Middle	0.3	1.9	9.4	1174.81	1.49	0.52	13.00	1.48	32.32	5.58	3.44	0.60	0.56	0.32	0.27	0.24	0.11	0.08	0.05
543	2019	Spring	AR	A17	West	5.7	5.9	9.3	1230.27	44.26	0.51	14.48	1.45	32.31	5.68	3.47	0.48	0.48	0.26	0.22	0.17	0.09	0.05	0.02
544	2019	Spring	AR	A9	Middle	0.3	1.7	9.4	1218.51	43.96	0.52	13.50	1.47	33.58	5.64	3.57	0.68	0.65	0.37	0.30	0.25	0.13	0.09	0.05
545	2019	Spring	TAR	TAR	N/A	0.3	0.7	14.6	1081.00	40.33	0.59	4.77	1.50	44.03	6.42	3.02	0.79	0.68	0.32	0.28	0.53	0.10	0.38	0.58
546	2019	Spring	AR	A9	East	0.9	1.2	9.7	1186.40	1.64	0.57	3.96	1.47	33.73	5.62	3.48	0.67	0.62	0.34	0.28	0.33	0.12	0.42	0.62
547	2019	Spring	CL	CL06-CL	Mixing	5.9	6.2	10.8	1272.28	48.00	0.53	11.82	1.47	37.23	5.41	3.45	0.70	0.66	0.36	0.29	0.30	0.13	0.11	0.10
548	2019	Spring	ER	ER	N/A	0.6	1.3	14.6	991.85	0.73	0.56	12.90	1.50	42.43	6.60	2.91	0.69	0.57	0.27	0.25	0.44	0.09	0.08	0.05
549	2019	Spring	AR	AR04-SB	Mixing	1.9	2.2	9.4	1168.50	1.41	0.52	13.61	1.46	32.16	6.02	3.42	0.64	0.59	0.34	0.28	0.25	0.12	0.08	0.04
550	2019	Spring	CL	CL06-CL	Mixing	0.3	6.2	10.9	1251.60	47.49	0.52	11.91	1.49	36.92	5.76	3.39	0.69	0.65	0.35	0.29	0.29	0.12	0.11	0.08
551	2019	Spring	AR	AR06-CL	Mixing	0.3	3	11.9	1336.26	49.52	0.52	14.17	1.48	40.11	5.76	3.37	0.68	0.65	0.34	0.27	0.26	0.12	0.08	0.04
552	2019	Spring	AR	A9	Middle	0.8	1.7	10.2	1180.07	1.56	0.52	14.24	1.47	33.91	5.45	3.32	0.60	0.56	0.32	0.26	0.23	0.11	0.07	0.04
553	2019	Spring	AR	AR06-CL	Mixing	2.7	3	12.1	1355.24	49.96	0.54	6.75	1.47	40.17	5.46	3.32	0.70	0.66	0.34	0.27	0.29	0.12	0.24	0.32
554	2019	Spring	MLC	MLC	N/A	0.2	0.3	13.7	1170.23	45.47	0.59	10.44	1.52	38.72	6.39	2.83	0.73	0.58	0.32	0.26	0.56	0.10	0.12	0.16
555	2019	Spring	AR	AR05-CL	Mixing	1.8	2.1	10.7	1281.03	48.21	0.53	12.62	1.50	35.29	5.60	3.30	0.58	0.55	0.33	0.27	0.25	0.12	0.08	0.05
556	2019	Spring	AR	AR05-CL	Mixing	0.3	2.1	11.0	1298.60	48.63	0.52	12.77	1.47	34.99	5.58	3.18	0.64	0.60	0.33	0.27	0.25	0.12	0.09	0.06
557	2019	Spring	CL	CL04-CL	Mixing	0.3	2.1	10.6	1197.60	10.29	0.52	13.62	1.46	33.33	5.39	3.14	0.62	0.58	0.33	0.27	0.25	0.11	0.07	0.05
558	2019	Spring	CL	CL04-CL	Mixing	1.8	2.1	10.9	1197.60	10.29	0.52	14.38	1.47	33.76	6.07	3.10	0.60	0.56	0.31	0.26	0.24	0.11	0.07	0.03
559	2019	Spring	CL	CL05-CL	Mixing	0.3	1.9	11.0	1244.05	10.48	0.53	11.53	1.48	34.66	5.52	3.15	0.64	0.60	0.33	0.27	0.26	0.11	0.10	0.09
560	2019	Spring	CL	CL03-CL	Mixing	0.8	1.1	10.4	1197.60	10.29	0.53	12.70	1.49	33.59	5.46	3.23	0.65	0.61	0.35	0.29	0.29	0.12	0.09	0.06
561	2019	Spring	AR	AR03-CL	Mixing	2.5	4.3	11.2	1341.24	10.86	0.53	14.55	1.48	36.03	5.54	3.22	0.58	0.54	0.30	0.25	0.24	0.10	0.06	0.03
562	2019	Spring	AR	AR04-CL	Mixing	1.6	1.9	11.2	1318.90	10.78	0.53	11.85	1.48	36.28	5.53	3.24	0.64	0.61	0.33	0.27	0.27	0.12	0.10	0.09
563	2019	Spring	AR	AR04-CL	Mixing	0.3	1.9	11.7	1317.78	10.77	0.54	12.74	1.49	35.52	5.70	3.04	0.61	0.56	0.32	0.25	0.26	0.11	0.08	0.07
564	2019	Spring	CL	CL05-CL	Mixing	1.6	1.9	10.4	1266.98	10.57	0.52	14.34	1.46	35.02	6.12	3.37	0.67	0.63	0.34	0.29	0.26	0.12	0.08	0.04
565	2019	Spring	AR	AR02-CL	Mixing	0.3	2.4	10.6	1327.81	10.81	0.55	11.54	1.49	32.39	5.88	3.06	0.58	0.53	0.31	0.25	0.27	0.11	0.09	0.08
566	2019	Spring	AR	AR01-CL	Mixing	1.5	2	10.4	1323.35	10.79	0.54	12.60	1.48	33.12	5.68	3.18	0.60	0.55	0.31	0.26	0.26	0.11	0.08	0.06
567	2019	Spring	AR	AR03-CL	Mixing	0.5	4.3	10.9	1316.74	19.37	0.66	2.41	1.50	36.81	6.10	3.38	0.70	0.64	0.34	0.28	0.45	0.12	0.79	1.40
568	2019	Spring	CL	CL02-CL	Mixing	2.2	2.5	10.6	1179.74	17.99	0.52	11.05	1.48	33.35	5.24	3.15	0.63	0.59	0.33	0.28	0.28	0.12	0.11	0.11
569	2019	Spring	CL	CL03-CL	Mixing	0.3	1.1	10.5	1190.40	18.10	0.53	12.58	1.49	33.13	5.49	3.16	0.63	0.59	0.34	0.28	0.28	0.12	0.09	0.07
570	2019	Spring	AR	Upstream MLC	West	1.5	1.7	12.2	1364.84	19.84	0.56	5.07	1.48	39.48	5.51	3.24	0.69	0.64	0.33	0.27	0.33	0.12	0.33	0.47
571	2019	Spring	AR	A9	East	0.3	1.2	10.3	1186.40	1.64	0.53	12.90	1.47	33.40	5.55	3.24	0.59	0.53	0.31	0.25	0.23	0.11	0.08	0.06
572	2019	Spring	AR	Upstream MLC	Middle	2.8	3.1	12.8	1378.39	19.97	0.52	12.94	1.46	39.84	5.59	3.11	0.65	0.62	0.32	0.26	0.24	0.12	0.09	0.07
573	2019	Spring	AR	Upstream MLC	Middle	1.4	3.1	12.3	1365.97	19.85	0.51	14.51	1.48	39.70	5.55	3.23	0.66	0.64	0.33	0.26	0.25	0.12	0.07	0.04
574	2019	Spring	AR	Upstream MLC	East	0.3	0.8	10.9	1226.91	18.47	0.52	13.26	1.47	35.47	5.43	3.25	0.62	0.59	0.32	0.27	0.25	0.11	0.08	0.05
575	2019	Spring	AR	Upstream MLC	West	1	1.7	11.9	1355.84	19.75	0.54	6.46	1.48	39.54	5.97	3.32	0.69	0.64	0.34	0.27	0.29	0.12	0.24	0.32
576	2019	Spring	AR	A5	West	0.3	2.7	10.4	1191.69	1.71	0.53	13.40	1.46	33.28	5.59	3.20	0.60	0.56	0.31	0.26	0.25	0.11	0.07	0.05
577	2019	Spring	AR	A9	Middle	1.4	1.7	10.4	1193.81	1.74	0.52	11.81	1.46	33.72	5.54	3.24	0.63	0.59	0.33	0.27	0.25	0.12	0.10	0.09
578	2019	Spring	AR	A9	West	3.1	3.5	10.1	1174.81	1.49	0.52	10.24	1.46	34.18	5.53	3.38	0.62	0.59	0.33	0.27	0.24	0.12	0.12	0.13
579	2019	Spring	AR	Upstream MLC	West	0.3	1.7	11.9	1370.48	19.89	0.55	5.59	1.47	39.33	5.57	3.30	0.71	0.66	0.34	0.28	0.32	0.12	0.30	0.43
580	2019	Spring	AR	A17	East	0.3	1.9	10.5	1102.63	118.10	0.54	7.45	1.47	32.11	5.60	3.06	0.58	0.52	0.30	0.25	0.27	0.10	0.17	0.21
581	2019	Spring	AR	A9	West	1.7	3.5	10.2	1305.65	146.81	0.51	14.19	1.45	33.97	5.54	3.33	0.60	0.57	0.32	0.26	0.21	0.12	0.07	0.04
582	2019	Spring	AR	Upstream MLC	East	0.6	0.8	11.0	1233.40	18.54	0.53	12.41	1.46	35.27	5.46	3.21	0.64	0.59	0.33	0.27	0.25	0.12	0.09	0.08
583	2019	Spring	AR	Upstream MLC	Middle	0.3	3.1	12.2	1321.19	19.41	0.51	14.32	1.45	40.39	5.48	3.31	0.69	0.65	0.34	0.27	0.25	0.12	0.08	0.05
584	2019	Spring	AR	A9	West	0.3	3.5	10.5	1319.40	148.79	0.56	4.81	1.47	34.17	5.54	3.25	0.65	0.60	0.33	0.27	0.30	0.12	0.32	0.47
585	2019	Spring	MKR	MKR	N/A	0.6	1.1	20.7	1214.14	133.73	0.52	15.73	1.48	65.33	5.65	3.16	1.08	1.00	0.36	0.28	0.53	0.11	0.11	0.07
586	2019	Spring	AR	AR02-SB	Mixing	5.7	6	10.4	1328.96	150.17	0.51	13.83	1.46	32.23	5.52	3.10	0.59	0.56	0.32	0.26	0.21	0.11	0.07	0.04
587	2019	Spring	AR	AR03-SB	Mixing	0.3	3.8	10.2	1308.82	147.27	0.60	3.18	1.47	32.55	5.72	3.19	0.60	0.55	0.31	0.26	0.35	0.11	0.48	0.73
588	2019	Spring	AR	AR01-SB	Mixing	0.3	2.7	9.9	1315.17	148.18	0.51	14.19	1.45	32.46	5.48	3.28	0.60	0.58	0.32	0.26	0.21	0.12	0.07	0.03
589	2019	Spring	AR	AR02-SB	Mixing	0.3	6	10.0	1317.28	148.49	0.53	10.36	1.47	32.57	5.45	3.26	0.60	0.56	0.32	0.27	0.25	0.11	0.11	0.10
590	2019	Spring	SB	SB04-SB	Mixing	0.3	1.1	13.7	1261.63	140.49	0.51	14.74	1.46	45.55	5.42	3.32	0.85	0.77	0.37	0.31	0.38	0.13	0.09	0.07
591	2019	Spring	AR	AR03-SB	Mixing	3.5	3.8	10.0	1305.65	146.81	0.52	13.56	1.47	32.17	5.54	3.22	0.58	0.55	0.31	0.26	0.24	0.11	0.07	0.04
592	2019	Spring	AR	AR04-SB	Mixing	0.3	2.2	10.1	1199.79	38.16	0.53	11.68	1.48	31.64	5.68	3.13	0.58	0.54	0.31	0.26	0.25	0.11	0.09	0.07
593	2019	Spring	AR	A17	East	1.1	1.9	10.2	1206.58	38.27	0.52	14.67	1.46	32.15	5.49	3.15	0.57	0.53	0.30	0.25	0.22	0.11	0.06	0.03
594	2019	Spring	AR	A17	East	1.7	1.9	10.4	1207.56	38.28	0.52	14.72	1.45	32.04	5.64	3.08	0.59	0.55	0.31	0.26	0.23	0.11	0.06	0.02
595	2019	Spring	AR	A17	Middle	1.6	1.9	10.6	1253.58	38.99	0.53	10.51	1.47	32.76	5.44	3.09	0.58	0.54	0.31	0.26	0.25	0.11	0.11	0.11
596	2019	Spring	AR	A17	Middle	1.1	1.9	10.2	1241.76	38.81	0.52	13.17	1.47	32.60	6.17	3.20	0.60	0.55	0.32	0.26	0.24	0.11	0.08	0.05
597	2019	Spring	AR	A17	West	0.3	5.9	10.1	1264.45	39.15	0.56	5.02	1.46	32.95	5.65	3.26	0.60	0.56	0.32	0.26	0.27	0.11	0.28	0.38
598	2019	Spring	AR	AR01-SB	Mixing	2.1	2.7	10.1	1242.75	38.83	0.53	11.59	1.47	31.76	5.74	3.14	0.59	0.54	0.31	0.26	0.24	0.11	0.09	0.08
599	2019	Spring	SB	SB01-SB	Mixing	0.5	1	16.5	1192.04	38.04	0.51	16.21	1.48	55.44	5.34	3.36	1.05	0.96	0.41	0.33	0.45	0.14	0.10	0.07
600	2019	Spring	AR	A5	Middle	0.3	2.1	9.2	1252.59	38.98	0.52	16.00	1.46	32.77	5.63	3.56	0.64	0.61	0.35	0.28	0.24	0.12	0.06	0.01
601	2019	Spring	AR	A5	Middle	0.9	2.1	9.4	1257.53	39.05	0.53	10.53	1.47	32.96	5.65	3.51	0.67	0.61	0.36	0.29	0.28	0.13	0.12	0.11
602	2019	Spring	AR	A5	Middle	1.8	2.1	9.4	1298.87	64.45	0.53	11.95	1.47	32.89	6.31	3.50	0.63	0.58	0.33	0.27	0.26	0.12	0.09	0.07
603	2019	Spring	AR	A5	East	0.3	2.4	9.9	1281.69	63.96	0.53	12.13	1.47	32.50	5.90	3.28	0.60	0.56	0.32	0.27	0.25	0.11	0.09	0.07
604	2019	Spring	AR	A5	East	1.2	2.4	9.5	1298.87	64.45	0.53	11.37	1.45	32.22	5.70	3.39	0.62	0.57	0.32	0.27	0.26	0.11	0.10	0.09
605	2019	Spring	AR	A5	East	2.1	2.4	9.2	1301.92	64.54	0.53	13.45	1.46	31.73	5.74	3.45	0.61	0.57	0.33	0.27	0.26	0.12	0.08	0.04
606	2019	Spring	PR	PR	N/A	0.5	0.8	14.7	1066.64	57.28	0.61	6.14	1.58	38.13	6.34	2.59	0.73	0.67	0.37	0.31	0.59	0.11	0.27	0.40
607	2019	Spring	MUR	MUR	N/A	0.5	0.9	17.2	1204.02	61.64	0.54	15.03	1.52	50.08	6.25	2.91	0.84	0.77	0.34	0.27	0.48	0.10	0.08	0.04
Note: upstream FMM, upstream MLC, A17, A9, and A5 refer to T1-T5.																								

Appendix IV: mainstem & tributary PCA scores

Sample ID	Season	River	Nickname	Group	Location	PC1 (50.0%)	PC2 (20.5%)	PC3 (16.3%)
459	Fall	AR	Upstream FMM	AR	West	-4.08306	0.84759	0.20062
460	Fall	AR	Upstream FMM	AR	Middle	-4.68968	0.31971	0.25408
456	Fall	AR	Upstream FMM	AR	East	-4.57898	0.2048	0.59056
259	Fall	AR	Upstream MLC	AR	East	0.74788	-1.6872	0.51087
467	Fall	AR	A17	AR	East	-0.29047	-1.60005	-0.8145
463	Fall	AR	A9	AR	West	-6.05697	-3.24395	-1.90414
404	Fall	AR	A5	AR	West	-1.38607	-1.13518	0.95211
423	Fall	BC	TR	TR	TR	4.06945	0.83704	3.70676
401	Fall	PR	TR	TR	TR	-0.03438	-0.15426	6.78356
403	Fall	HR	TR	TR	TR	9.90437	-5.67647	0.49849
267	Fall	AR	Upstream MLC	AR	Middle	-2.06317	-0.73716	0.55226
405	Fall	AR	Upstream FMM	AR	West	-7.77301	-0.25732	2.23325
416	Fall	AR	A5	AR	East	-3.05257	-1.95006	0.38103
417	Fall	AR	A5	AR	East	-1.36087	-1.11209	0.7354
418	Fall	AR	A5	AR	East	-0.70225	-0.4639	0.49479
420	Fall	AR	A5	AR	Middle	-1.37455	-0.84851	0.99908
421	Fall	AR	A5	AR	West	-1.23777	-0.48792	0.84003
283	Fall	AR	Upstream MLC	AR	East	-0.37281	-2.35766	0.83518
424	Fall	AR	Upstream MLC	AR	West	-2.9956	0.36197	1.46422
425	Fall	AR	A5	AR	West	-1.56157	-0.20093	1.09868
427	Fall	AR	A5	AR	Middle	-1.707	-0.39654	0.02894
430	Fall	MKR	TR	TR	TR	7.84804	-3.7007	3.19797
432	Fall	AR	Upstream FMM	AR	Middle	-4.22284	0.49418	0.72227
435	Fall	AR	A5	AR	Middle	-2.55517	-1.08605	0.05406
449	Fall	TAR	TR	TR	TR	0.8793	-0.62648	2.4217
450	Fall	MUR	TR	TR	TR	2.12519	-1.35138	3.15296
451	Fall	SB	TR	TR	TR	4.68339	-2.80778	0.85221
452	Fall	AR	A9	AR	West	-1.92933	-0.91309	-0.0894
453	Fall	AR	A9	AR	Middle	-2.23705	-0.95532	-0.04411
455	Fall	AR	A9	AR	Middle	-2.23909	-1.2413	0.07387
284	Fall	AR	Upstream MLC	AR	East	0.69724	-1.7864	0.58329
457	Fall	AR	A9	AR	West	-1.43206	-0.77621	-0.58538
458	Fall	ER	TR	TR	TR	-3.26852	-1.75252	2.39241
285	Fall	AR	Upstream MLC	AR	West	-3.23622	0.70117	1.61596
286	Fall	AR	Upstream MLC	AR	West	-2.74913	0.55015	1.47559
289	Fall	AR	Upstream MLC	AR	Middle	-2.79602	-0.76104	1.25794
465	Fall	AR	Upstream FMM	AR	Middle	-5.02758	0.87181	0.75222
308	Fall	MLC	TR	TR	TR	4.74163	1.40901	4.73857
468	Fall	AR	A17	AR	West	-3.02729	-0.16408	-0.41403
470	Fall	AR	A17	AR	East	-4.72124	-3.10354	-1.56691
471	Fall	AR	A17	AR	Middle	-0.97692	-2.61797	-1.78848
472	Fall	CL	TR	TR	TR	0.49958	-2.46891	-0.54078
475	Fall	AR	A17	AR	West	-4.59182	-0.05413	-0.106
476	Fall	AR	A17	AR	Middle	-0.45351	-1.93626	-1.5901
478	Fall	AR	A9	AR	East	-1.24852	-1.04676	-0.70015
479	Fall	AR	A17	AR	Middle	-0.12167	-1.7939	-0.33511
480	Fall	AR	A17	AR	West	-4.33277	-0.98225	-0.41875
482	Fall	AR	Upstream FMM	AR	East	-3.91677	1.2912	0.52611
483	Fall	LFC	TR	TR	TR	2.28404	-3.48382	2.11889
485	Fall	AR	Upstream FMM	AR	East	-4.01912	0.56226	0.06416
501	Spring	AR	Upstream FMM	AR	West	0.4049	5.71592	0.48353
502	Spring	AR	Upstream FMM	AR	Middle	-0.40766	1.80368	-0.18904
503	Spring	AR	Upstream FMM	AR	East	-0.27745	2.38794	-0.192

570	Spring	AR	Upstream MLC	AR	West	2.40785	3.44894	-1.18959
580	Spring	AR	A17	AR	East	0.31939	1.74226	-0.49265
577	Spring	AR	A9	AR	Middle	1.08953	0.16159	-1.31382
576	Spring	AR	A5	AR	West	0.49031	-0.26919	-0.99337
511	Spring	CL	TR	TR	TR	2.0629	0.23699	-1.29596
512	Spring	AR	A5	AR	West	1.88182	3.04069	-1.01447
517	Spring	AR	A5	AR	West	1.07154	0.98798	-1.19849
525	Spring	HR	TR	TR	TR	6.26197	-1.25828	-1.14421
530	Spring	LFC	TR	TR	TR	6.19347	-0.49841	-0.29894
531	Spring	AR	Upstream FMM	AR	East	-0.25389	1.71589	-0.00924
539	Spring	AR	Upstream FMM	AR	Middle	-0.1183	1.03949	-0.60079
540	Spring	AR	A9	AR	East	1.78996	0.86433	-1.28794
541	Spring	AR	A17	AR	West	1.6865	0.13284	-1.54947
542	Spring	AR	A17	AR	Middle	0.63288	-0.33778	-1.22755
543	Spring	AR	A17	AR	West	-1.08256	-1.22652	-2.19073
544	Spring	AR	A9	AR	Middle	1.92906	-0.31518	-1.68341
545	Spring	TAR	TR	TR	TR	1.82465	4.22519	2.0401
546	Spring	AR	A9	AR	East	2.28042	3.90301	-1.10107
548	Spring	ER	TR	TR	TR	-0.35977	0.52339	2.51771
552	Spring	AR	A9	AR	Middle	0.6289	-0.72109	-1.22858
554	Spring	MLC	TR	TR	TR	0.71104	2.45443	2.51583
504	Spring	AR	Upstream FMM	AR	West	-0.20516	1.00537	-0.36857
571	Spring	AR	A9	AR	East	0.32067	-0.10678	-1.01623
572	Spring	AR	Upstream MLC	AR	Middle	1.2622	0.00763	-1.47049
573	Spring	AR	Upstream MLC	AR	Middle	1.52274	-0.52633	-1.30913
574	Spring	AR	Upstream MLC	AR	East	0.98798	-0.38181	-1.17975
575	Spring	AR	Upstream MLC	AR	West	2.02187	2.6365	-1.10776
506	Spring	AR	Upstream FMM	AR	Middle	-0.51497	1.16816	-0.48377
507	Spring	AR	Upstream FMM	AR	West	-0.42246	1.50376	-0.14425
578	Spring	AR	A9	AR	West	1.2104	0.51243	-1.49258
579	Spring	AR	Upstream MLC	AR	West	2.63099	3.12348	-1.52835
505	Spring	AR	Upstream FMM	AR	East	0.23973	1.49026	-0.66074
581	Spring	AR	A9	AR	West	0.79504	-0.61997	-2.11277
582	Spring	AR	Upstream MLC	AR	East	1.13539	0.13705	-1.22289
583	Spring	AR	Upstream MLC	AR	Middle	1.78573	-0.61232	-1.73862
584	Spring	AR	A9	AR	West	1.96407	3.43237	-1.53742
585	Spring	MKR	TR	TR	TR	3.72304	-0.73091	0.90251
593	Spring	AR	A17	AR	East	-0.03456	-0.86651	-1.25746
594	Spring	AR	A17	AR	East	0.17497	-0.77306	-1.15918
595	Spring	AR	A17	AR	Middle	0.51763	0.81363	-1.20822
596	Spring	AR	A17	AR	Middle	0.2561	0.14028	-0.76475
597	Spring	AR	A17	AR	West	1.21472	3.21713	-1.39907
599	Spring	SB	TR	TR	TR	4.5869	-1.02997	-0.0137
600	Spring	AR	A5	AR	Middle	1.22387	-1.24048	-1.86324
601	Spring	AR	A5	AR	Middle	1.83339	0.96868	-1.54315
602	Spring	AR	A5	AR	Middle	0.84328	0.68465	-1.32845
603	Spring	AR	A5	AR	East	0.5458	0.47075	-1.25121
604	Spring	AR	A5	AR	East	1.02709	0.69367	-1.93653
605	Spring	AR	A5	AR	East	0.89785	0.00906	-1.73452
606	Spring	PR	TR	TR	TR	1.58311	4.29169	4.11604
607	Spring	MUR	TR	TR	TR	1.64846	0.09162	2.19615

Note: upstream FMM, upstream MLC, A17, A9, and A5 refer to T1-T5.

Appendix V: mixing zone PCA scores

Sample ID	Season	River	Nickname	Location	PC1 (55.3%)	PC2 (24.2%)
402	Fall	AR	AR02-HR	AR-HR	-3.99249	0.02827
403	Fall	HR	HR01-HR	HR	11.34822	-2.98244
309	Fall	AR	AR05-CL	AR-CL	-2.57713	-1.64599
310	Fall	CL	CL05-CL	CL	-0.57267	-2.36897
400	Fall	AR	AR04-HR	AR-HR	-4.31827	-0.52914
277	Fall	CL	CL05-CL	CL	0.04626	-2.35697
288	Fall	AR	AR05-CL	AR-CL	-2.28223	-1.33921
406	Fall	CL	CL02-CL	CL	0.51127	-1.73047
407	Fall	AR	AR01-HR	AR-HR	-4.41532	-0.03298
408	Fall	HR	HR02-HR	HR	8.11238	-2.52189
409	Fall	HR	HR02-HR	HR	5.8576	-3.10543
410	Fall	AR	AR04-HR	AR-HR	-4.47191	0.11876
411	Fall	AR	AR01-HR	AR-HR	-3.75246	-0.08386
412	Fall	HR	HR04-HR	HR	3.97034	-2.62785
413	Fall	AR	AR02-HR	AR-HR	-5.51396	-0.9119
414	Fall	HR	HR03-HR	HR	4.52352	-3.08594
415	Fall	AR	AR03-HR	AR-HR	-5.20318	-0.10198
426	Fall	AR	AR03-HR	AR-HR	-4.52843	-0.06398
428	Fall	CL	CL04-CL	CL	-0.54567	-2.49098
429	Fall	AR	AR04-CL	AR-CL	-3.44612	-0.75197
431	Fall	AR	AR01-CL	AR-CL	-5.54543	-0.45251
433	Fall	AR	AR04-CL	AR-CL	-3.34515	-0.73896
434	Fall	CL	CL03-CL	CL	-0.36464	-2.18085
436	Fall	AR	AR02-CL	AR-CL	-1.97385	-0.85354
437	Fall	AR	AR01-CL	AR-CL	-5.77843	0.19843
438	Fall	AR	AR04-SB	AR-SB	-1.11501	-1.56518
439	Fall	SB	SB02-SB	SB	0.79692	-1.32281
440	Fall	SB	SB03-SB	SB	0.16981	-1.72501
442	Fall	AR	AR03-SB	AR-SB	-1.92987	-1.31826
443	Fall	AR	AR02-SB	AR-SB	-2.06873	-1.28649
444	Fall	SB	SB04-SB	SB	0.43239	-0.90136
445	Fall	SB	SB02-SB	SB	-0.67091	-1.99616
446	Fall	SB	SB03-SB	SB	0.30457	-1.04796
447	Fall	CL	CL04-CL	CL	-0.18079	-1.90602
448	Fall	SB	SB04-SB	SB	-0.99162	-1.78067
451	Fall	SB	SB01-SB	SB	4.96682	-1.73733
454	Fall	CL	CL03-CL	CL	-0.49292	-1.84189
461	Fall	AR	AR03-CL	AR-CL	-4.75888	-0.37694
462	Fall	CL	CL01-CL	CL	0.04179	-2.33013
464	Fall	CL	CL02-CL	CL	0.69652	-1.90314
466	Fall	AR	AR01-SB	AR-SB	-1.56603	-1.8596
469	Fall	AR	AR03-SB	AR-SB	-3.86187	-2.8321
472	Fall	CL	CL01-CL	CL	0.31382	-2.37681
473	Fall	AR	AR02-SB	AR-SB	-2.47517	-1.64006
474	Fall	AR	AR04-SB	AR-SB	1.27072	-2.5373
477	Fall	AR	AR03-CL	AR-CL	-5.57749	0.57896
481	Fall	AR	AR01-SB	AR-SB	-5.89188	-3.80455

484	Fall	AR	AR02-CL	AR-CL	-3.07383	-1.18346
500	Spring	AR	AR01-HR	AR-HR	-0.84109	2.27053
508	Spring	HR	HR01-HR	HR	7.02734	-0.0324
518	Spring	AR	AR02-CL	AR-CL	0.38118	0.96902
511	Spring	CL	CL01-CL	CL	1.44336	0.65971
549	Spring	AR	AR04-SB	AR-SB	0.35218	0.03789
513	Spring	AR	AR05-HR	AR-HR	-0.74928	0.40484
514	Spring	HR	HR05-HR	HR	1.42273	2.45293
515	Spring	SB	SB02-SB	SB	2.40604	-0.86983
516	Spring	CL	CL01-CL	CL	1.38487	0.6475
509	Spring	AR	AR04-HR	AR-HR	0.44472	3.34689
519	Spring	SB	SB03-SB	SB	4.82503	0.07862
520	Spring	HR	HR05-HR	HR	1.57174	2.5314
521	Spring	HR	HR03-HR	HR	0.04521	1.24169
522	Spring	HR	HR04-HR	HR	2.12156	0.70872
523	Spring	HR	HR02-HR	HR	3.48421	-0.14989
524	Spring	AR	AR02-HR	AR-HR	-1.28536	0.96161
525	Spring	HR	HR01-HR	HR	6.46544	0.22508
526	Spring	AR	AR01-HR	AR-HR	-0.31293	5.44551
527	Spring	AR	AR02-HR	AR-HR	-0.76049	2.20348
528	Spring	SB	SB04-SB	SB	1.61939	2.64953
529	Spring	HR	HR04-HR	HR	2.21917	5.12159
532	Spring	HR	HR02-HR	HR	4.69578	0.7267
533	Spring	AR	AR03-HR	AR-HR	-0.6142	5.64274
534	Spring	AR	AR05-HR	AR-HR	0.3069	1.61672
535	Spring	AR	AR01-CL	AR-CL	0.19233	1.08713
536	Spring	AR	AR03-HR	AR-HR	-1.26582	2.48724
537	Spring	HR	HR03-HR	HR	0.04651	1.09577
538	Spring	AR	AR04-HR	AR-HR	0.4798	1.36121
547	Spring	CL	CL06-CL	CL	1.72095	0.94599
510	Spring	CL	CL02-CL	CL	1.34123	0.33152
550	Spring	CL	CL06-CL	CL	1.12836	0.87172
551	Spring	AR	AR06-CL	AR-CL	1.04911	0.17941
553	Spring	AR	AR06-CL	AR-CL	1.49098	2.95976
555	Spring	AR	AR05-CL	AR-CL	0.19466	0.35163
556	Spring	AR	AR05-CL	AR-CL	0.50249	0.48903
557	Spring	CL	CL04-CL	CL	0.35611	-0.24462
558	Spring	CL	CL04-CL	CL	-0.47444	-0.20318
559	Spring	CL	CL05-CL	CL	0.41136	0.74044
560	Spring	CL	CL03-CL	CL	0.79795	0.35748
561	Spring	AR	AR03-CL	AR-CL	-0.34251	-0.12919
562	Spring	AR	AR04-CL	AR-CL	0.58734	0.88711
563	Spring	AR	AR04-CL	AR-CL	-0.2449	0.70804
564	Spring	CL	CL05-CL	CL	0.76915	0.18198
565	Spring	AR	AR02-CL	AR-CL	-0.71209	1.25917
566	Spring	AR	AR01-CL	AR-CL	-0.18463	0.74427
567	Spring	AR	AR03-CL	AR-CL	0.82437	7.30806
568	Spring	CL	CL02-CL	CL	0.52972	0.6367

569	Spring	CL	CL03-CL	CL	0.36334	0.37265
586	Spring	AR	AR02-SB	AR-SB	-0.11825	-0.13771
587	Spring	AR	AR03-SB	AR-SB	-0.0401	5.32446
588	Spring	AR	AR01-SB	AR-SB	0.24538	-0.36445
589	Spring	AR	AR02-SB	AR-SB	0.20469	1.24443
590	Spring	SB	SB04-SB	SB	2.97001	0.27704
591	Spring	AR	AR03-SB	AR-SB	-0.17767	0.08549
592	Spring	AR	AR04-SB	AR-SB	-0.47125	0.53554
598	Spring	AR	AR01-SB	AR-SB	-0.39467	0.74278
599	Spring	SB	SB01-SB	SB	4.48641	-0.07084

Note: upstream FMM, upstream MLC, A17, A9, and A5 refer to T1-T5.

Appendix VI: water quality measurements and major ions

Sample ID	Velocity (ft/s)	Water Temperature (°C)	Pressure (mmHg)	DO (% L)	DO (mg L^{-1})	Conductivity (µs cm^{-1})	pH	ORP (mV)	TP (P µg/L)	NO2NO3 (N µg/L)	NH4 (N µg/L)	Cl (mg/L)	SO4 (mg/L)	Al (µg/L)	Ca (mg/L)	Fe (mg/L)	K (mg/L)	Mg (mg/L)	Na (mg/L)
259	2.5	2.6	742.6	94.7	12.61	142.6	8.5	141.6	13	< 2	< 3	16.37	14.10	4.2	22.81	0.29	1.01	6.71	17.07
267	2.7	2.8	742.2	90.5	11.88	177.6	8.7	122.9	5	34	10	4.78	30.90	5.3	35.76	0.06	1.36	9.76	12.48
277	1.7	3.4	743.4	92.7	12.04	152.9	8.5	158	12	55	15	14.42	17.44	8.5	24.90	0.23	1.08	7.24	16.39
283	1.3	2.9	742.8	96	12.6	144.5	8.5	143.8	14	208	7	16.56	14.09	6.7	22.53	0.28	0.98	6.60	16.80
284	2.1	2.9	742.7	92.8	12.23	143.4	8.5	143.4	15	51	< 3	16.53	14.00	5.4	22.82	0.29	1.00	6.70	17.01
285	2.3	2.9	742	92.3	12.17	184.3	8.7	135.6	6	959	< 3	2.94	34.08	5.1	38.39	0.06	1.42	10.40	11.68
286	1.6	3.5	742	92.2	11.96	185.8	8.7	130	5	29	< 3	2.83	34.49	8.1	38.61	0.06	1.41	10.38	11.51
288	2.3	3.3	743	93.9	12.23	169.3	8.6	155.4	5	56	10	7.78	26.61	7.9	32.28	0.10	1.27	8.98	13.72
289	2.4	3.4	742.5	95.4	12.38	180.1	8.7	125.6	7	43	< 3	4.97	30.94	6.3	36.40	0.10	1.36	9.90	12.60
308	0.7	1.2	742.8	98.9	13.54	341.6	8.6	157.3	9	5	26	70.51	35.73	5.9	38.39	0.48	1.47	11.87	73.40
309	2	3.7	743.1	93.9	12.05	169.1	8.6	154.5	9	18	< 3	8.50	25.86	6.3	31.80	0.16	1.22	8.79	13.71
310	2	3.3	743.3	94.1	12.29	153.4	8.5	156	12	32	< 3	14.64	17.56	11.6	25.20	0.25	1.05	7.21	16.03
400	3.5	5.2	737.1	97.4	11.94	194.3	8.7	155.6	6	59	< 3	2.33	35.02	6.2	38.70	0.10	1.46	10.49	11.46
401	0.9	3.1	743.1	97.2	12.75	266.9	8.4	101.4	26	79	12	7.09	40.89	< 3.6	51.07	0.25	2.85	14.41	24.83
402	3.6	4.4	740.2	94.6	11.92	156.7	8.7	129.3	4	14	< 3	2.31	35.60	8.6	38.77	0.05	1.42	10.44	11.21
403	1.8	1	741.8	91.1	12.67	87	8.4	138.2	47	< 2	6	2.57	9.02	33.2	19.90	0.94	0.78	5.70	13.91
404	1.7	4.3	742	92.4	11.72	160.1	8.5	104.2	8	40	4	14.26	30.55	6.6	33.31	0.13	1.25	9.30	17.55
405	3.3	4.1	746.1	91.7	11.76	158.4	8.5	191.9	5	14	< 3	2.25	38.25	7.4	38.73	0.04	1.40	10.56	10.89
406	2.8	3.9	748.6	93.4	12.1	126.3	8.3	168.6	18	14	5	20.90	7.32	5.2	17.00	0.34	0.83	5.25	17.66
407	1.9	3.3	741.2	91.1	11.81	165.2	8.7	128.3	6	41	11	2.35	35.91	7.5	38.40	0.05	1.41	10.33	11.13
408	1.8	3.3	739.6	93.7	12.15	136.8	8.5	132.9	26	23	23	2.49	23.44	18.7	29.84	0.47	1.12	8.21	12.45
409	2.7	3.3	739.8	94	12.2	130.3	8.5	134.2	27	10	3	2.50	22.77	18.8	29.18	0.48	1.10	8.02	12.54
410	4.1	5.5	737.2	94.6	11.54	168.7	8.7	153.7	5	45	11	2.37	35.59	6.6	37.92	0.06	1.41	10.19	11.24
411	1.3	3.9	740.9	91.8	11.78	183.6	8.6	122.4	5	15	4	2.37	36.07	4.9	38.67	0.05	1.44	10.42	11.32
412	2.4	4.8	736.9	93.9	11.67	145.4	8.6	158.4	18	8	4	2.47	28.37	15.8	33.08	0.30	1.25	9.00	12.00
413	3.9	4	740.5	93.5	11.94	152.9	8.7	123.3	5	16	< 3	2.32	35.99	6.7	38.53	0.05	1.43	10.35	11.21
414	0.7	4.5	737.6	98.3	12.33	165	8.6	152.8	20	< 2	< 3	2.48	26.49	17.4	32.00	0.37	1.21	8.73	12.33
415	2.9	4.5	738.6	96.4	12.13	191.1	8.6	148.7	5	113	24	2.36	36.08	7.7	38.03	0.05	1.42	10.21	11.12
416	2.6	5.4	742.6	96.8	11.91	156.8	8.5	150.1	9	17	4	9.42	29.81	6.1	32.75	0.12	1.25	9.11	14.56
417	2	4.6	743.1	91.9	11.56	161.9	8.5	154.3	8	12	< 3	9.60	29.85	5.7	32.97	0.12	1.23	9.11	14.56
418	2.5	4.8	742.9	92.8	11.63	153.2	8.5	152.2	8	14	< 3	9.57	30.00	5.6	32.78	0.12	1.22	9.02	14.41
420	1.9	5.5	742.1	92.7	11.34	176	8.5	129.2	9	48	< 3	9.37	30.23	5.3	32.81	0.12	1.23	9.04	14.39
421	2.4	4	748.7	90.9	11.62	174.5	8.5	139.7	8	67	< 3	14.39	30.86	4.1	32.97	0.15	1.26	9.07	17.31
423	0.8	4.4	742.8	93.3	11.77	655	8.3	156.7	7	51	< 3	71.44	139.69	4.8	108.76	0.20	2.36	27.30	90.11
424	2.5	3	741.7	91.3	12.02	183.7	8.7	142.2	5	41	< 3	3.16	34.72	8.6	37.56	0.06	1.41	10.01	11.55
425	2.2	4.2	741.9	91.2	11.59	189.1	8.5	113.3	8	50	< 3	14.32	30.89	4.0	33.18	0.12	1.25	9.11	17.25
426	2.6	5	738.2	97.3	12.07	195.5	8.6	151.8	5	46	< 3	2.36	36.17	4.9	38.20	0.05	1.42	10.17	11.07
427	2	5	742.2	92.5	11.5	173.9	8.5	125.8	9	219	< 3	9.35	30.21	4.0	32.91	0.12	1.25	9.09	14.49
428	1.8	5.2	746.6	94.4	11.78	116.4	8.4	209	15	291	< 3	16.55	14.26	4.7	21.76	0.28	0.95	6.35	16.07
429	2	5.5	746	93.3	11.56	165.8	8.5	197.3	7	59	< 3	5.78	31.64	6.0	34.12	0.12	1.29	9.36	12.37
430	0.6	3	749.2	96.1	12.73	123.6	8.4	180.3	28	< 2	4	2.40	11.77	8.7	20.90	0.54	0.69	6.88	17.56
431	3.1	7	743.7	97.1	11.5	142.8	8.6	190.8	4	25	< 3	2.19	38.96	5.2	38.24	0.04	1.41	10.43	10.81
432	3.2	5.6	745.4	95.9	11.82	152.5	8.6	183.6	4	48	< 3	2.19	38.91	6.7	37.93	0.04	1.40	10.30	10.59
433	2.9	5.8	746.2	94.8	11.61	151.8	8.5	198.2	7	18	< 3	5.64	31.90	< 3.6	34.58	0.11	1.32	9.53	12.56
434	4.4	4.6	747.4	93.6	11.84	139.4	8.4	197.7	14	13	< 3	14.58	17.14	6.5	23.94	0.26	1.03	6.93	15.76
435	2.3	4.4	742.1	91.5	11.53	165.3	8.5	120.3	8	22	< 3	9.50	30.31	6.4	33.00	0.12	1.25	9.12	14.53
436	3.7	3.9	748.9	97.2	12.56	175.3	8.5	168	8	48	< 3	5.80	31.35	6.1	33.98	0.12	1.29	9.35	12.50
437	2.4	7.3	743.7	97.7	11.49	122.1	8.6	198.8	5	21	4	2.21	39.07	8.6	38.20	0.04	1.39	10.37	10.66
438	1.5	7.5	740.7	95.9	11.2	177	8.4	224.4	10	12	< 3	8.87	26.15	7.8	29.30	0.16	1.16	8.22	13.26
439	2.3	7.2	742	97.2	11.44	173.7	8.5	220.4	16	10	< 3	6.67	20.44	7.8	28.54	0.30	1.03	8.23	14.36
440	0.3	7.7	741.3	98.3	11.41	170.2	8.4	218.6	11	3	< 3	8.66	23.85	7.1	28.58	0.21	1.11	8.12	13.66
442	2.1	7.4	740.5	94.5	11.1	174.3	8.4	225.1	10	96	< 3	8.45	26.85	8.2	29.71	0.15	1.19	8.35	13.04
443	2.6	7.3	739.7	94.2	11.03	172.3	8.4	268.3	10	18	< 3	8.13	27.64	12.2	31.82	0.18	1.16	9.56	12.85
444	0.8	7.7	741	99.1	11.5	177.2	8.4	220.6	12	72	< 3	8.71	23.99	8.3	30.53	0.22	1.09	9.36	13.83
445	0.9	7.7	742.1	94.2	10.96	171.4	8.4	218.9	12	15	< 3	9.37	23.87	10.2	29.78	0.21	1.07	9.16	13.76
446	0.5	7.7	741.6	97.8	11.37	172.6	8.4	220.3	12	7	< 3	8.81	24.04	9.9	30.39	0.22	1.07	9.36	13.75
447	2.1	5.5	746.7	96.4	11.94	115.8	8.3	196.8	14	8	< 3	16.56	14.53	7.6	23.15	0.30	0.92	7.38	16.46

448	0.8	7.8	741.1	98.3	11.34	176.3	8.4	222.2	12	34	< 3	8.73	23.92	9.0	30.24	0.22	1.06	9.29	13.76
449	0.2	6.3	749.4	95.2	11.59	157.9	8.3	206.6	21	< 2	< 3	4.36	39.81	8.9	39.95	0.49	1.77	12.53	17.82
450	1.2	4	749.5	99.2	12.91	213.8	8.5	202.4	11	94	< 3	5.33	21.34	5.4	48.76	0.24	1.13	13.14	14.73
451	1.1	4.4	738.3	105.5	13.2	163.8	8.4	150.1	24	< 2	< 3	2.22	15.19	10.8	31.54	0.52	0.87	10.10	15.58
452	2	5.9	749.7	94	11.56	139.1	8.4	191.5	8	18	< 3	8.13	29.77	9.9	33.20	0.13	1.16	9.94	13.23
453	2	5.4	749.7	94.3	11.74	121.9	8.4	202.6	9	31	< 3	8.38	29.29	6.9	32.86	0.13	1.15	9.86	13.11
454	5.7	4.6	747.6	93.2	11.82	135.3	8.4	197.2	13	6	< 3	14.50	17.47	9.5	25.28	0.27	0.97	7.88	15.39
455	1.7	5.5	749.7	94.2	11.72	134.1	8.4	201.4	9	24	< 3	8.43	29.35	7.0	33.48	0.13	1.16	10.01	13.32
456	2.2	6	744.8	93	11.35	164.6	8.6	193.1	5	6	< 3	2.23	38.96	12.1	40.36	0.05	1.32	11.74	10.64
457	2.9	5.3	749.7	95.3	11.91	136.9	8.4	185.8	9	6	< 3	8.18	29.87	9.7	33.17	0.13	1.18	9.91	13.25
458	1.1	4.7	749.2	102.7	13.04	130.1	8.4	237.1	12	< 2	< 3	1.07	15.20	4.8	25.33	0.22	1.11	7.89	10.39
459	3.1	4.2	746.9	93.8	11.9	138.9	8.5	181.2	4	14	< 3	2.28	38.96	7.4	40.44	0.04	1.33	11.72	10.77
460	4.5	4.8	745.8	91.7	11.56	155.2	8.6	176.4	4	13	< 3	2.19	39.09	10.5	41.38	0.06	1.39	11.50	10.88
461	2.4	5.4	748.1	96.5	11.92	196.9	8.6	180.5	5	8	< 3	2.35	38.50	9.5	41.45	0.05	1.38	11.60	11.21
462	2.6	6.2	743.8	95.1	11.55	90.4	8.2	180.3	18	2	< 3	32.09	5.42	9.5	16.53	0.35	0.77	5.41	18.24
463	3.1	5.6	749.6	93.2	11.54	178.6	8.4	179.9	8	6	< 3	8.21	29.85	10.3	33.66	0.14	1.18	9.69	13.52
464	2.5	4.4	748.4	95.6	12.21	128.6	8.2	168.3	17	7	< 3	21.35	7.45	8.4	17.96	0.35	0.81	5.73	18.26
465	4	5.1	745.7	96	11.93	145.4	8.6	179.8	5	10	< 3	2.20	39.22	11.7	40.71	0.04	1.34	11.35	10.71
466	2	7.4	739.2	96.3	11.2	175.4	8.4	174.8	11	8	< 3	9.34	25.53	8.8	30.66	0.18	1.11	8.94	13.55
467	1.6	8.1	737.3			174.5	8.4	215.5	11	25	< 3	10.80	22.94	9.5	28.82	0.20	1.06	8.47	14.00
468	2.9	7.9	739.6			185	8.5	234	7	55	< 3	4.24	34.80	11.2	36.71	0.08	1.26	10.51	11.21
469	3.3	7.9	740.2	96.9	11.27	179.8	8.4	226.9	10	3140	< 3	8.63	26.69	10.6	31.54	0.16	1.13	9.10	13.26
470	1.5	7.9	737.3			173.9	8.4	230.8	11	15	< 3	10.72	23.30	10.5	29.27	0.20	1.06	8.55	14.00
471	0.9	9.8	737.7			168.8	8.4	156.8	11	5	< 3	9.91	24.30	11.0	30.02	0.19	1.10	8.77	13.77
472	3.2	5.7	744.1	94.9	11.62	98.8	8.2	167.5	19	12	< 3	21.72	5.42	6.9	16.77	0.36	0.77	5.48	18.31
473	3.6	7.4	739.6	94.3	11	179.5	8.4	289.2	10	52	< 3	9.02	25.98	9.1	31.14	0.17	1.14	9.02	13.49
474	2.6	7.4	740.7	95.2	11.13	177	8.4	225.5	7	26	< 3	4.13	35.16	9.0	37.15	0.08	1.28	10.52	11.27
475	2.2	11	739.1			214.8	8.4	185.5	9	7	< 3	8.09	27.83	10.2	32.37	0.15	1.15	9.30	12.98
476	0.9	7.9	737.6			175.8	8.4	197.8	11	4	< 3	10.00	24.39	8.7	29.90	0.19	1.09	8.71	13.74
477	2.2	5.4	748.1	94.9	11.83	197	8.6	185.5	5	24	< 3	2.36	38.71	10.2	41.41	0.05	1.36	11.57	11.20
478	1.6	5.9	749.7	96	11.83	131.8	8.4	204.8	8	14	< 3	8.48	29.56	11.6	33.60	0.14	1.18	9.64	13.56
479	0.9	8	737.3			170.8	8.4	199.6	11	8	< 3	9.93	24.50	7.9	30.25	0.20	1.11	8.80	13.76
480	3	7.7	740			192	8.5	174.6	7	152	< 3	4.84	33.68	8.4	36.22	0.09	1.25	10.24	11.49
481	2.7	7.7	738.9	97.7	11.3	177.1	8.4	172	10	8	< 3	9.33	25.57	10.1	30.93	0.18	1.12	8.91	13.57
482	2.5	6	744.9	94.3	11.48	160.1	8.6	191	4	12	< 3	2.25	39.30	11.6	41.04	0.04	1.36	11.39	10.89
483	0.5	2.9	744.2	102.5	13.45	275.7	8.4	253.2	15	17	< 3	2.13	69.03	12.3	51.15	0.53	1.76	18.66	32.78
484	2.9	4	748.7	97.5	12.59	174.7	8.5	165.2	8	9	< 3	5.89	31.74	10.9	36.58	0.13	1.26	10.27	12.72
485	2.8	5.8	745.2	93.6	11.48	166	8.6	188.3	4	36	< 3	2.25	39.17	10.1	40.96	0.04	1.37	11.37	10.87
500	0.7	12	741.1	99.5	10.49	248.2	8.3	428.1	11	9	<3	4.19	26.62	7.3	40.45	0.04	2.37	10.03	13.71
501	1	12.2	740.5	88.8	9.26	238.7	8.3	165.5	11	<2	<3	3.75	26.37	8.7	39.12	0.04	2.31	9.82	13.55
502	1.4	12.9	740	91.9	9.43	242	8.3	391	9	8	<3	3.68	26.24	9.0	39.32	0.04	2.28	9.81	13.23
503	1.1	13.3	739.7	94.6	9.63	245.4	8.3	382.6	9	31	<3	3.72	26.34	9.9	39.15	0.04	2.28	9.80	13.37
504	1.3	12	740.5	88.9	9.33	235.5	8.3	165.1	10	12	<3	3.75	26.40	5.6	40.23	0.04	2.36	10.10	13.91
505	1.2	12.7	739.8	93.7	9.68	241.6	8.3	294.8	11	<2	<3	3.74	26.45	8.0	39.15	0.04	2.28	9.85	13.37
506	1.6	13.1	740.3	89	9.12	243.5	8.3	216.4	9	28	<3	3.67	26.29	7.0	39.47	0.06	2.29	9.87	13.24
507	1.4	11.9	740.6	80.1	8.36	236.2	8.2	159.1	11	<2	<3	3.78	26.57	5.3	39.58	0.04	2.30	9.92	13.65
508	0.2	9.5	740.9	104.6	11.69	196.3	8.2	266.2	27	<2	<3	5.39	17.92	13.8	28.74	0.51	2.06	8.36	19.04
509	1.2	11.4	745.9	90.4	9.68	263.5	8.3	154.8	13	198	<3	3.87	27.21	8.3	40.52	0.04	2.18	10.11	13.01
510	1.3	13.4	743.4	104.2	10.62	192.8	8.1	254.7	14	<2	<3	19.82	7.34	6.4	17.31	0.21	1.18	5.43	18.08
511	0.8	13.6	742.7	97.5	9.85	185.9	8.1	324	13	75	<3	20.38	6.54	5.6	16.43	0.23	1.15	5.27	18.23
512	0.5	17.4	739.4	104.7	9.73	252	8.2	260.4	11	69	<3	8.03	22.27	9.3	32.18	0.06	1.54	8.27	12.57
513	1	13.6	745.2	100.5	10.21	283.7	8.3	388.3	14	46	<3	3.88	27.22	11.4	40.99	0.04	2.20	10.20	13.13
514	1.4	13.3	744.9	97.2	9.92	279.8	8.3	408.2	15	75	<3	4.00	26.45	9.1	39.45	0.07	2.16	9.94	13.49
515	0.3	18.8	739.2	110.4	10	244.4	8.5	280.7	19	196	<3	2.20	9.09	5.4	30.24	0.31	1.45	8.98	13.41
516	0.7	13.7	742.5	98.1	9.83	184.2	8.0	383.6	14	49	<3	20.31	6.50	6.8	16.42	0.22	1.14	5.24	18.22
517	0.4	17.6	739.3	103.2	9.57	257.2	8.2	266.9	11	47	<3	8.01	22.33	4.5	32.01	0.05	1.55	8.20	12.58
518	1.2	14.9	743.7	101	9.95	290.8	8.3	280.5	13	825	<3	3.77	26.62	9.5	40.31	0.04	2.16	9.96	12.78
519	0.1	19.3	739.3	113.2	10.14	247.3	8.5	288	17	<2	<3	2.15	9.04	6.0	30.11	0.30	1.44	8.94	13.49

520	1.5	13.3	745.1	101.9	10.45	280.4	8.3	315.9	13	<2	<3	4.06	26.55	8.6	39.56	0.07	2.19	9.95	13.73
521	1.2	14.1	741.9	101.6	10.22	264.9	8.3	331	12	8	<3	4.36	26.71	11.9	40.13	0.05	2.39	10.06	14.32
522	0.5	11.7	745.4	103.2	11.08	267.4	8.3	342.4	16	10	<3	4.16	26.19	14.2	39.06	0.09	2.18	9.88	14.17
523	0.4	13.2	741.6	102.9	10.53	236	8.3	375.5	20	29	<3	5.03	21.58	10.3	33.46	0.29	2.20	9.06	17.23
524	1.1	12.4	741.1	100.8	10.46	252.4	8.3	380.6	11	24	<3	4.26	26.87	8.3	40.43	0.04	2.41	10.04	13.90
525	0.2	10.3	740.8	98.5	10.76	204.5	8.2	195.7	26	106	<3	5.35	17.91	11.2	28.45	0.48	2.05	8.26	18.99
526	0.9	11.3	741	101.6	10.76	245.1	8.3	311.7	12	6	<3	4.21	26.66	8.1	40.71	0.06	2.43	10.06	13.86
527	0.8	12.5	741.1	102.4	10.49	256.2	8.3	403.1	11	<2	<3	4.29	26.95	9.4	40.44	0.04	2.39	10.03	13.92
528	0.4	19	739.8	110	9.95	248.4	8.4	291.3	16	49	<3	5.17	12.01	9.9	29.15	0.20	1.42	8.30	13.41
529	0.4	11.9	745.3	100.1	10.5	272	8.3	422.6	16	18	<3	4.16	26.20	8.4	37.87	0.09	2.14	9.60	13.76
530	0.41	10.9	739.7	106.4	11.4	187.3	8.1	176.5	15	<2	6	1.42	30.07	10.9	23.51	0.27	2.43	8.88	18.44
531	1	13.7	739.6	95.9	9.69	249	8.3	318.9	11	23	<3	3.75	26.42	7.3	39.12	0.04	2.31	9.79	13.48
532	0.5	12.8	741.6	105.7	10.82	240.4	8.2	249.2	19	2865	<3	4.94	21.99	8.9	33.10	0.25	2.21	9.00	16.99
533	1.5	13.9	741.8	102.7	10.3	265.4	8.3	353.8	12	<2	<3	4.29	26.95	7.7	40.70	0.03	2.37	10.07	13.81
534	1.5	12.7	745.2	102.7	10.69	276.7	8.3	315.6	13	15	<3	3.87	27.33	7.9	39.98	0.04	2.16	9.91	12.80
535	1.2	13.7	744.4	101.8	10.3	282.1	8.3	238.7	14	7300	<3	3.77	26.84	7.1	39.97	0.03	2.16	9.88	12.72
536	1.6	13.8	741.8	100.5	10.23	261.1	8.3	301.3	13	32	<3	4.28	26.85	7.3	40.07	0.04	2.36	9.92	13.67
537	1.4	14	742	103.5	10.41	265.1	8.3	313.3	13	53	<3	4.36	26.61	12.1	39.54	0.05	2.35	9.90	14.13
538	0.9	11.8	745.4	105.5	11.02	270.4	8.3	373.4	14	13	<3	3.88	27.36	10.5	39.68	0.03	2.16	9.87	12.87
539	1.5	12.9	740.2	94.4	9.7	241.8	8.3	369.5	19	48	<3	3.69	26.34	11.0	38.88	0.04	2.29	9.71	13.22
540	0.6	16.5	742.6	99.5	9.54	225.7	8.1	461.8	13	48	<3	7.62	18.79	6.8	29.49	0.05	1.49	7.61	11.92
541	1.2	14	744.8	97.8	9.89	216.9	8.2	236.2	13	46	<3	3.54	21.96	8.3	32.62	0.04	1.50	8.24	9.19
542	1	14.7	744.5	93.6	9.32	221.2	8.2	265	12	29	<3	7.72	19.20	8.4	30.06	0.06	1.43	7.79	11.80
543	0.7	14.3	744.7	94.1	9.45	223.1	8.2	250.5	13	64	<3	3.30	22.22	9.1	32.47	0.04	1.50	8.18	9.07
544	0.8	15.1	742.5	99.9	9.8	217.4	8.1	324.3	13	46	<3	7.47	18.93	7.6	29.52	0.05	1.49	7.55	11.62
545	0.07	17	742.5	103.8	9.78	302.3	8.1	265.8	18	17	<3	2.89	35.67	5.8	39.58	0.30	1.92	11.36	15.17
546	0.6	16.5	742.6	97.7	9.34	225.8	8.2	369.1	13	74	<3	7.66	18.90	5.0	29.77	0.07	1.52	7.63	11.90
547	0.7	15.9	743.1	103.7	10.02	209.9	8.1	365.4	13	6	<3	11.37	12.88	9.4	26.03	0.11	1.57	6.88	14.25
548	0.4	17.3	742.4	104.5	9.85	193.1	8.4	266.3	15	9	<3	1.28	15.21	<3.6	25.59	0.19	1.49	7.13	9.56
549	0.8	18	740.3	104.8	9.64	241.5	8.2	331.5	12	53	<3	10.01	17.93	7.1	28.50	0.07	1.38	7.51	13.04
550	0.9	16.8	743.2	105.8	9.94	221.7	8.1	348.7	14	13	<3	11.67	12.78	5.9	25.57	0.11	1.55	6.78	14.32
551	1	16.4	743.5	163.9	9.94	227.9	8.1	268.6	16	14	<3	3.71	17.65	8.9	32.80	0.05	1.88	8.02	10.46
552	0.7	15.5	742.6	98.5	9.61	219.8	8.2	361.7	13	43	<3	7.45	18.92	4.8	29.18	0.05	1.47	7.49	11.59
553	0.7	16.5	743.4	98.4	9.36	228	8.1	356.1	15	11	<3	3.61	17.53	5.2	32.82	0.05	1.88	7.99	10.36
554	0.6	16.3	743.8	101.8	9.81	376.3	8.3	262.7	8	17	<3	12.25	51.19	<3.6	47.47	0.03	2.90	13.03	28.22
555	0.7	14.6	742.1	104.1	10.24	244.4	8.1	263.8	15	19	<3	7.49	18.27	6.6	31.82	0.07	1.83	8.07	13.04
556	0.9	15	742.2	105.7	10.38	247.3	8.0	237.9	53	23	<3	7.26	18.52	89.9	32.63	0.28	1.86	8.26	13.02
557	1.4	14.5	742.5	100.5	10.02	199.1	8.0	261.3	14	19	<3	17.39	9.47	11.5	20.43	0.17	1.32	5.98	17.05
558	1.2	14.3	742.4	98.7	9.89	198.7	8.0	269.5	13	8	<3	17.41	9.42	5.8	20.20	0.16	1.31	5.93	17.02
559	0.9	15	741.8	106.4	10.42	227.9	8.1	264.9	14	11	<3	12.32	14.26	7.6	26.49	0.11	1.59	7.11	15.16
560	0.6	13.3	743	102	10.32	190.1	8.0	256.5	14	45	<3	19.07	7.63	5.1	18.46	0.18	1.22	5.71	17.58
561	1.8	13.5	743.1	102.8	10.47	249.5	8.2	228	16	8	<3	3.54	21.32	6.4	36.53	0.04	2.04	8.92	11.36
562	0.6	14.6	742.7	102.5	10.2	256.7	8.2	266.1	15	992	<3	3.54	21.27	4.4	36.42	0.04	2.04	8.92	11.37
563	0.7	14.3	742.9	104.3	10.43	254.6	8.1	257.8	17	3	<3	3.54	21.42	18.8	36.76	0.06	2.05	8.95	11.41
564	0.8	15.3	741.9	104.7	10.26	230.8	8.1	272.6	14	8	<3	12.36	14.13	6.2	26.40	0.11	1.60	7.08	15.22
565	1.6	14.4	744	102.7	10.25	286.1	8.3	280.7	16	37	<3	3.80	26.81	10.0	39.44	0.04	2.14	9.74	12.64
566	0.9	14.2	744.2	101.8	10.17	287.8	8.3	324.4	14	18	<3	3.80	26.88	5.5	38.67	0.06	2.23	9.39	12.81
567	2	12.8	743.1	97.7	10.1	243.3	8.1	172.1	15	50	<3	3.57	21.49	7.2	35.48	0.05	2.08	8.54	11.40
568	1	13.6	743.3	100.3	10.12	193.5	8.1	370.2	15	12	<3	19.25	8.09	<3.6	17.38	0.20	1.25	5.24	17.78
569	0.7	13	743	102	10.51	186.7	8.0	244	14	14	<3	19.17	7.53	8.2	17.78	0.21	1.25	5.41	17.53
570	0.2	14.2	744.5	101.2	10.19	225.6	8.1	243.4	20	49	<3	4.08	19.01	28.2	33.15	0.11	2.05	7.96	11.29
571	0.7	15.9	742.8	98.6	9.5	222.8	8.2	310.1	14	48	<3	7.68	18.89	5.6	28.26	0.06	1.52	7.13	11.82
572	0.8	15.6	744.4	100.2	9.75	226.8	8.2	346.2	16	11	<3	2.83	18.01	5.8	32.38	0.05	1.96	7.67	10.00
573	1	15.5	744.6	103.6	10.06	226.8	8.2	342.8	15	55	<3	2.85	18.02	4.2	32.26	0.05	1.93	7.65	9.91
574	0.5	15.3	744.2	104.2	10.23	198	8.0	293.3	13	13	<3	15.88	10.29	<3.6	21.12	0.14	1.42	5.89	16.44
575	0.4	13.9	744.6	98.4	9.95	225.5	8.1	202.5	15	70	<3	4.10	19.06	<3.6	32.89	0.05	2.03	7.91	11.25
576	0.6	17	739.4	105.6	9.91	249.7	8.1	221.7	11	60	<3	8.20	22.53	<3.6	30.49	0.06	1.57	7.63	12.50
577	0.6	15.7	742.7	98.8	9.57	220.5	8.2	426.5	13	41	<3	7.48	19.00	<3.6	28.38	0.06	1.50	7.14	11.73

578	0.7	14.9	742	98.7	9.67	217	8.2	449.5	13	214	<3	6.14	20.42	6.8	29.54	0.05	1.57	7.35	10.94
579	0.4	13.4	744.8	102	10.46	222.9	8.1	189.3	16	65	<3	4.11	19.11	<3.6	33.76	0.05	2.05	8.08	11.43
580	0.8	15.6	744	97.8	9.48	227.5	8.2	289.7	12	18	<3	11.45	17.14	6.6	26.34	0.08	1.40	6.89	13.83
581	1	14.8	741.9	98.9	9.76	217.3	8.1	378.8	14	79	<3	6.27	20.22	<3.6	29.04	0.05	1.56	7.26	11.05
582	0.5	15.6	744	103.5	10.02	198.8	8.0	354	14	18	<3	15.95	10.27	5.4	20.82	0.15	1.39	5.80	16.26
583	1.1	14.9	744.6	105	10.3	222.4	8.2	267.2	16	77	<3	2.85	18.12	3.9	32.21	0.05	1.94	7.65	9.92
584	1	14.5	742.1	99	9.84	214.6	8.1	194.4	13	193	<3	6.44	19.99	6.3	28.77	0.06	1.55	7.21	11.11
585	0.2	18.6	742.2	104.8	9.56	269.9	8.5	224.4	16	16	<3	6.18	23.66	5.7	26.21	0.27	2.00	8.37	23.48
586	1	17.1	741.3	103.1	9.69	237.1	8.1	337.2	13	46	<3	7.22	19.82	4.5	29.39	0.09	1.49	7.46	11.48
587	1.1	18.1	741.1	106	9.75	242.6	8.1	308.5	13	50	<3	9.75	18.08	<3.6	27.65	0.08	1.44	7.15	13.07
588	0.4	17.6	742.6	104	9.61	238.1	8.2	282.9	12	177	<3	8.76	18.74	4.8	28.23	0.07	1.46	7.22	12.39
589	1.1	17.7	741.8	105.9	9.8	241.3	8.1	280.9	12	42	<3	7.37	19.55	3.7	29.04	0.06	1.47	7.42	11.67
590	0.4	19	739.9	111.5	10.04	245.7	8.4	294.7	15	160	<3	5.86	12.79	4.6	27.65	0.19	1.42	7.67	13.31
591	0.8	17.8	740.8	105.1	9.73	240.7	8.2	314.5	12	25	<3	9.59	18.16	<3.6	27.29	0.08	1.41	7.04	12.68
592	0.9	18.3	740.7	106.5	9.71	245.7	8.1	304.1	12	299	<3	9.91	18.01	<3.6	27.49	0.08	1.43	7.11	13.08
593	0.8	16.2	743.7	99.2	9.5	231.7	8.2	301.4	12	64	<3	11.24	17.13	3.9	26.23	0.08	1.40	6.86	13.75
594	0.5	16.3	743.4	100.2	9.58	232.3	8.2	301.3	12	27	<3	11.32	17.12	5.2	26.37	0.08	1.40	6.89	13.81
595	0.7	15.2	744.2	96.9	9.54	225.9	8.2	291.3	12	20	<3	7.81	19.25	<3.6	28.56	0.06	1.45	7.27	11.75
596	0.8	14.9	744.3	98.2	9.7	222.3	8.2	285.4	12	22	<3	7.79	19.26	<3.6	29.67	0.10	1.48	7.73	11.74
597	1.3	13.5	744.9	102.1	10.39	219.2	8.2	206.6	13	78	<3	3.92	21.75	<3.6	31.89	0.05	1.50	8.06	9.37
598	0.4	17.4	742.3	104.1	9.55	238.6	8.2	300.8	12	298	<3	8.70	18.74	<3.6	29.04	0.07	1.44	7.59	12.27
599	0.3	15.4	742.9	113.5	11.07	224.7	8.3	281.2	16	48	<3	2.10	8.97	5.5	29.60	0.29	1.44	8.77	13.22
600	0.8	17.8	739.2	100.5	9.27	239.8	8.1	278.8	11	114	<3	6.87	22.41	6.3	31.06	0.05	1.50	7.95	11.30
601	0.8	18.1	739.2	101.2	9.24	249	8.1	284.3	11	46	<3	6.88	22.39	6.0	31.37	0.05	1.52	7.97	11.29
602	0.6	18.1	739.1	99.4	9.17	248.5	8.2	288.8	11	50	<3	6.87	22.39	3.6	30.94	0.05	1.52	7.90	11.27
603	0.7	18.4	738.9	97.5	8.84	246	8.2	281.2	11	67	<3	8.28	21.08	4.4	30.30	0.05	1.48	7.72	11.99
604	0.7	18.4	738.8	100.8	9.24	248.3	8.2	286.3	12	45	<3	8.30	21.11	4.8	30.24	0.05	1.48	7.74	11.97
605	0.4	18.5	738.8	104.6	9.52	251.7	8.2	287.6	12	34	<3	8.32	21.11	5.7	30.60	0.06	1.50	7.81	12.08
606	0.1	17.9	738	104.7	9.5	366.7	8.0	271.4	21	49	<3	5.47	83.55	<3.6	38.96	0.16	3.65	11.70	23.12
607	0.4	20.3	736.8	111.7	9.71	366.6	8.5	238.7	11	201	<3	7.82	24.37	<3.6	49.19	0.14	1.68	10.65	15.49